DESIGN AND DEVELOPMENT OF AN ON-MACHINE PROFILE MEASUREMENT SYSTEM FOR AN ELID GRINDING MACHINE

Mohammad Sazedur Rahman

B.Sc in Mechanical Engineering

Bangladesh University of Engineering & Technology

A THESIS SUBMITTED

FOR THE DEGREE OF MASTER OF ENGINEERING

Department of Mechanical Engineering

National University of Singapore

2007

ACKNOWLEDGMENTS

The author would like to express his deepest and heartfelt thankfulness and appreciation to his supervisor, Professor Dr. Mustafizur Rahman and former supervisor Dr. Lim Han Seok, for their invaluable guidance, continuous support and encouragement throughout the research work. Whenever any problems arose they were there to give some of their valuable moments and helped to come out of that problem. Their comments and advice during the research have contributed immensely towards the success of this work. In addition, their patient guidance and suggestions have also helped the author in learning more.

The author also would like to thank National University of Singapore (NUS) for supporting his research by the research scholarship and to Workshop 2, Advanced Manufacturing Lab (AML) and Micro Fabrication Lab for the state of the art facilities and support without which the present work would not be possible. His heartfelt appreciations will also go to Mitutoyo Association of Science and Technology, Japan for their generous financial support towards the development of this on-machine measurement device.

The author would also like to thank the following staffs for their sincere help, guidance and advice: Mr. Neo Ken Soon, Mr. Lee Chiang Soon, Mr. Lim Soon Cheong, Mr. Tan Choon Huat, and Mr. Chua Choon Tye. He also acknowledge helpful co-operation from NUS Spin-off company MiktroTool Pvt. Limited's staff Mr. Atiqur Rahman.

The author would again offer his appreciation for the support and encouragement from his research colleagues and lab mates who have encouraged and helped him along the way. His appreciation goes to Tanveer Saleh, Majharul Islam, Wang Zhigang, Altabul Quddus, Sadiq M Alam, Masheed Ahmad, Indraneel Biswas and many more.

Last but not least his heartfelt thank to his family members who have always been there to support him in all kinds of ways and prayed for his better performance.

CONTENTS

CHAPTER 3 DESIGN AND DEVELOPMENT

CHAPTER 4: EXPERIMENT SETUPS

CHAPTER 5: RESULTS AND DISCUSSION

CHAPTER 6: CONCLUSIONS AND RECOMMENDATIONS

SUMMARY

Recent improvement of optoelectronic industry has put some stern challenge to the people in the arena of manufacturing to generate aspheric surface on hard and brittle material. Dimensional accuracy and surface quality is also needed to meet the requirements of high end optical devices. When the world of manufacturing is so much competitive to give the best product and most economical price it is really a challenge for the lens manufacturers to ensure lower price with high precision.

Improvement of dimensional accuracy of the finished product is one of the prime goals of this study. Shifting towards more sophisticated machine tool will definitely improve the accuracy of the finished product. But not necessarily this is a wise decision in every case. However it was found that in practical cases there are some quasi-static systematic errors which reduce the dimensional accuracy of the finished product. Over the years it has been proved that, software compensation is a very economical way of controlling these errors and improving the dimensional accuracy of the finished product.

Electrolytic in Process Dressing (ELID) grinding has established itself as a very efficient process for generating submicron level surface on hard and brittle materials which is a basic requirement of an aspheric lens. In this study a fully functional 4 axis CNC ELID grinding machine has been developed. To incorporate the machining of free form surface one workpiece rotational axis was also attached to this system.

On-machine measurement systems were developed in this study to measure ground surface profile and diameter of the grinding wheel. A very efficient on-machine profile measurement system has been developed based on Coordinate Measurement Machine (CMM) principle to check the ground surface profile during machining. Wheel wear was also measured at some regular interval to find out the latest wheel diameter possible. Tool path in the NC program was updated with this change in wheel diameter.

Free form surfaces were generated on BK7 glass and Perspex with and without compensating the tool path. Profile of the finished workpiece was measured in a commercially standard CMM machine and significant improvement of dimensional accuracy was reported.

Surface roughness was also measured using some standard roughness measuring equipment available in the lab. Different roughness parameters obtained were analyzed. In order to investigate the surface integrity the machined surface was observed under SEM and optical microscope with very high magnification.

LIST OF TABLES

LIST OF FIGURES

CHAPTER ONE

INTRODUCTION

1.1 SIGNIFICANCE OF RESEARCH

The hasty market progress in optoelectronics industry has led to increasing demands for machining aspheric and other free-form surfaces on hard and brittle materials with very high profile accuracy which in turn puts stern requirements on the manufacturing equipment.

Optical elements get expensive in proportionate with its precision and application. Even in case of consumer products it is expensive enough if we leave the case of very high quality aspherical mirrors used in astronomical observatory. In case of consumer products the biggest challenge the manufacturers are facing now a days is to present highly accurate product at a very competitive price. The aspheric surfaces used in the optical systems can control the aberrations and reduce the number of elements without diminishing image quality and thereby results lighter optical systems. Even asymmetrical and eccentric surfaces can eliminate obscurations to improve the image quality [Derk Visser et al, 1985; C.S. Han et al, 2004]. So application of aspheric lenses in optical systems makes it possible to improve system performance without increasing the price. As a result optical components of large sized aspheric surface have gained significant importance and indispensability.

Glasses exhibit desirable optical properties needed for advanced optical instruments [C.S. Han et al.]. High hardness and brittleness make it very difficult to machine glasses frees from subsurface damages using conventional turning or grinding machines. As a result, proficient and cost-effective manufacturing techniques for generating high quality aspheric surfaces on glass with very accurate profile are still a challenge faced by manufacturers.

According to market expectations on required accuracy of optics and the international optics standard (ISO 10110), an overall machining accuracy better than 200 nm is expected. Currently available commercial machines cannot fully meet these requirements [Qian et al]. Aspheric components needed to be with higher form accuracy than other traditional devices especially when the wavelength used in modern optics are progressively smaller [Yousef A. et al.]. Where as non-rotational symmetry causes manufacture of such optical elements made of brittle materials considerably more difficulty, so these elements are more expensive and rare. Ductile mode machining of hard and brittle materials like glass and ceramics to optical quality is now considered as an emerging technology.

Single point diamond turning with a fast tool servo is a more conventional way to engender high quality freeform surfaces, but the number of materials machinable with this method is limited. In most of the cases free form surfaces are generated by grinding and then followed by lapping or polishing to achieve the surface finish in sub-micron level. Grinding and polishing aim to improve the forming and dimensional accuracy as

well as the surface finishing. Both processes play an important role as they are at the end of the manufacturing chain. So researchers have tried to improve the grinding process over the years.

Wet grinding, owing to its ability to produce superb form accuracy and surface integrity on hard and brittle materials, remains as one of the most important and feasible machining technologies to date [Shinya Moritaa et al.]. Usually a rough aspheric form is generated by grinding or milling followed by very time consuming lapping and polishing process to get rid of damaged layers or tool marks which were created my rough cutting and provide a high quality surface. But it is impossible for this polishing process to improve the form accuracy and it can even make it worse. So over the years researchers have tried for innovative ideas to make this grinding process more efficient in grinding aspheric surfaces with higher form accuracy.

Loading, dulling and shedding on a grinding wheel frequently occur under inappropriate grinding conditions which causes a blur machined surface. The working surface of a grinding wheel is dressed at a certain interval to avoid the burning. Electrolytic in process dressing(ELID) grinding introduced by Murata et al in the year of 1985 is a very efficient process of achieving mirror surface finish on very hard and brittle material like glass, wafer etc. ELID grinding method was further improved by Ohmori and Nakagawa in 1990 and they succeeded in establishing this process in any conventional grinding machine with minimal amount of modifications [H. S Lim et al.].

So by replacing the normal grinding with the ELID it is possible to reduce the lapping and polishing time without compromising with the surface quality.

One of the very significant factors for the better performance of optical elements is the form accuracy of the lenses it uses. In practice, the machined part dimension deviates from the desired value owing to many quasi-static systematic errors: geometric error of machine tool, thermally induced distortions of machine tool elements, error arising from the static deflection of machine- fixture-workpiece-tool system under the cutting force and other errors such as those arising from clamping force, tool wear etc. The machining accuracy is commonly determined by the kinematics accuracy of NC machine tool and a big portion of machines used are with low kinematic accuracy, which prevents many manufacturing enterprises from producing high quality products. Software based error compensation is a method of anticipating the combined effect of all these above factors on workpiece accuracy and suitably modifying the NC program. Owing to its reliance on modification of software rather than hardware, it is considered to be a direct and very economical method of achieving higher machining accuracy without having resort to higher accurate machine. Although a considerable research work have been reported to improve the kinematic accuracy of the machine tool which are too sophisticated to implement, there are few programs that focus on modifying the NC code to compensate the movement error [Saroti et al.].

Since it is not possible to get the desired form in single shot, the ground surface profile is needed to be measured to compensate in the NC program. The main problem in

measuring the surface profile is that, if it is removed from the machine the accuracy will be gone. So the measurement needed to be done without removing the workpiece form the machine which is called on-machine measurement. So in this study one of the primary goals was to develop an on machine measurement system for measuring the ground surface profile.

Grinding wheel diameter is one of the key factors in determining the tool path in the NC program. This tool path needed to be updated from time to time as wheel diameter changes due to wear. So in this study wheel diameter was also measured during the process to change the tool path in the NC program.

1.2 SCOPE OF THIS STUDY

Scope of this study can be briefly summarized as follows:

- Design and develop a fully functional 4 axis CNC ELID grinding machine for performing ELID grinding process on hard and brittle material.
- Design and develop a turn table for using it as an attachment in providing rotary motion to the workpiece.
- Design and develop an on-machine measurement system for measuring the free form surfaces machined in the machine.
- Measure the grinding wheel diameter regularly to compensate wheel wear in the tool path of the NC program.
- Fabricate aspheric surface on hard and brittle material with regular update of tool path in the NC program.

- Study on different factors responsible for the dimensional accuracy of the free form surface machined by ELID grinding process.

1.3 ORGANIZATION OF THE DISSERTATION

There are six chapters in this dissertation. In this chapter background of this study was discussed. Also scope and research objectives were summarized.

Chapter 2 is divided into 9 sections giving a comprehensive review of the literature. The ELID process is discussed in details. Research works done on profile measurement and error compensation are also reported.

Chapter 3 describes the design and development of the experimental setups. Factors considered during design and different components used are also mentioned in details in this chapter.

Chapter 4 contains experimental setups in details. It also explains the procedures of the experiments. There is a brief description of the different standard instruments used for measurement in this study.

Chapter 5 presents different informations gathered by the experiments. It also analyzed the results obtained.

Chapter 6 concludes the thesis with a summary of contribution. Further recommendations are also provided to move forward with this study in future.

CHAPTER TWO

LITERATURE REVIEW

"When you can measure what you are speaking about and express it in numbers you know something about it; but when you cannot measure it you cannot express it in numbers, your knowledge is meager and of unsatisfactory kind." Lord Kelvin

2.1 INTRODUCTION

Measurements are done to gain reliable quantified information about our real world. Although everybody has accepted the importance of metrology in manufacturing still it is often regarded as a cost factor and very seldom as a value adding activity. So in many cases one of the most important aims of production engineers is to reduce metrology costs to an absolute minimum. In this study a very economical and efficient on-machine profile measurement system has been developed to measure the profile of the ground surface generated by ELID grinding process.

ELID grinding has great potentialities in the field of manufacturing high precision optical lenses due to its ability to produce high quality surface on hard and brittle materials. Dimensional accuracy is one of the most important factors for a lens to be qualified for being used in optical industry. In this chapter after describing the basic mechanism of ELID grinding some works dedicated to improve the dimensional accuracy of a finished product will be reviewed. Lastly, different works done on the development

of a very economical way to improve the dimensional accuracy free form surfaces machined by ELID grinding was studied.

2.2 HISTORICAL BACKGROUND OF ELID GRINDING PROCESS

The ELID technique was originated from Japan, and most of the works reviewed were reported from Material Fabrication Lab, RIKEN, Japan. Murata et al. [Murata et al., 1985] introduced ELID in 1985 for the application of abrasive cut-off of ceramic. The structural ceramics are highly difficult to grind due to its hard and brittle nature. Normally for grinding harder materials, the softer grade grinding wheels have been used. But, the softer grinding wheels have the problem of large diameter decrease due to wheel wear. Therefore, stronger bond with harder abrasives have been selected for grinding hard and brittle materials. When the grits are worn out, a new layer in the outer surface is electrolyzed and necessary bonding is removed from the grinding wheel surface in order to realize grit protrusion. The results of the experiments performed with different grades of grinding wheel showed that the grinding force was reduced to a significant amount when the in-process dressing was done. Even though the surface finish is not a major criterion in abrasive cut-off, the surface roughness also improved due to the application of the ELID. The experiments show that ELID is an effective process of increasing surface quality even though it has some problems like rust formation due to electrolyte application [Murata et al., 1985].

Ohmori et al. [Ohmori and Nakagawa, 1990] further improved ELID suitable for super-abrasive grinding wheels. Different types of grinding wheels have been used along with ELID grinding [Ohmori et al., 1999, 2000]. The grinding wheels used in ELID are broadly classified into the following:

- Metal-bonded diamond grinding wheels and
- Metal-resin-bonded diamond grinding wheels

The grades of the grinding wheels are ranging from #325 to #300,000, which have an average grit size from 38 μm to 5 nm. The basic ELID system consists of a metal bonded diamond grinding wheel, an electrode, a power supply and an electrolyte [Ohmori and Nakagawa, 1990].

2.3 DEVELOPMENT ELID GRINDING

Periodic dressing of grinding wheels is cumbersome and also produces inaccuracy during the process. The main requirement for a grinding wheel is its ability to replenish the topography and promotes an uninterrupted grinding (or with minimum interruptions). When grinding is performed with conventional grinding wheels (other than metal-bonded), the worn out grits are removed automatically by the grinding force and the grits beneath come into contact with the workpiece. This is known as the 'self-sharpening' effect as shown in Figure 2.1. This effect makes the in-process dressing necessary and grinding becomes continuous. The conventional wheels are also prepared with certain porosity in order to provide space for chip and coolant [Malkin, 1987; Shaw, 1996]. However, the wheels have the properties described above are suitable for machining metals or materials with less hardness and they are not recommended for grinding harder material because of intense diminution of wheel diameter. Therefore, wheels with high bonding strength are quite suitable in order to withstand higher grinding forces generated during grinding.

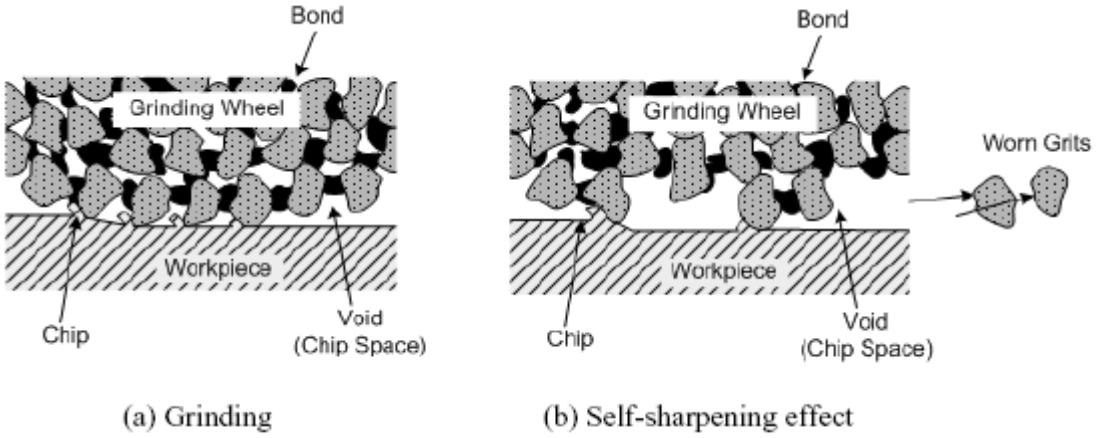

Figure 2.1: Self-sharpening effect of the conventional grinding wheel

Though the metal-bonded grinding wheels possess excellent properties for grinding hard and brittle materials, its usage was not widespread because they are not suitable for continuous usage due to their poor self-sharpening effect and there is no space for chip and coolant because the grits are bonded in the metal matrix. The metal bond around the grit should be removed to a certain amount in order to produce grain protrusion as well as space for coolant and chip flow. The necessary bond material is removed electrochemically by anodic dissolution, but when the grit size of the grinding wheel becomes smaller, problems such as wheel loading and glazing are encountered which impedes the effectiveness of the grinding wheel. Therefore, an additional process is necessary in order to rectify the above problems and promotes uninterrupted grinding using metal-bonded grinding wheels. The concept of the ELID is to provide uninterrupted grinding using harder metal-bonded wheels. The problems such as wheel loading and glazing can be eliminated by introducing an ‘electrolyze cell’ (anode, cathode, power source and electrolyte) during grinding, which stimulates electrolysis whenever necessary to protrude sharp grids during the grinding process continuously.

2.4 ESSENTIAL COMPONENTS OF THE ELID

An electrolyze cell is the unique component in ELID grinding process to facilitate the self-sharpening effect on the grinding wheels. The cell is created using a conductive grinding wheel, an electrode, electrolyte and a power supply. Figure 2.2 shows the schematic illustration of the ELID system. The metal-bonded grinding wheel is made into a positive pole and the electrode is made into a negative pole. In the small clearance of approximately 0.1 to 0.3 *mm* between the positive and negative poles, electrolysis occurs through the supply of the grinding fluid and an electrical current. Different components of a basic ELID grinding system will be discussed in the subsequent sections.

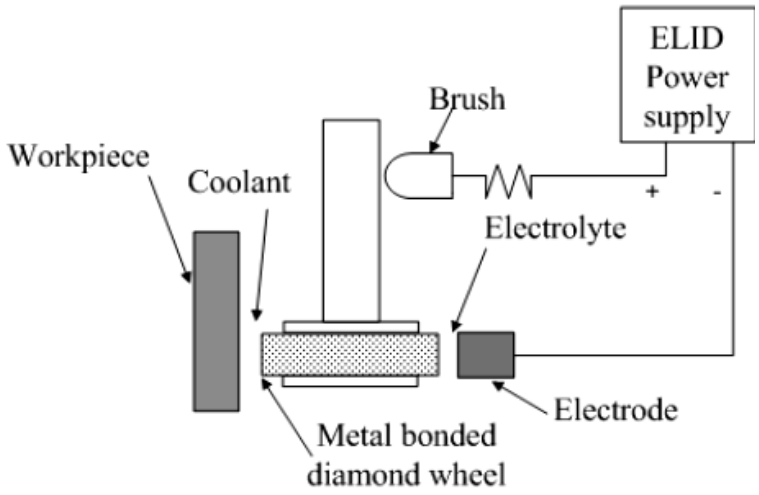

Figure 2.2 Schematic illustration of the ELID system

2.4.1 The ELID-grinding wheels

The ELID grinding wheels are made of conductive materials *i.e.* metals such as cast iron, copper and bronze. The diamond layer is prepared powder metallurgy mixing the metal and the diamond grits with certain volume percentage. The prepared diamond layer is attached with the steel hub as shown in Figure 2.3. The grinding wheels are

available in different size and shapes. Among them the straight type and the cup shape wheels are commonly used.

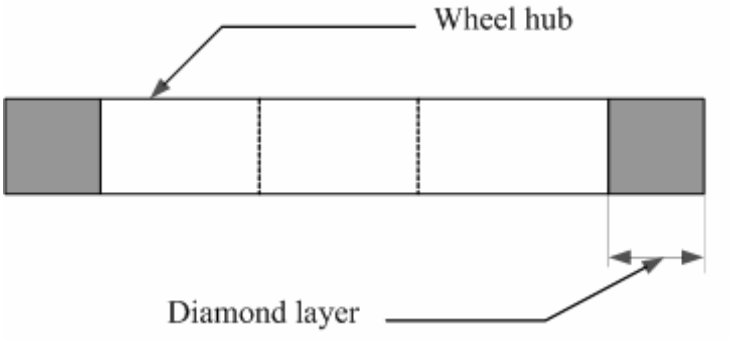

Figure 2.3: Metal bonded grinding wheel.

2.4.2 The electrode

The size of the electrode can be chosen in such a way that there is no hindrance for the machining process. However, higher grinding wheel speed reduces the effect of electrolysis. Hence the size of the electrode should be sufficient to produce the effect of in-process dressing. Generally the size of the electrode can be chosen from one-sixth to one-fourth of the grinding wheel perimeter. The thickness of the electrode is made by 1 – 2 *mm* more than the width of the grinding wheel [Ohmori and Nakagawa, 1990]. The electrode used in this study has channels drilled inside the electrode with opening in the circular periphery so that electrolyte was directly injected at the gap between electrode and wheel.

2.4.3 Material for the ELID electrode

Material such as copper, graphite and stainless steel are commonly used as the electrode materials. The metal ions of the anode migrate to the cathode and become a thin layer on the surface, which needs to be galvanized. Therefore, care should be taken

selecting the cathode material. To predict the reactions during electrolysis, the "electrochemical electromotive series" is used. Metals with a more noble character than copper will not react, but fall down as an anode mud. However, metals with a standard potential less than copper will also be electrolyzed and migrate at the cathode. When grinding with copper bonded grinding wheels, the Cu2+ ions in solution is precipitated on the cathode, and a more pure copper layer is formed than before. The pollution from the grinding wheel will not react but fall down to the ground as the anode mud. Therefore, the cathode is always pure and conductive when used with copper or bronze bonded wheels.

2.4.4 Electrode-Wheel Gap

The gap between the electrodes should be more than the oxidized layer formed on the grinding wheel surface and also sufficient for electrolyte flow. Recommended gap between electrode and wheel is 100 – 300 μm which cannot be maintained throughout the process because of the wheel wear. The gap should be measured using the gap sensor and it is adjusted by an automatic gap adjustment system [Lee, 2000].

2.4.5 Electrolyte

The electrolyte plays an important role during in-process dressing. The performance of the ELID depends on the properties of the electrolyte. If the oxide layer produced during electrolysis is solvable, there will not be any oxide layer on the wheel surface and the material oxidized from the wheel surface depending on the Faraday's law.

However, the ELID uses an electrolyte in which the oxide is not solvable and therefore the metal oxides are deposited on the grinding wheel surface during in-process dressing.

2.4.6 Power sources

Different power sources such as AC, DC and pulsed DC have been experimented with the ELID. The applications and the advantages of different power sources were compared, and the results were described in the previous studies [Ohmori, 1995, 1997]. However, the recent developments show that the pulsed power sources can produce more control over the dressing current than other power sources.

2.5 MECHANISM OF THE ELID GRINDING

The mechanism of the ELID grinding can be explained as shown in Figure 2.4. After truing, the grains and bonding material of the wheel surface are flattened. It is necessary for the trued wheel to be electrically pre-dressed to protrude the grains on the wheel surface. When pre-dressing starts, the bonding material flows out from the grinding wheel and an insulating layer composed of the oxidized bonding material is formed on the wheel surface. This insulating layer reduces the electrical conductivity of the wheel surface and prevents excessive flow out of the bonding material from the wheel. As grinding begins, diamond grains as well as the layer gradually wears out. As a result, the electrical conductivity of the wheel surface increases and the electrolytic dressing restarts with the flow out of bonding material from grinding wheel. The protrusion of diamond grains from the grinding wheel therefore remains constants. This cycle is repeated during the grinding process to achieve stable grinding.

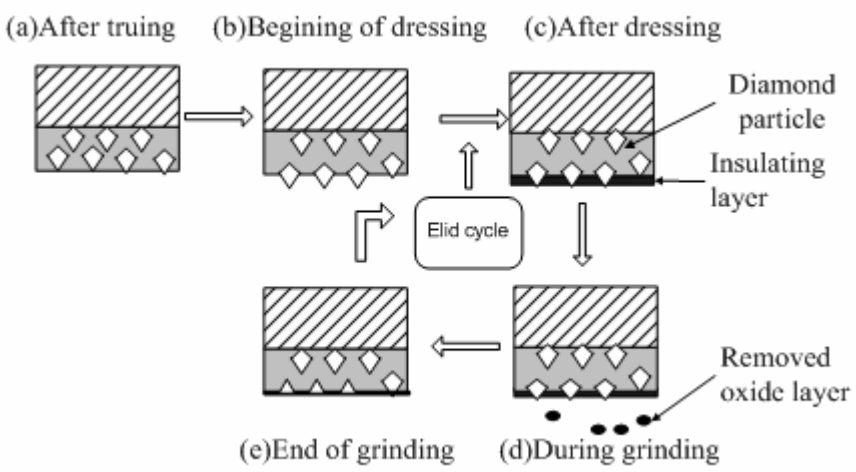

Figure 2.4: Principle of the ELID grinding process

2.6. MACHINE DEVELOPMENT FOR GENERATING ASPHERIC SURFACE

Application of precision ELID grinding is a promising solution to the market demands for aspheric lenses in optical industries due to its ability in generating freeform surface with a reasonable surface roughness and subsurface damage, hence drastically reducing subsequent polishing process time without impairing form accuracy. Very few satisfactory machines are available by now, because most of the freeform generators on the market are originally designed and developed for single-point diamond turning (SPDT), with options for grinding by refitting the machine with a tool spindle or eventually with an additional ELID set-up.

Under the supervision of J. Qian et al. a European project “Nano Grind” have been launched to develop an ultraprecision 5-axis grinding machine and relevant processing techniques for realizing curved surfaces with optical quality by means of

nano-precision grinding based on ELID technology. The prototype machine was still under development and construction. Research work related to machine development has followed well-known principles of precision engineering. This paper discusses the innovative features of the prototype design.

Hao-Bo Cheng et al. have designed a six-axis machining system in Tsinghua University and for fabricating large off-axis aspherical mirrors with sub-aperture lapping techniques. The new system is based on computer-controlled optical surfacing (CCOS), which combines the faculties of grinding, polishing, and on-machine profile measuring, has the features of conventional loose abrasive machining with the characteristics of a tool having multiple degrees of freedom moving in planar model.

Shaohui Yin et al. adopted the following steps for ultraprecision fabrication of the large special Schmidt plate:

(1) Conventional (rough) grinding,

(2)ELID arc-enveloped grinding,

(3) Polishing.

Conventional (rough) grinding aimed to remove a lot of materials to generate approximate sphere, ELID arc-enveloped grinding was used to obtain higher form accuracy and desired surface roughness so that polishing period could be shorten; polishing aimed to obtain better surface roughness and less damaged layer. ELID arc enveloped grinding experiments were carried out using no. 325, 1200 CIFB diamond cast-iron bond wheels and grinding characteristics such as attainable form accuracy,

surface roughness were investigated. Furthermore, some measures to improve form accuracy were discussed and verified.

2.7 On-machine profile measurement

2.7.1 3D shape Measurement

Peisen S. Huang et al. have developed a novel high-speed phase shifting technique for 3-D shape measurement with a potential measurement speed of 100 Hz. It takes advantage of the unique color channel switching characteristic of a digital-light-processing (DLP) projector with one digital micromirror device (DMD) chip. By removing the color filter and properly synchronizing the projection of fringe patterns by the DLP projector and the acquisition of images by the CCD camera, three phase-shifted fringe patterns can be obtained within 10 ms. This makes it possible to achieve a maximum measurement speed of 100 Hz or 100 3-D shape measurements per second if the sampling speed of the CCD camera is fast enough. A compensation algorithm was developed to eliminate the effect of the gray-scale curve distortion of the digital projectors, and as a result, satisfactory results were obtained. Experimental results showed that this method could be used to measure the 3-D shapes of slowly moving objects, which has been difficult to accomplish by the traditional phase shifting 3-D shape measurement systems.

2.7.2 Non-Contact Probe

Ming Chang et al. have developed a micrograting projection system for non-contact profilometric measurement of small-form parts. The key technologies in the

implementation of this probe include the projection fringe method, lateral shearing interferometry and phase shifting interferometry. The measurement resolution of object height is dependent on the projected grating pitch and grating incidence angle and can reach the order of submicron. The experimental setup is inexpensive and very easy to manage with simple instruments, remote sensing, good accuracy, and insensitivity to environmental noise. This system has the potential to be a low-cost and efficient probe for the inspection of small form parts in industrial applications.

Young Kee Ryu et al. have developed a low-cost and simple non-contact optical sensor composed of a hologram laser unit from a CD player to measure the surface and the thickness of the transparent material such as glass simultaneously. They overcome the wavelength variation due to temperature change a by employing thermoelectric cooler (TEC) and improved the sensor performance in the real world where the ambient temperature varies.

Pei-Lum et al. investigated the influence of different working parameters on lapping and polishing of aspheric lens. On the basis of effective methods to improve the form accuracy was identified. They proposed for use of use of asphalt layer for polishing which helped to remove the crack layer and improve form accuracy.

Wei Gao et al have developed a combined method to measure profiles that include high-frequency components whose spatial wavelengths are shorter than the probe interval. It combined the generalized 2-point method with the inclination method. It is

suitable for measuring discontinuous profiles that include step-wise variations and abrupt changes. He discussed the influences of the setting error of the probe interval and the positioning error of sampling when the combined method was used to measure a step-wise profile. Results of theoretical analyses showed that these errors cause the same kind of evaluation errors in the profile measured with the combined method and large profile evaluation errors are caused by the edge part of a step-wise profile. An automatic selection method that can select the standard area properly and quickly is developed to improve the accuracy of the combined method. A machined surface with a stepwise profile is measured by using two capacitance-type displacement probes. Experimental results confirm the effectiveness of the combined method.

2.7.3 Optical Reference Profilometer

Stephan R. Clarket al. developed an optical reference profilometer which is basically a coordinate measurement machine (CMM) configuration that utilizing a special optical referencing frame to provide a stable and accurate surface measurement. This referencing frame provides several mechanical advantages that make it possible to use lower precision mechanical components while still maintaining high measurement accuracy. It also reduced measurement sensitivity to thermal variations of the environment. By utilizing a superinvar metering rod network, this CMM system is essentially thermally insensitive to temperature changes of the order of 1°C. This special feature makes the optical reference profilometer functional at a high measurement accuracy level in an open laboratory environment. This system appears to be scalable to

larger sizes, and may present some novel design concepts for use in future CMM development.

2.7.4 Phase-shifting image digital holography

Ichirou Yamaguchi et al. have developed a system for measurement of shape and deformation of diffusely reflecting surfaces by phase-shifting digital holography. The difference of the reconstructed phases before and after tilt of the object illumination beam provides the contour lines of the surface height, while before and after object deformation delivers those of object displacement. This method enables measurements of both the surface shape and deformation of 3-D objects of various sizes with the same optical system and processing software. Suppression of speckle noise is also discussed. Although the setup is the same as electronic speckle pattern interferometry with a phase-shifted reference beam, the present method is more flexible because phase information can also be used for numerical reconstruction of the defocused region of a 3-D object.

N. R. Sivakumar et al. have developed a measurement system using a modified Michelson interferometer in combination with an instantaneous phase-shifting interferometer (IPSI) for high speed measurement of large flat surfaces. Since instantaneous phase shifting does not depend on the conventional mechanical actuators for phase shifting, the vibration-related inaccuracies are largely avoided. Moreover, all the phases are captured simultaneously. This has reduced the environmental, vibration and other external effects considerably. No mechanical movement is involved, thus minimizing the errors due to nonlinearity and vibration induced by the phase shifter itself.

2. 7.5 Optical inverse scattering phase method

A. Taguchi et al. have proposed a new optical measuring method which can be applied to the in-process measurement of three-dimensional micro-profiles with accuracy in the nanometer order. No scanning process is required. Employing Fourier phase retrieval algorithm, three-dimensional micro-profiles are reconstructed from only the measured Fraunhofer diffraction intensity. Computer simulations and actual measurements were performed for the verification of the proposed method. The optical inverse scattering phase method offers the advantage of measuring a three-dimensional profile within the whole area illuminated by the laser beam simultaneously.

2.7.6 Multi-Iteration CMM

E.B. Hughes et al have designed a high accuracy CMM based on iteration technique where spatial coordinates are determined solely from measurements of displacement of a moving probe relative to a number. A prototype measuring station has been designed, built and tested. The design of the measuring station has been optimized to minimize uncertainties due to beam steering.

2.7.7 Compact high-accuracy CMM

The trend towards miniaturization in manufacturing has led to a requirement for a coordinate measuring machine (CMM) capable of measuring tiny features on small components. A compact CMM has been designed and built by G.N. Peggs et al. which had a working volume of a cube of side 50 mm, and a measurement uncertainty estimated to be 50 nm. The machine utilized a self-calibrated solid cube to provide a geometrical

reference that is transferred into the CMM by means of a combination of three, mutually orthogonal, mirrors, six laser interferometers and three dual axis autocollimators. In situ measurement of the mirrors' flatness and orthogonality and redundancy of measurement were used to minimize systematic uncertainties.

2.7.8 Nano-CMM probe

A 3D nano-position sensing probe based on leaser trapping technology was developed by Y. Takaya et al. It served as an important technology in the development of the nano-CMM used in micro-fabrication systems. They discussed the laser trapping probe whose principle is based on the dynamic properties of optically trapped particles and the Linnik microscope interferometer. Its potentials as a nano-CMM probe were investigated in fundamental experiments. Single-beam gradient-force optical traps of silica particles in air were successfully demonstrated by using an object lens. Positional detection accuracy of 30nm was also confirmed through measurements of fringe changes with the shifts of the probe sphere.

2.8. ERROR COMPENSATION

Peisen S. Huang et al. have presented an error compensation method for a full-field 3-D shape measurement system based on a digital fringe projection and phase shifting technique. The error map of the system is first established by comparing the measured coordinates with the coordinates defined by a coordinates measuring machine (CMM) at selected sample points within the measurement volume. An eight-point interpolation algorithm based on the Shepard’s method is then used to compensate for the

errors in the measured coordinates. Experimental results showed that the accuracy of the system was improved by more than 60% after error compensation.

Inadequate shop floor friendliness is a major reason why traditional software based error compensation approaches have failed to be accepted by industry. Z.Q. Liu et al. have developed a compensation approach that relies solely on post-process and on-machine measurements of parts previously machined on the same machine. The approach is based on a new method of error decomposition and a simple model of machine deflections induced by the cutting force. The approach is verified by independent measurements of the various model parameters. It is also shown that the machine tool can be made to act as its own dynamometer.

On machining processes the unbalance of wheel and vibration of spindle have great impact on workpiece accuracy and roughness. Y. Zhang et al. developed a mathematical model which leads to the error of the workpiece surface profile due to parameters variation of wheel and spindle on the workpiece surface.

H. J. Jing el al. have successfully reduced the machining error by modifying NC program according the kinematic error of a machine tool. A compensation algorithm was built along with a software system to modify the NC program according to the kinematic error. The cutting results showed an enhancement of 40% sphericity error, over 50% dimension error and an average of 25% in roundness error were achieved by modifying NC program.

2.8.1 Improvement of form accuracy

T. Enomoto et al. tried to improve the form accuracy by considering the form generation mechanism. Countermeasures are proposed to overcome the problem that, in grinding an asymmetrical surface, the surface profile concavely deviates from the ideal profile. By experimentally investigating the form generation mechanism, it was found that grindability deteriorated on the outward surface owing to direct contact between the wheel bond and the workpiece. Using a hard bonded wheel improved form accuracy, and traversing the wheel outward from the workpiece centre achieved both high form accuracy of less than 120 nm p-v and good roughness ranging from 20 to 40 nm Ry.

2.8.2 Improvement of machining accuracy

T. Kawai et al have improved the Machining Accuracy of a 5-Axis Ultraprecision machine tool by laminarization and mirror surface finishing. Air bearings are often used in ultraprecision machine tools requiring high accuracy. With increasing the high accuracy for machine tools, it is required to pay attention to micro-vibration with nanometer order. The fluctuation in compressed air applied to air bearings causes the air turbulence, which results in the micro-vibration. The study presented the laminarization by the optimal design of piping and air bearing surfaces as well as mirror surface finishing, so that the laminarization can be realized to suppress the micro-vibration. From experimental results, it was found that the surface roughness of workpieces can be drastically improved by using a revised ultraprecision machining center.

2.8.3 Error mapping

H. Schwenke et al have presented a novel approach for the mapping of geometric errors of machine tools and coordinate measuring machines by a single tracking interferometer. The concept is based on interferometric displacement measurements between reference points that are fixed to the base and offset points fixed to the machine head. The experimental comparison with an independent technique on a high accuracy CMM demonstrated the agreement of parameters in the sub-micron range. Thus, the method proved to be suitable for the highest accuracy demands. Furthermore, it has almost no limitation for the maximum size of the working volume. It does not require any alignment of equipment and yields a very simple data structure, which can be evaluated by the developed software with very little additional information from the operator. The method has also been tested on a large horizontal arm machine and on a smaller high precision machine tool.

2.9. SURFACE ROUGHNESS

Jung-Sik Heo et al. have investigated Grinding characteristics of conventional and ELID methods in difficult-to-cut and hardened brittle materials. They have compared the grinding characteristic at the SCM415 that is one of the difficult-to-cut materials due to hardened brittle using the CBN wheel and the 38P wheel that increased the toughness and hardness at the WA wheel and analyzed the tendency of grinding force and surface roughness from various working conditions such as spindle speed and depth of cut. In order to verify the variation of grinding force and to evaluate the surface roughness examinations were conducted in general grinding and ELID grinding. Finally they have

come to the conclusion that the ELID grinding can do mirror-like grinding and grinding force at the CBN stably maintained regardless of grinding condition change.

Y. Namba et al. ground 11 kinds of typical optical glass by the ultra-precision surface grinder having a glass-ceramic spindle of extremely-low thermal expansion with various cup-typed resin-bonded diamond wheels. It was found that if it is possible to grind the glass pieces in ductile mode, the surface does not contain a micro-crack under the surface. The surface roughness is related with grain size, feed per wheel revolution and glass material, not with depth of cut. Super-smooth surfaces less than 0.2nm rms, 2nm R_{max} had been obtained by the ultra-precision grinding.

CHAPTER THREE

DESIGN AND DEVELOPMENT

3.1 INTRODUCTION

One of the major goals of this study was the design and development of different components of the experimental setup which includes an ultra precision ELID grinding machine, a turn table, an on-machine surface profile and another on machine wheel wear measurement system. The ultimate goal was to develop an ELID grinding machine which is capable of generating surfaces at submicron level and in corporate the high quality optical surface generating ability in machining aspheric lenses with higher form and profile accuracy. The wheel profile measurement system was basically developed for enhancing the roundness of the grinding wheel by controlled electrolysis. In this study it was used for measuring the wheel profile and from that generates the average wheel diameter.

3.2 DESIGN AND DEVELOPMENT OF ELID GRINDING MACHINE

Initial target of this study was to develop a 4 axis CNC ELID grinding machine which is capable of generating a surface in submicron level. The project included dismantling of a robust wire cut EDM machine, testing the concrete bed and gantry structure for stability to be used in the new machine, fabrication of necessary physical structures and finally installation of a controller developed in the lab.

3.2.1 Design Considerations

- Dismantle the robust wire cut EDM machine situated in the workshop 2.
- Installation of servo motor along with driver to the machine in place of stepper motor.
- Replace the open loop controller with a closed loop one and thereby improve the accuracy.
- Design and fabricate necessary components for setting up the physical structure of the ELID grinding system such as electrode holder, mountings for setting up limit switches, linear scales and controller panel to the machine.

3.3 THE NEW ELID MACHINE

A 4-axis CNC ELID grinding machine along with a DC power supply was developed to perform the ELID process. The schematic design of the machine is given in the figure 3.1(a). This design has been implemented on an existing WEDM machine. Figure 3.1(b) shows the photograph of the developed system. Detailed information about the newly developed grinding system is given in table I. All the four axes are controlled by servo motors. The system arranged as gantry structure, two pillars, a crossbeam and a base form main frame of the machine. A special type of electrode was used which has the cavity inside the body and a pump is used to inject electrolyte right at the gap between the wheel and electrode. Stroke length, resolution, natural frequency and damping ratio of the 3 translation axes are shown in the table 3.1. Rated speed of the grinding spindle is also shown in this table. Three steeper motor used in the three translational axes were replaced by three TBL- j Series servo motors matched with TBL-I Driver. Three

Mitutoyo linear scales were used with these three axes to ensure higher resolution. The linear scale incorporated with Y axis was not in operation and its resolution was determined by setting up parameters in the corresponding driver. One Panasonic MSMA series motor along with a MSDA series driver from the same manufacturer was used for the grinding spindle. Detail specification of these motors and drivers are given in table B1 of Appendix B.

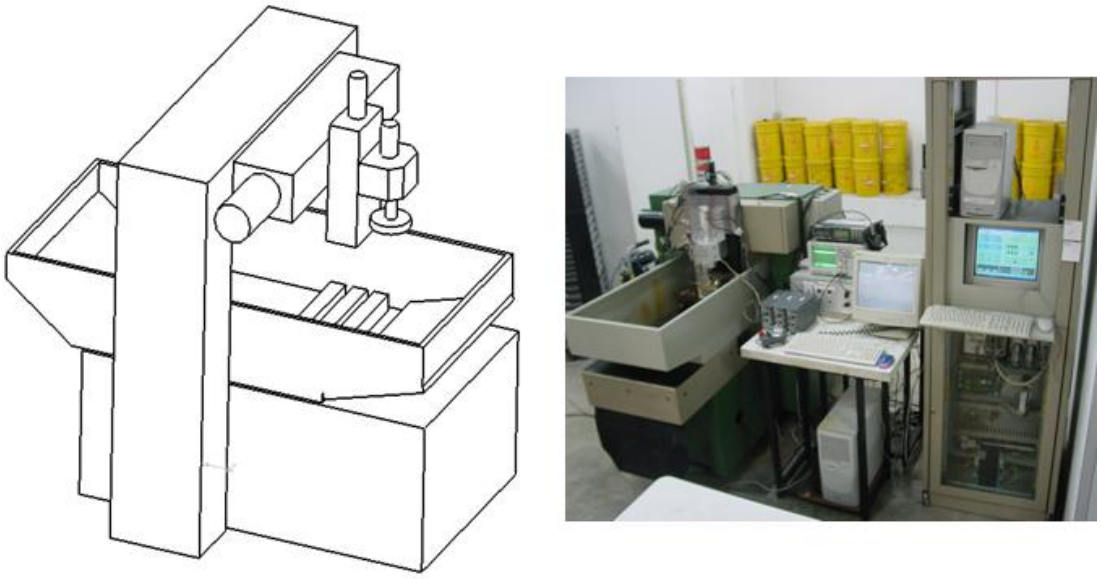

(a) (b)

Figure 3.1 (a): Schematic design of the ELID Machine (b): Photograph of the developed system

Table 3.1: Specifications of the ELID Grinding Machine

Parameters	X	Y	Z
Full Stroke(mm)	250	250	150
Resolution(microns)	0.1	0.25	0.1
Accuracy(microns)	35	500	40
Repeatability(microns)	22	500	2

Natural frequency(Hz)	817	2000	1429
Damping Ratio	0.0765	0.086	0.014
Rated Spindle speed	2000 RPM		

3.3.1 The Power Supply

Power supply is the heart of the ELID grinding technology. A square pulsed DC power supply has been designed and fabricated to generate power for the ELID cell. Important technical data of the developed power supply are given in table 3.2.

Table 3.2: Technical Specifications of the DC power supply

Parameters	Values
Voltage(volts)	20,40,60,80,100
Peak Current(A)	2
T_{on} (micro second)	8,10,14,30
T_{off} (micro second)	5,8,20

3.3.2 Fabrication of the electrode-holder:

This is one of the many parts that were designed and developed to improve the basic structure of the ELID grinding machine.

3.3.2.1 Design Considerations:

- Previously electrode was attached in the machine with the help of a magnet which was very troublesome to set and it was not a very reliable way to fix the electrode

whereas the gap between electrode and the grinding wheel is a very significant parameter for ELID grinding.

- Another important factor in the new system is that the spindle material was aluminum which is not magnetic. So it was necessary to find some other way for attaching the electrode to the machine spindle.
- For the measurement of wheel profile there should be some mechanism to hold sensors at a certain distance apart from the wheel targeting right at the grinding wheel cutting edge.

The CAD drawing and real image of this part made with Perspex is shown in figure 3.2 (a) and (b) respectively.

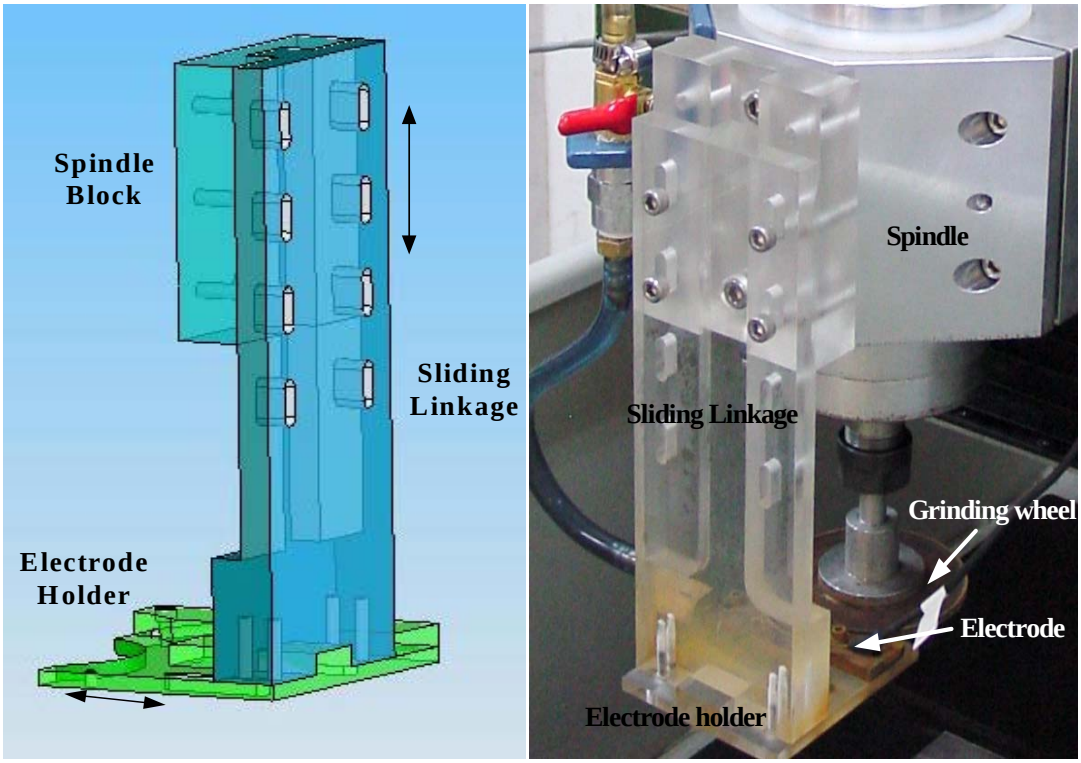

(a) (b)

Figure 3.2: (a) CAD drawing (b) Real image of the Electrode-holder

3.3.3 The Electrode-Holder

Basically there are three parts of this electrode-holder mechanism- Spindle block, sliding linkage and the electrode holder. Spindle block is fixed with the spindle and sliding linkage can move vertically to fix the position of electrode holder accurately with the grinding wheel. The electrode holder can be moved horizontally to control the gap width between grinding wheel and electrode. In the electrode holder there was also accommodation for the inductive sensor used for wheel profile measurement.

3.3.4 The Turntable

A turntable has been designed and fabricated to provide rotary motion to the workpiece during grinding of aspheric surfaces. It is capable of rotating at 300 rpm and has an inherent backlash of 4 μm. There were two roller bearings at the front side to take the axial load applied during the grinding process and one ball bearing at the rear side just to take the normal load. CAD drawing of the turntable is shown in figure 3.3. Figure 3.4 (a) and (b) shows picture taken of the turntable from front and rear sides. This table is driven by a lead wire type induction motor manufactured by SPG in Korea. Specification of this motor is attached in table B2 of Appendix B. Initially two angular contact roller bearings were used in one side of the shaft as this type of bearings are very suitable to take axial loads. Later it was found that electrolyte goes in and caused corrosion which jammed the main shaft during grinding. So ultimately these roller bearings were replaced by sealed type ball bearing so that it was protected from corrosion caused by electrolyte going inside.

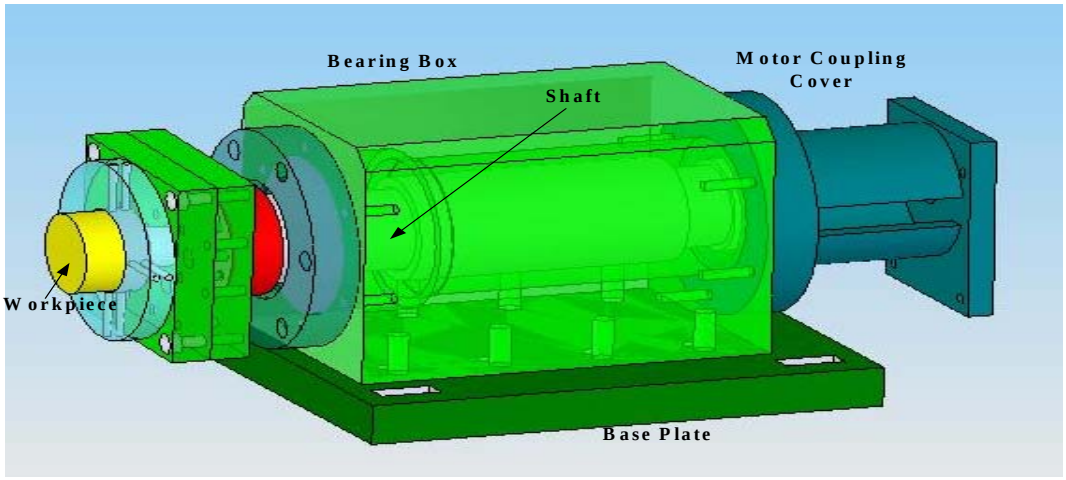

Figure 3.3: CAD drawing of the turn table

(a) (b)

Figure 3.4: picture of the turn table from (a) front and (b) rear side

3.4 DESIGN AND DEVELOPMENT OF AN ON-MACHINE PROFILE MEASUREMENT SYSTEM

One of the most important targets of this study was to design and develop an on-machine measurement system to measure the profile of a free form surface machined in the newly developed ELID grinding machine. An on-machine measurement (OMM) system based on CMM principle has been developed in this study to check the profile of ground surface. Coordinate measuring machines (CMM) have become more and more important in measurements and authentication of dimensional excellence of

manufactured products. In most cases touch trigger probe is an integral part of the CMM to evaluate the position of the axis indicated by the contact of the probe tip. The measurement uncertainty of CMM process is mainly due to the very machine where the probe is attached although the some common errors result from the probe system. However many factors were considered during designing this on-machine measurement system.

3.4.1 Design Considerations

- Select an appropriate probe for measurement.
- Design and fabricate necessary setup for attaching the probe to the machine and interfacing with the machine controller.
- Development of measurement software.

3.4.2 Selection of Appropriate Probe:

Probe is the most important and sophisticated hardware of this measurement system. So selection of a probe which can serve the purpose of measurement as well as cost effective is major concern while designing this on-machine measurement system. The main reason for choosing a touch probe is it's adaptability with the controller installed in this machine. There is a built in function in the controller which stops all the movement of machines translational axis when it receives a signal from the input ports. A touch probe is capable of generating a binary signal and this phenomenon was the main reason for choosing a touch probe for this system.

3.4.3 LP2 probe head

LP2 touch probe manufactured from Renishaw was chosen for many reasons which are such as:

- Short overall length - it is very much Compact in size.
- It is suitable for use on machines with limited Z travel. Adjustable spring force- Trigger forces should generally be kept as low as possible for optimum measurement accuracy. However, heavy stylus assemblies, which are sometimes required for complex measurement tasks, can cause the probe to false trigger under inertial loads. This can be combated by adjusting the probe spring force. Available with High spring force LP2H.
- Available with double diaphragms (DD) - Double diaphragms are used in applications requiring extra sealing.
- All steel construction which protects against sudden impact

Detailed specification of the LP2 touch probe used is given in table B3.

3.4.4 Selection of Stylus

A stylus is that part of the measuring system which makes contact with the component causing the probe mechanism to displace. The generated signal enables a measurement to be taken. Successful gauging depends very much on the ability of the probes stylus to access a feature and then maintain accuracy at the point of contact. Maximum rigidity of the stylus and perfect sphericity of the tip are vital. Several factors were considered while choosing the stylus:

A. Keep the styli short

Probing with the minimum stylus length for your application is the best option. Longer stylus will be susceptible to more bending or deflects resulting lower accuracy.

B. Minimize joints

Joints introduce potential bending and deflection points. Therefore joint should be kept as minimum as possible.

C. Keep the ball as large as possible

There are two reasons for this, Firstly, it maximizes ball/stem clearance thereby reducing the chances for false triggers caused by 'shanking out' on the stylus stem; Secondly, the larger ball reduces the effect of the surface finish of the component being inspected.

Considering above factors one tungsten carbide straight stylus was selected tipped with ruby ball. Ruby is an extremely hard material and hence stylus wear is minimized. It is also of low density, keeping tip mass to a minimum, which avoids unwanted probe triggers caused by machine motion or vibration. Tungsten carbide stems are used for maximizing stiffness with either small stem diameters required for ball diameters of 1 mm and below or lengths up to 50 mm. Detail specification of the stylus is given in the table B4.

3.4.5 Design and development of the probe setup

A CAD drawing and a photograph of the developed OMM are shown in figure 3.5 (a) and (b) respectively. The probe is fixed in probe holder which is attached with plate 3 which is again fixed with plate 1. The L-shaped plate 2 is working as a link between the

piston rod of an air cylinder and LM block pair joined together by plate 1. A single way solenoid valve was used to control the air flow in and out of the cylinder. Necessary voltage required was maintained in the solenoid valve coil by a 24V relay. The piston rod is linked with a block which vertically moves the probe on an LM guide. So it was possible to move the probe up during grinding and save it from hazardous grinding conditions. The reason for using a single way solenoid valve is that it automatically retracts while machine is stopped for any emergency purpose and thereby safeguard the sensitive touch probe from any unwanted collusion with other machine components.

An FS1i female socket was used for holding the probe head. The stylus is attached to a tripod structure inside the probe head, whose three cylindrical arms are supported by three pairs of crossed cylinders. An electric current normally flows through the tripod arms and cylinders. When the stylus moves, one of the contacts breaks and a binary signal comes out from the probe head. The female socket powered from a 24 V supply contains an integral interface which converts this binary signal into a voltage free solid state relay(SSR) output for transmitting to the CNC machine controller. The internal structure of the probe is such that during undisturbed state signal continuously comes out from the output. A simple circuit was fabricated to reverse this output signal so the exact moment of contact between the stylus tip and surface to be measured was made possible. With the built in interface and compact size of Φ25mm×L45.5 mm these sockets eliminate the need for a separate interface within the control cabinet and thus make the installation simpler. Detail of this female socket is given in table B5. Output from this

female socket is connected to the input 1 of the I/O board of the machine controller through the circuit mentioned before for reversing the signal.

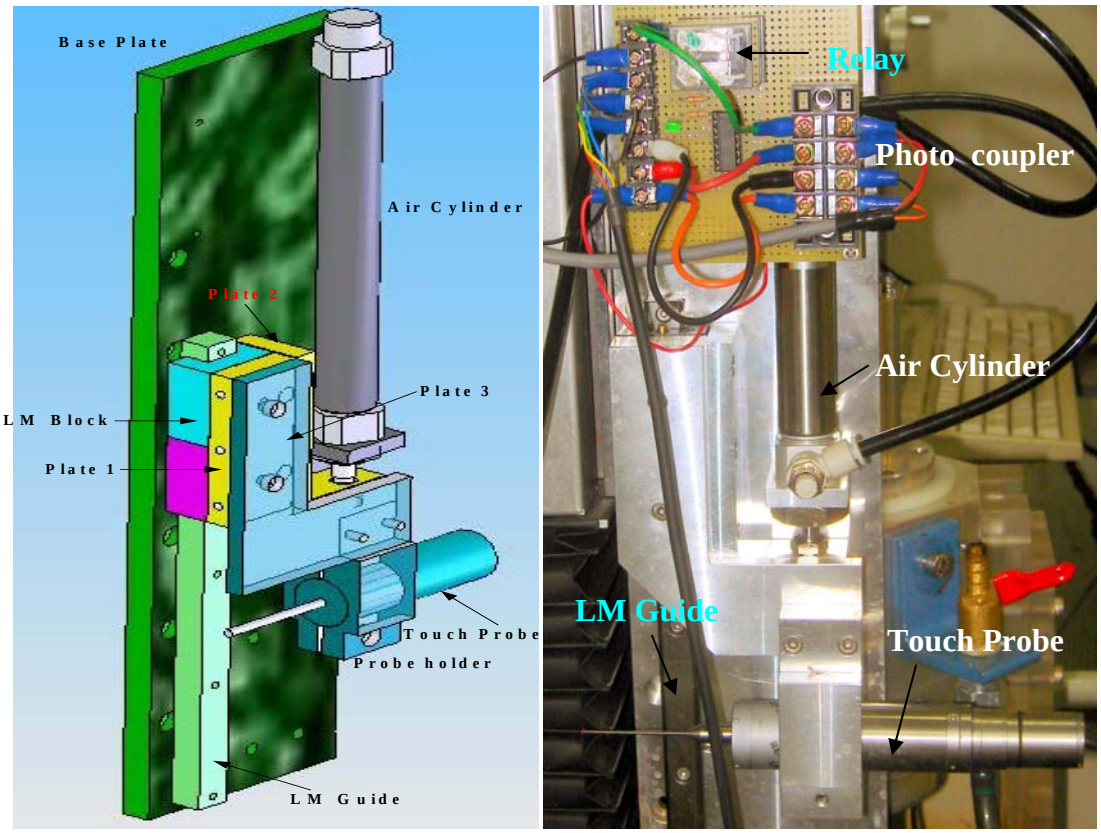

(a) (b)

Figure 3.5: (a) CAD Drawing and (b) Photograph of the on-machine profile measurement system

3.4.6 Measurement Software

The graphical user interface (GUI) was developed using BORLAND C++ builder to measure the co-ordinates on a ground surface without removing the workpiece form the machine. Buttons for standard operation of a CNC machine such as movement of all the translational axes, MPG (Manual Pulse Generator) operation control were there. Options are given to control the speed of the axis movement and speed of the spindle rotation.

Two more buttons were there to activate the air cylinder and vertically move the touch probe. A schematic diagram of the GUI developed to perform the coordinate measurement using the developed system is shown in figure 3.6.

After manually setting the starting point for scanning it will ask the user for the values of X limit and Z limit for defining the maximum area of the measurement. It is also possible to set the resolution in X and Z direction. After setting all the parameters the system will start the measurement right after pushing the Scan button. All these scanned points are then used to calculate the profile of the ground surface.

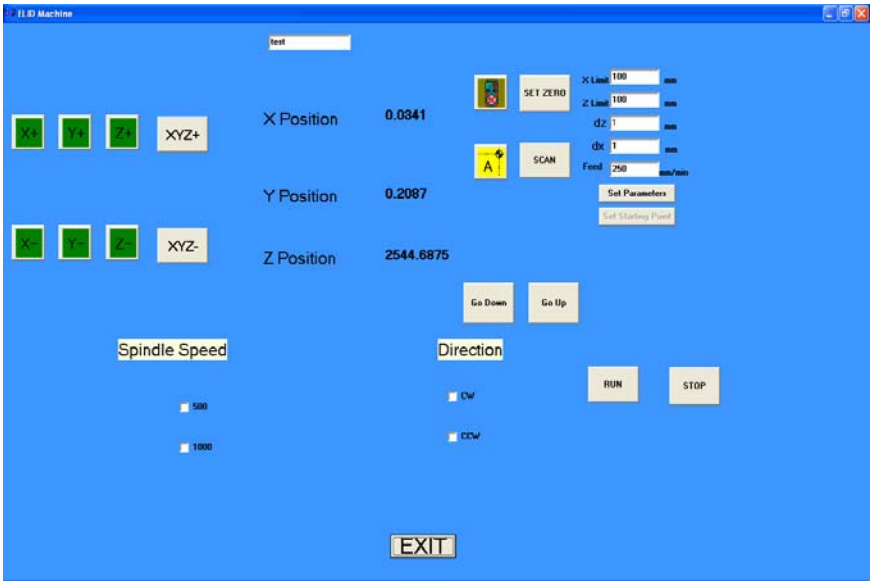

Figure 3.6: GUI of the Measurement software

3.4.7 Working Principle of the Measurement System

The basic operation of this system is based upon the CMM principle. Like many other CMM machines it uses a touch probe to measure the coordinates on the aspheric surface that has just been machined. During grinding process the probe is placed up from the wheel and workpiece, so that electrolyte can not splash on it. When measurement is

needed to be done grinding is stopped and probe is lowered down by the air-cylinder. The touch probe is then taken at a position which is such a distance apart from the surface that the stylus tip will not touch the workpiece while it moves over the workpiece in X, Z direction. Then this point is set as the origin of the measurement system. After this the probe moves in the Y direction until it touches the machined surface. As soon as it touches the surface a signal is sent to controller which stops all the movement of the machine axes. Then another query is sent to the controller to know the real position of the machine which is converted into coordinate of the contact point of the stylus tip with the aspheric ground surface. A graphical user interface (GUI) was developed for measuring the co-ordinates where it is possible to set the maximum measuring length in X and Z direction and also the grid size of the measurement. After setting all the parameters the system will start the measurement right after pushing the Scan button. All these scanned points are then fed into a MATLAB program where radius of each circle consisting those arrays of points are calculated and the biggest radius will be the radius of the generated aspheric surface. Figure 3.7 showed one position of the touch probe while measuring the coordinates.

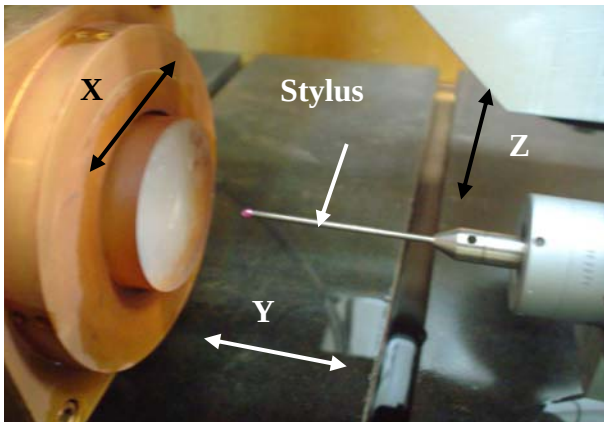

Figure 3.7: Working Principles of the measurement system

3.5 In Process Wheel Monitoring System

Previously Katsushi Furutani et al. used pressure sensor for measuring in process wheel topography. This method is actually affected by the turbulence flow of the cutting fluid and also electromagnetic properties of the workpiece material. In this paper an inductive sensor KEYENCE EX305, EX-201 was used to measure the profile of the grinding wheel. It actually gives the value the gap between probe tip and edge of the wheel. Using these gap values the diameter of the grinding wheel can be calculated. The measured profile can be used to calculate the tool wear, which later will be needed for machining compensation of the grinding process considering the change in diameter of the wheel due to its wear. Study has shown that the accuracy of the sensor is effected by wet condition so all the measurements of the wheel profile was taken after making the wheel as dry as possible. Specification of this inductive sensor is given in table B7 and resolution of the sensor is 0.04 mm according to the information given in the table. This resolution is sufficient for calculating the wheel wear with the duration of machining followed in this study.

3.5.1 Working principle of the system

Working principle of the wheel profile measurement system is shown in figure 3.8. After setting the grinding wheel in the spindle the sensor was set in a position at a distance apart from the edge of the grinding wheel. Output of the sensor was recorded at this moment. This gap value will act as a reference in calculating wheel radius. After grinding for several hours these gap values were recorded at many points equally spaced around circumference of the wheel. If gap value at any point is larger than the previous

value it means that wheel has more worn at that point and wheel radius is calculated at that point by subtracting the difference of the two gaps from the original wheel radius.

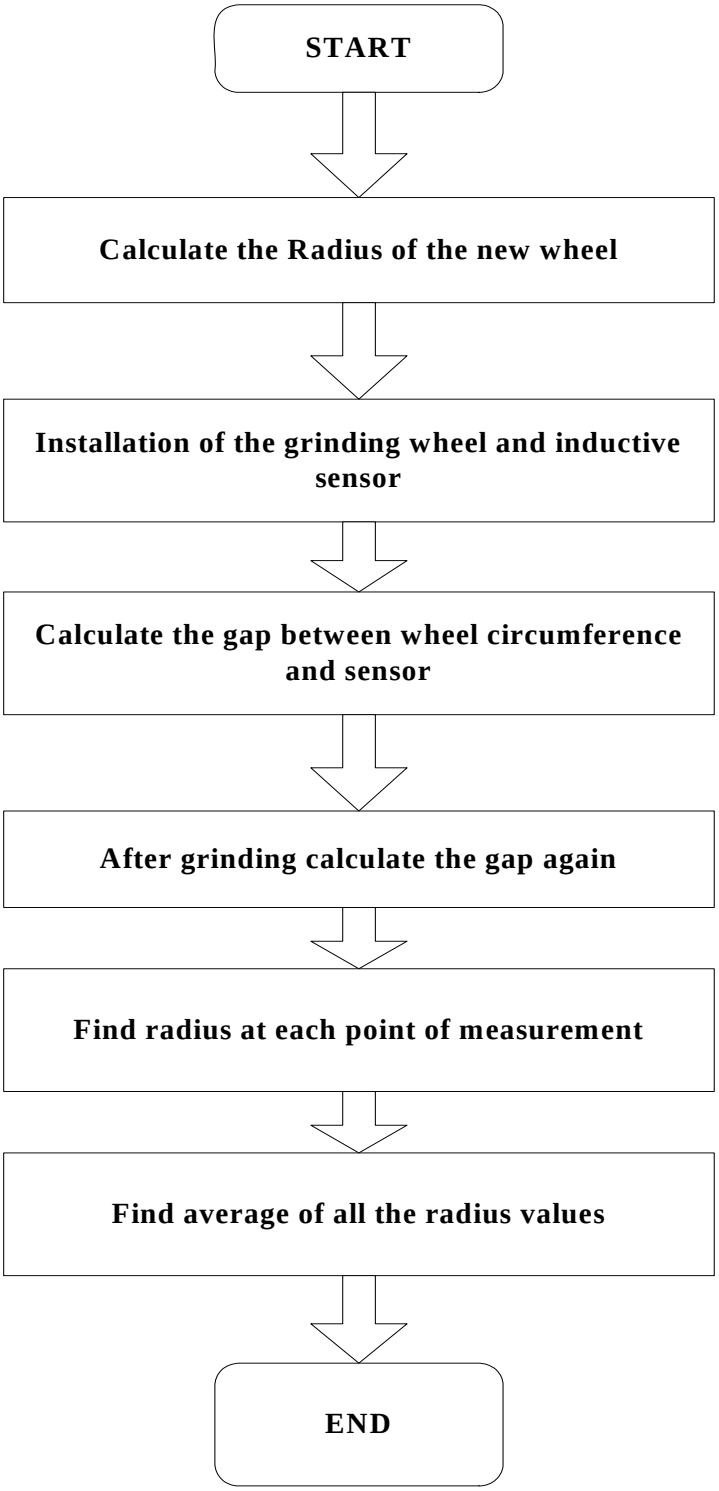

Figure 3.8: Flow chart to calculate wheel radius from in-process wheel monitoring system

On the other hand if the gap is smaller than the reference gap it means wheel is larger at that particular point. Wheel radius at that point is calculated by adding the gap difference to the original wheel diameter. Later overall wheel radius is calculated by averaging all the radius value calculated at points uniformly distributed around the circumference of the wheel.

CHAPTER FOUR
EXPERIMENTAL SETUPS

4.1 INTRODUCTION

In this study, experiments were carried out basically to investigate the performance of the developed systems and justify their application in generating free form surface. The newly developed on-machine measurement system was attached to the new machine and experiments were carried out. Experiments were carried out in workshop 2 and MicroFabrication Lab. Other measurements on the finished workpiece were carried out with the state of the art equipments located in the Advanced Manufacturing Lab (AML). This chapter describes the details of the experimental setup and the experimental procedures used in this study.

4.2 DETAILS OF EXPERIMENTAL SETUP

A photograph of the experimental setups used in this study is shown in figure 4.1. This experimental setup mainly comprises of the following members:

- A 4 Axis CNC machine tool
- A turn-table
- An ELID power supply
- An on-machine profile measurement system
- On-machine wheel wear measurement mechanism.

Several influential members of this experimental setup will be discussed in the following sections.

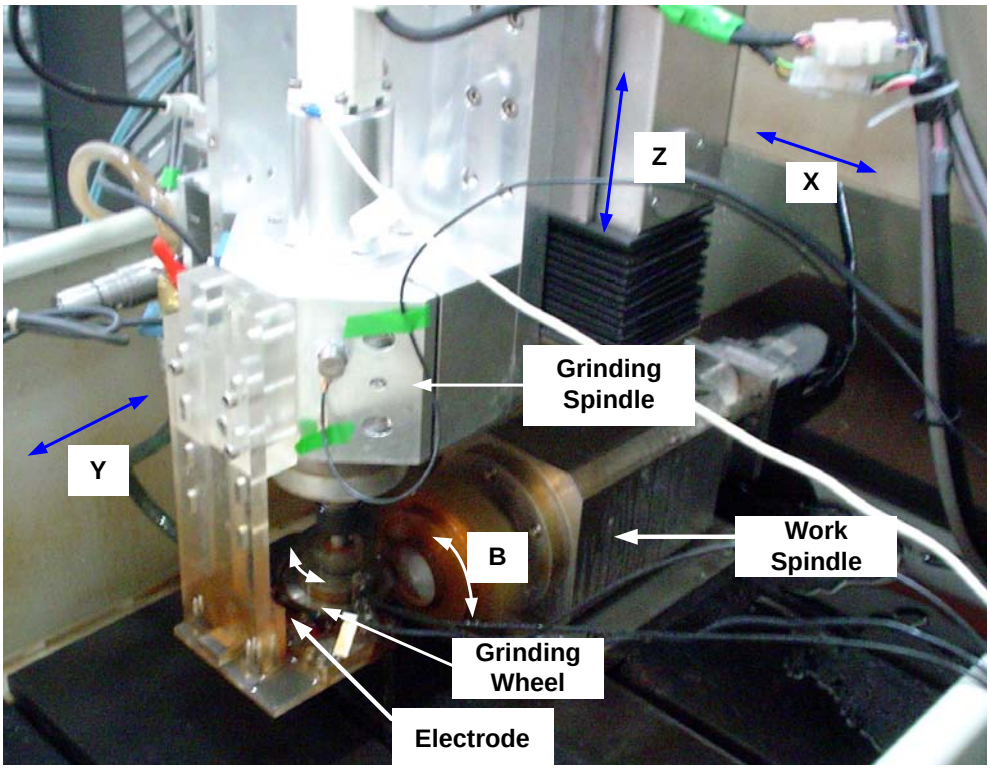

Figure 4.1: ELID Grinding system developed

4.2.1 CNC ELID Grinding Machine

The developed CNC ELID grinding machine was used for machining the workpiece to generate free form surfaces mainly on hard and brittle materials. Details of this CNC grinding machine tool are:

- Size of the machine tool: 150 cm (l) X 102 cm (w) X 145 cm (h)
- Size of the control Cabinet: 75 cm (l) X 65 cm (w) X 215 cm (h)
- Each axis has optical linear scale with the resolution of 0.1 μm, and full closed feedback control ensured accuracy of sub-micron.

4.2.2 Workpiece material

Glass has been chosen as the workpiece material mainly for two reasons. Firstly, glass is very much suitable material for ultraprecision grinding as it is uniform without any grain, slip or twin. Secondly, the BK7 glass is a widely used material in optical industries due to its excellent properties such as transparency, homogeneity, isotropy, hardness, durability and high chemical resistance. However in this study first spherical surface was machined on Perspex to inspect the performance of the systems developed. Photographs of the glass and Perspex workpiece used in this study are showed in figure 4.2.

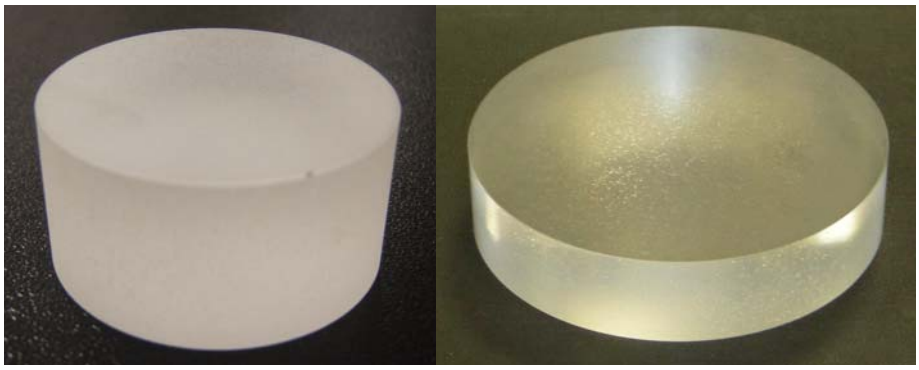

(a) (b)

Figure 4.2: workpiece used for grinding (a) BK7 glass (b) Perspex

4.2.3 Mounting of workpiece:

Proper mounting of the workpiece in the machine is more important in this case due to rotation of the workpiece given by the turntable. The Perspex specimen was attached by a thin layer of wax (NX-AF/EW: NEXSYS) applied to the circular step on the mounting plate to ensure the rotational symmetry of the workpiece. The adhesive chosen have superior strength to withstand high force and temperature during grinding. But it was not possible to ensure perfect uniformity of the thin layer of wax applied

which resulted into the inclination of workpiece surface. Another problem was due to difference in cooling rate cracks appeared on the workpiece dismantling the workpiece from the plate. To overcome these problems, later experiments were carried out with glass piece clamped on the mounting plate with screws from four sides. The CAD drawing of the modified workpiece mounting mechanism is shown in figure 4.3.

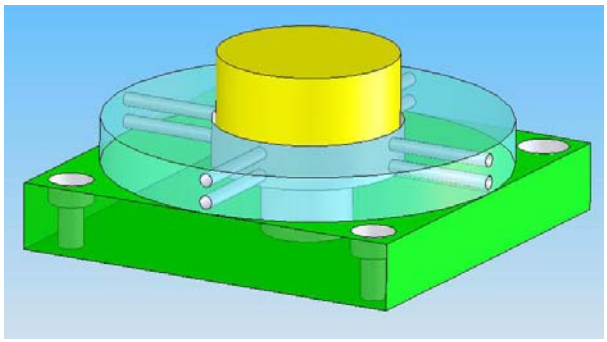

Figure 4.3: CAD drawing of workpiece mounted on the mounting plate

4.2.4 Grinding wheels

Grinding wheels consists of abrasive grains known as grits, and the bonding material to hold the grits together. Diamond or CBN grits are generally preferred as super-abrasive grit material for their extreme hardness suitable for machining hard and brittle material. In the ELID grinding wheels the bonding-materials used are cast iron, cast iron-cobalt, copper, bronze and copper-resin bonded. Experiments that were carried out in this study with Cast Iron bonded Diamond (CIB-D) grinding wheel.

4.2.5 Electrolyte

The electrolyte GC-7 supplied from NEXSYS Corporation, Japan, was diluted with water in the ratio of 1:50 and made alkaline to use as an electrolyte and coolant for

the experiments. This electrolyte is stored in a tank of 30 liter capacity and pumped from there using a pump of 1/8 HP capacity.

4.2.6 Pre-dressing

Pre-dressing is the process of producing grain protrusion on the grinding wheel active-surface by eroding the bonding material around the grits. The grinding wheel was mounted on the machine spindle, the electrode was placed in position and the gap was adjusted to 100 – 300 μm. Then the electrolysis was started with the supply of electrolyte and current. The pre-dressing conditions used in this study were 100 V, 1A, ON-time – 30 µs and OFF-time 5 µs and spindle rotation of 1000 rpm. Pre-dressing was performed for 30 minutes before starting the grinding process.

4.2.7 Wear measurement of the grinding wheel

Wear measurement is a very vital part of this study. Wheel diameter needs to be updated from time to time for changing the tool path in the NC Program and compensate the tool wear during grinding. The developed on machine measurement system was used for measuring the wheel wear. A digital slide calipers was also used for the measurement of grinding wheel diameter at regular interval during grinding.

4.3 STANDARD MEASURING EQUIPMENT USED

4.3.1 Mahr OMS-400 CMM Machine

Basic structure of this machine is like a CNC machine equipped with three types of sensor/camera- touch probe, leaser triangulation and video camera. Most common

applications of this machine are dimensional measurement, profile measurement; angularity and digitizing. Of the three types of sensor touch probe was used to measure the ground surface profile based on CMM principle. Machine path was programmed to read coordinates of the several uniformly distributed points on the ground surface from which later radius of the profile was calculated using some built-in software comes with the machine. Due to the higher reliability this profile radius was taken as reference for calculating accuracy of the machined part. Both repeatability and resolution of this machine is 0.1 inch operating temperature range is 63-73 ºF. A photograph of the CMM machine used in this study is shown in figure 4.4.

Figure 4.4: Picture of the Mahr OMS-400 CMM Machine

4.3.2 Mitutoyo FORMTRACER

A Mitutoyo FORMTRACER CS-500 equipped with a cone type stylus was used to measure the surface roughness and form accuracy of the free form surface

machined during the experiments. Higher traversing capacity of the stylus in Z direction enables this machine to be used for measuring surface roughness of the aspheric surface. This machine was also used to check the radius of the ground surface profile. A photograph of the Mitotoyo FORMTRACER used in this study is shown in figure 4.5. Detail specifications of this machine are given in table 4.1.

Figure 4.5: Picture of the Mitutoyo FORMTRACER CS-500

Table 4.1: Specification of the Mitutoyo machine

Resolution	0.00625µm (X); 0.0020µm (Z)
Measurement Pitch	0.002 mm
Roughness pitch	0.0005 mm
Cut off	0.025

4.3.3 Taylor Hobson Machine:

The Taylor Hobson Talysurf Model 120 stylus profiler is a precision metrology instrument used for measuring surface texture is shown in figure 4.6. All measurement

functions are programmable and extensive analysis functions are available in the Windows-based measurement/analysis software. This machine was used to measure the surface roughness of the ground surface in this study. Due t its range limitation it is mainly suitable for measuring surface roughness of flat surface where probe range in z direction is not big. Even though this machine was used for measuring surface roughness due to its better reliability taking shorter sampling length to keep the stylus range within limit. Detail specifications of this machine are given in table 4.2.

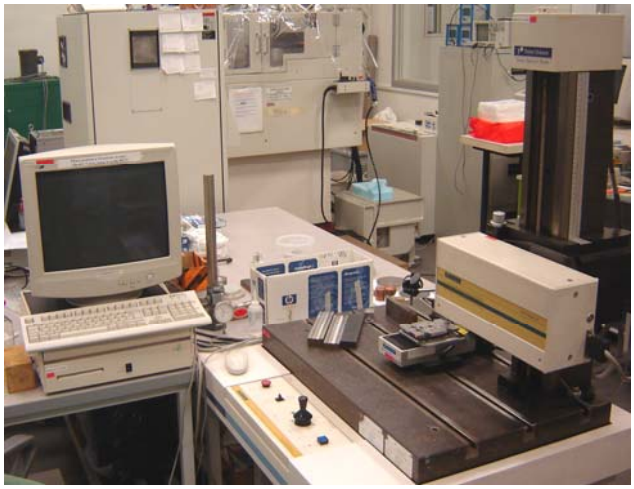

Figure 4.6: Picture of the Taylor Hobson Talysurf Model 120

Table 4.2: Specification of the Taylor Hobson machine

Traverse speeds	1.0 mm / sec and 0.5 mm/sec (+/- 5%)
Column traverse	450 mm
Stylus range	6 mm range
Stylus tip radius	1.5 - 2.5 micron
Stylus force over full range	0.7 - 1.0 mN

4.3.4 Keyence VHX digital Optical Microscope:

A Keyence VHX 100 Digital Optical Microscope Shown in figure 4.7 was used to observe different characteristics of the free form surface ground in the new machine. It is equipped with an 18 Mega Pixel, high resolution digital Camera and aided by lenses with maximum of 3000X magnifying capacity. It comprises of two main units- one to take the image and another one is the software part to analyze this image taken and generate different kinds of information needed.

Figure 4.7: Picture of the Keyence VHX Microscope

4.3.5 Jeol JSM-5500 Scanning Electron Microscope:

A scanning electron microscope (SEM), Jeol JSM-5500 was used to investigate the surface integrity of the ground surface. The BK7 glass piece was observed under SEM but due to size constrains the Perspex workpiece was not inspectable under SEM. Maximum value of magnification and accelerating voltage that can be attained by the microscope are 50000X and 30 KV. A photograph of the SEM used in this study is shown in figure 4.8.

Figure 4.8: A Photograph of Jeol JSM-5500 Scanning Electron Microscope

4.4 DETAIL EXPERIMENTAL PROCEDURES

4.4.1 Generation of tool path

By definition a lens or mirror surface that has been altered from spherical in order to reduce optical aberrations is called aspheric surface. The generic equation used to describe optical surface shapes takes the form of the determination of the sag Z of the surface at any point h, where h is the height from the optical axis.

$$Z = \frac{ch^2}{1+\sqrt{1-\varepsilon c^2 h^2}} + A_4 h^4 + A_6 h^6 + A_8 h^8 + A_{10} h^{10} + \ldots\ldots\ldots$$

Where, c is the curvature of the base sphere (at the optical axis or vertex), ε is the conic constant or measure of conic shape of the surface and A_4, A_6, A_8, A_{10}, A_{12} are the aspheric coefficients. This conic constant ε is also related to other common ways of describing a conic section such as:

ε = (1 + k) = (1 – e2); here k is the conic coefficient and e is the eccentricity

Clearly, if A4 = A6 = A8 = A10 = A12 etc. = 0 then the surface described is a pure conic. If also e = 0 then ε = 1 and the equation simplifies to that describing a sphere.

In this study aspheric surface was generated while the grinding wheel rotating at a high speed approaches from outer diameter to the center of the rotating workpiece. Orientation of grinding wheel and workpiece during machining is shown in Figure 4.9. Ideally the grinding wheel should be moved in such a way that there will always be single point contact between the wheel and workpiece. To accomplish this grinding wheel radius (QN), radius of the workpiece (AN) and radius of the spherical surface to be machined (ON) were taken into consideration. At the beginning the grinding wheel was in contact with the workpiece surface to set the origin of the working coordinate system as shown in the figure 4.10.

If C is the position of the spindle axis at the starting point than from simple geometry the location of the spindle can be calculated in a way that wheel will always be touching the workpiece at point N which is also the end point of the circular arc. In this way it is possible to calculate all the points of the tool path so that the wheel will be touching the workpiece only at one point.

X coordinate of the point Q, $OP = \dfrac{OM \times OQ}{ON}$

Y coordinates of the point Q, $CB = OC - OB$,

Here $OC = OQ = ON + NQ$ and $OB = PQ = \sqrt{OQ \times OQ - OP \times OP}$

Value of OM was reduced form its maximum value which is equal to radius of the workpiece (AN) to zero and contact point N moves from the edge of the workpiece

toward its center. In this way different values of X, Y coordinate along the tool path was calculated.

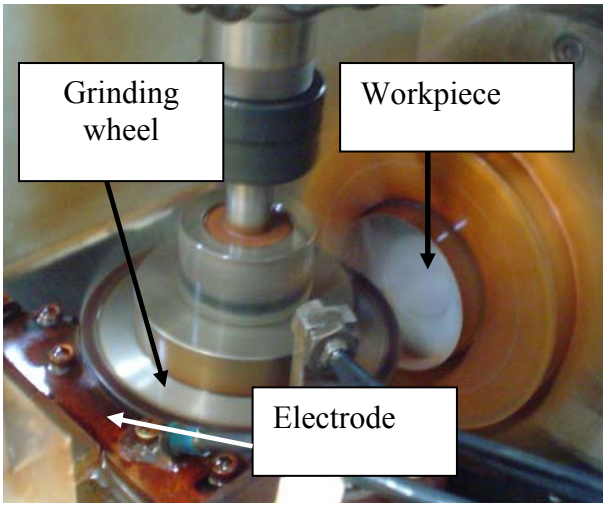

Figure 4.9: Workpiece-wheel orientation during machining

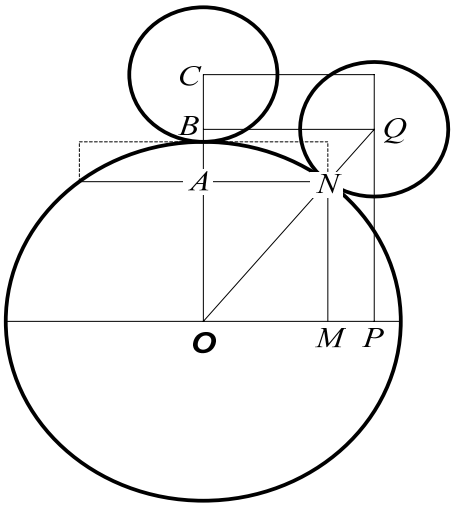

Figure 4.10: Schematic of the tool path

4.4.2 Experimental procedure

A complete schematic of the experimental setup is shown in figure 4.11. Positive and negative terminals of the power supply are connected to the spindle and electrode

respectively. Signal from the probe is directly fed into the controller for reading the coordinates.

All the values of experimental parameters are mentioned in Table 4.3. Different steps of the experiment are shown in figure 4.12. First of all the workpiece was fixed with the base plate in a way such that center of the workpiece coincides with the rotational axis of the turn-table. The turntable was attached on the machine after checking the alignment properly. In the mean time coordinates of the tool path was generated for grinding an aspheric surface with desired profile radius. NC program was prepared to grind aspheric surface on hard and brittle material with this tool path. Economic grinding was aimed by rough grinding with a lower grade grinding wheel followed by finishing with higher grade of grinding wheel to optimize the wheel wear [E. S. Lee et al]. Machining was stopped to measure the wheel diameter and NC program was updated to compensate the wheel wear. This process was repeated several times until the whole surface was machined and an aspheric surface was generated.

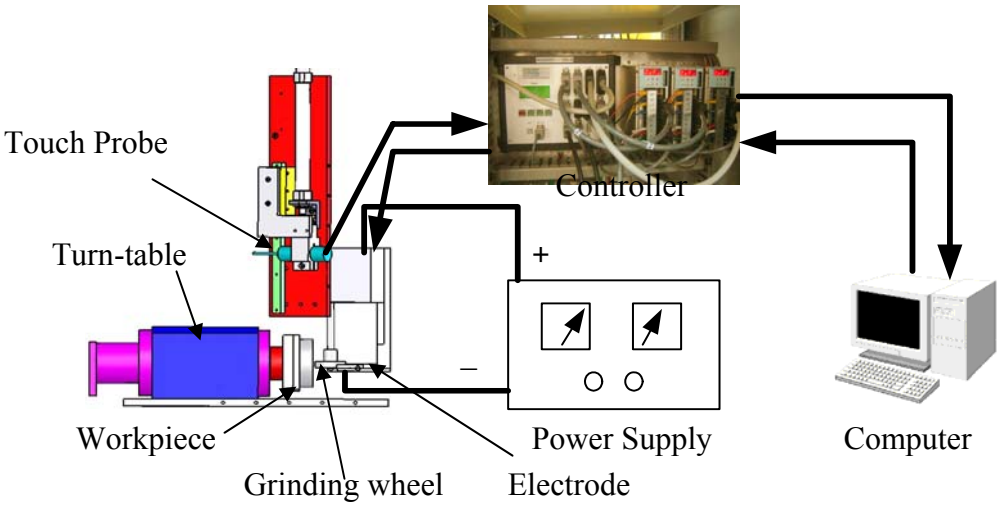

Figure 4.11: Schematic illustration of the experimental setup

Table 4.3: Parameters of the experiment

Workpiece	BK7 Glass (Φ40 mm); Perspex (Φ80 mm)	
Desired Profile diameter	200 mm(Glass); 500 mm (Perspex)	
Grinding wheel	CIB-D; Φ75 mm thickness 3 mm #1200 (Roughing); #4000 (Finishing)	
Electrode	Injection type Copper Electrode	
Electrolyte	CG-7 (Diluted in water with a ratio of 15:1)	
Applied current and voltage	0.3 A and 100V	
Spindle speed	1500 RPM	
Workpiece Speed	275 RPM	
T_{ON} and T_{OFF}	30µs and 5 µs	
Feed Rate	Perspex	Glass
	250-500 mm/min	300 mm/min (Roughing) 50 mm/min (Finishing)
Depth of cut	Perspex	Glass
	5 µm (Roughing) 3 µm (Finishing)	2 µm (Roughing) 1 µm (Finishing)

This whole cycle of profile and wheel radius measurement, error calculation and NC program generation continues until error value reaches under a tolerable limit. During finishing operation low feed speed and depth of cut were maintained to improve surface quality and minimize the level of subsurface cracks.

Finally the finished part was removed form the machine to measure the profile radius in the CMM machine. Surface roughness was measured in the Taylor-Hobson form Talysurf-120 machine and informations required for calculating form accuracy was gathered from the Mitutoyo CS-500 form tracer. Ground surface quality of the finished workpiece was observed under SEM and Keyence optical microscope.

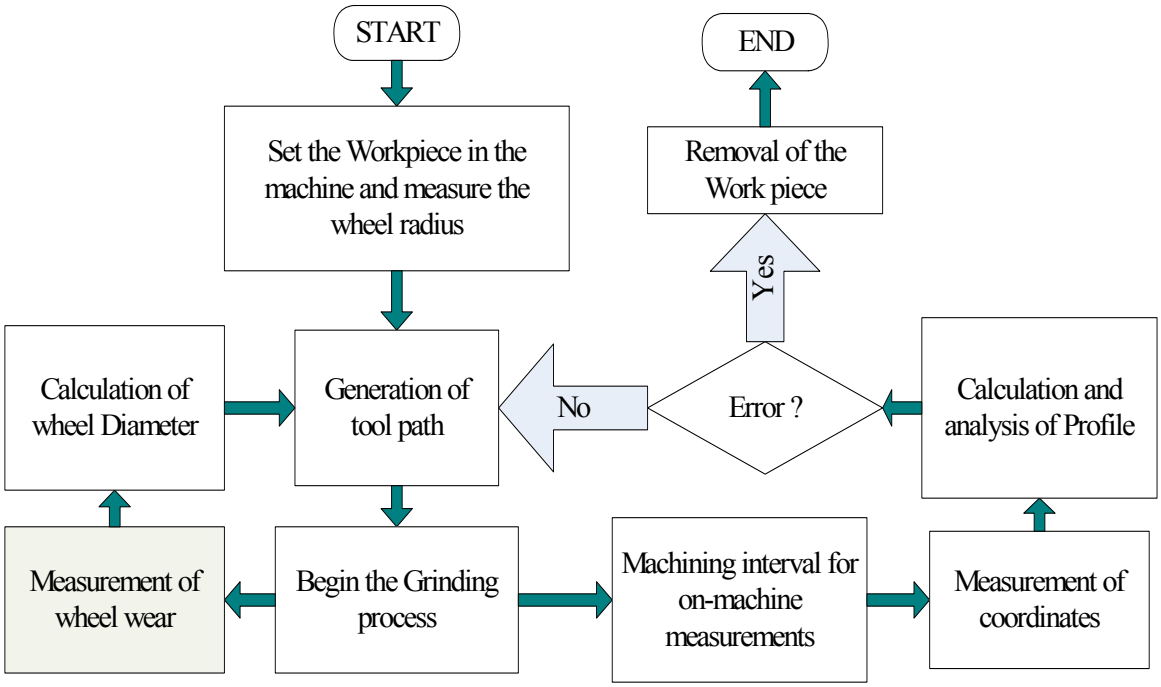

Figure 4.12: Block diagram of the experimental process

In order to observe the influence of software compensation over the dimensional accuracy of the machined part, another BK7 workpiece was machined in the same setup but without software compensation to achieve a profile of 100 mm radius. In this case ground surface profile or wheel wear was not measured during the grinding process to

update the tool path in the NC program. Afterwards profile of the finished workpiece was measured in the CMM machine.

CHAPTER FIVE

RESULTS AND DISCUSSION

5.1 INTRODUCTION:

The primary objective of this study was to machine free form surfaces on hard and brittle materials by ELID grinding process. To ensure this first of all a CNC ELID grinding machine was developed. Then on-machine measurement systems were developed to check the ground surface profile and wheel wear. All of these newly developed systems were scrutinized by performing some standard tests. One Perspex workpiece was machined to see how capable is the new system in generating free form surfaces on hard and brittle material. Later one BK7 workpiece was machined to generate an aspheric surface on it with software compensation. Another BK7 workpiece was machined under the same condition without software compensation to study the effect of software compensation in dimensional accuracy of the machined surface. In this chapter all the results have been summarized and discussed in details.

5.2 REPEATABILITY AND ACCURACY OF THE MACHINE TOOL

Repeatability and accuracy are the two most important parameters for determining efficient use of a machine tool. Since the machine tool used in this study was a newly developed machine these parameters need to be determined by some standard experiments.

Repeatability of the CNC ELID grinding machine was tested by following some standard testing manuals using laser interferometer. The laser interferometer reading for all the three translations namely X, Y and Z are given in figure 5.1(a), 5.1(b) and figure 5.1(c) respectively.

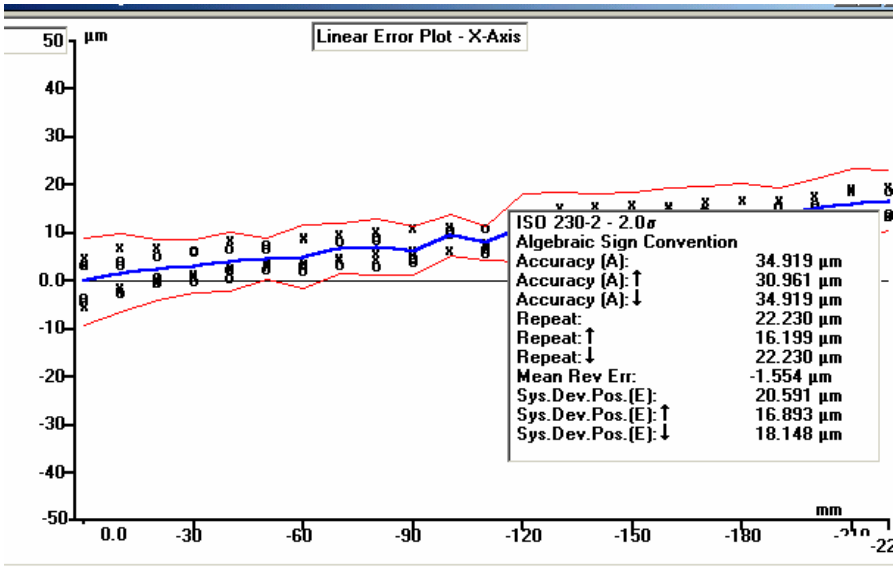

Figure 5.1(a): Interferometer reading for X axis

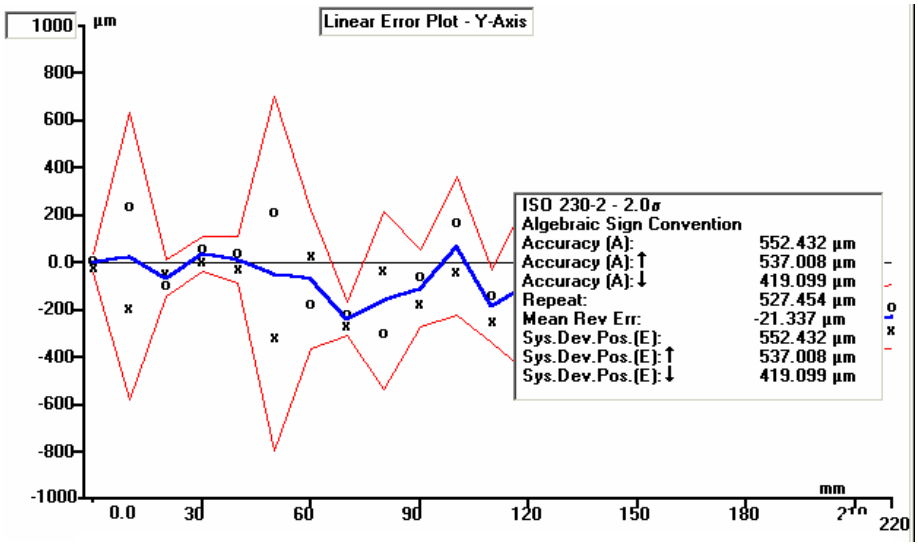

Figure 5.1(b): Interferometer reading for Y axis

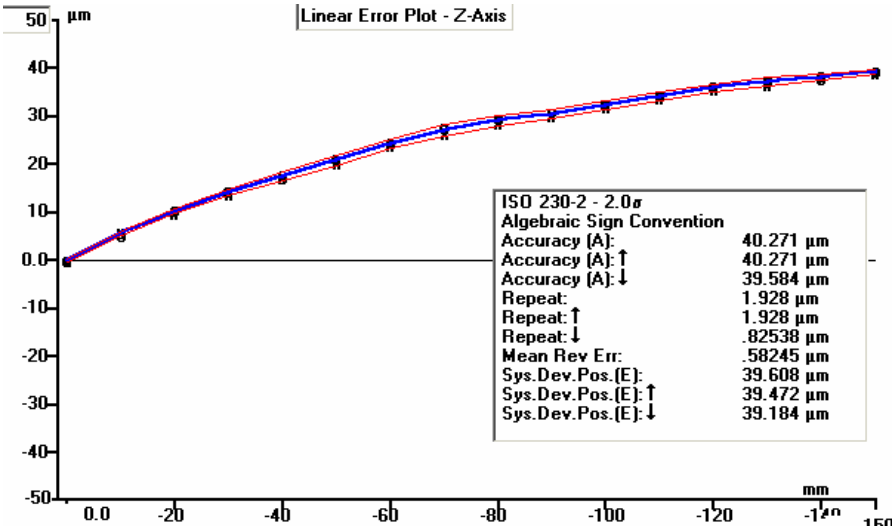

Figure 5.1(c): Interferometer reading for Z axis

From the above figures it is readable that repeatability of X, Y and Z axes are 35 µm, 500 µm and 2 µm respectively. The reason behind the lower repeatability of the X and Y axis is mainly due to the inaccuracy incorporated with the motors used in these two axes. The motors used in X and Y axes did not have sufficient power to hold the axes very rigidly resulting a lower control rigidity. This lower control rigidity resulted lower accuracy of these two axes. Whereas the motor used in the Z axis was different from the motors used in the other two translational axes and had enough power to ensure better control rigidity resulting to a more accurate Z axis.

5.3 REPEATABILITY AND ACCURACY OF THE OMM SYSTEM

The ground surface profile was measured with the newly developed on-machine measurement system and when the value reaches under tolerable limit it was removed from the machine. This is self explanatory of the high significance of the new

on-machine measurement. If the measurement system is not able to produce a reliable value the ultimate decision of stopping the machining process would be taken based on wrong information. If it gives a value that is too much bigger than the actual value it will lead to the extra machining time as well as wastage of other resources. Too much lower value than the actual value will also create problem in achieving the desired profile radius. And once removed from the machine means the machining coordinates will be reset again which is very much detrimental for the overall accuracy of the process. So reliability of the on-machine measurement system is one of the most important factors for ensuring greater accuracy of the machined surface profile.

In order to check the repeatability of the system a commercially manufactured convex lens was taken and measured for a grid size of 10 mm×1 mm at a feed speed of 250 mm/min. The coordinates measured were then used to calculate the radius of the surface measured during machining and this process was repeated five times for the same setup. The same lens was also measured five times in a CMM machine to find out the radius. Different values of the radius were then plotted as shown in the figure 5.2

The average of the five values measured in the developed OMM system and CMM were 74.9714 mm and 72.0233 mm respectively. One probable reason for the better repeatability of the CMM machine is that in case of CMM machine points measured were same for all the five cases but for the newly developed system the points were not same for all the five cases. Because in the new system the reference point of measurement needs to be setup before each individual set of measurement.

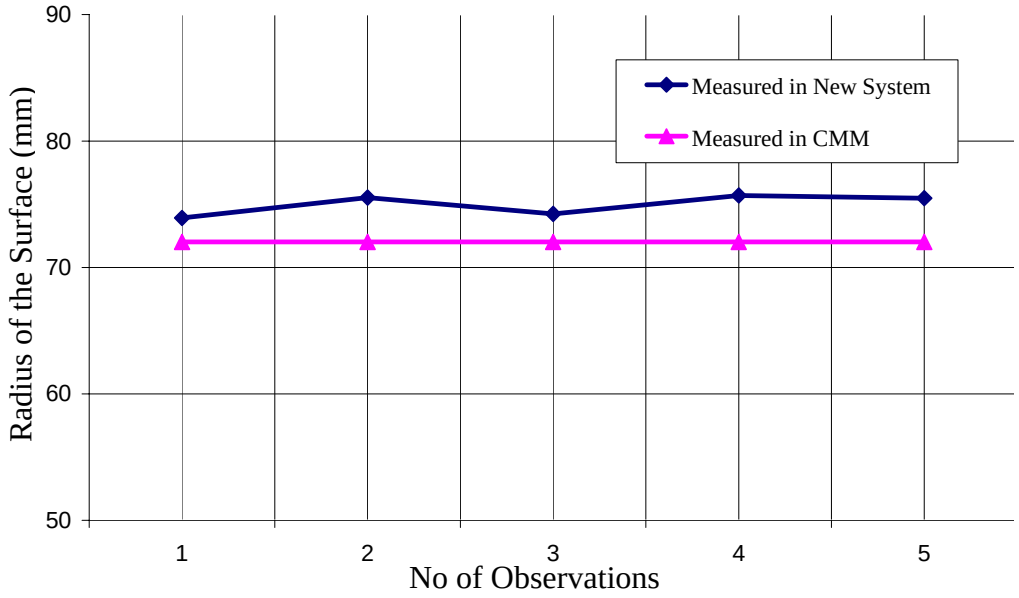

Figure 5.2: Repeatability and accuracy test of the measurement system

5.4 WHEEL WEAR MEASUREMENT

Wheel diameter is a major factor in determining the tool path for grinding an aspheric surface. Oxide layer forms in ELID grinding and breaks away from the wheel which causes a significant wear. So it is very important to measure the wheel diameter during machining and change the tool path at regular intervals.

In this study wheel diameter was measured several times during machining of the BK7 glass piece and coordinates were calculated based on this change of wheel diameter. Table 5.1 contains wheel radius and corresponding maximum value of Y coordinate calculated at different time interval during grinding of the workpiece. This newly calculated coordinates were then fed into the tool path of NC program to compensate the wheel wear.

While machining the Perspex workpiece tool path was generated taking the wheel radius as 37.5 mm and with that value the maximum removal depth was 3.2207 mm for achieving a surface with a radius of 250 mm where diameter of the workpiece was 80 mm. In this way after machining for several hours when the tool was almost in contact with the workpiece for the whole path the machining was stopped and profile of the wheel as well as ground surface was calculated.

Table 5.1: Change in tool path with wheel diameter change

Grinding Wheel	Time (Hour)	Measured Wheel Radius (mm)	Maximum Y coordinate value (mm)
CIB-D #1200	0	37.500	2.7781
	2	37.499	2.7780
	9	37.382	2.7757
	16	37.196	2.7865
	23	36.983	2.7676
CIB-D #4000	0	35. 531	2.7383

It can be seen from the figure 5.3 that the wheel radius has been changed into 37.4 mm. So new tool path was generated based on the new diameter of the worn wheel. Now the maximum depth of material removal was 3.6706mm. From Figure 5.3 it can be safely said that the wear of the wheel is quite substantial. This may be due to the grinding force which breaks the oxide layer formed during ELID and consequently facilitates the breaking of the layer enhancing the wear rate of the wheel

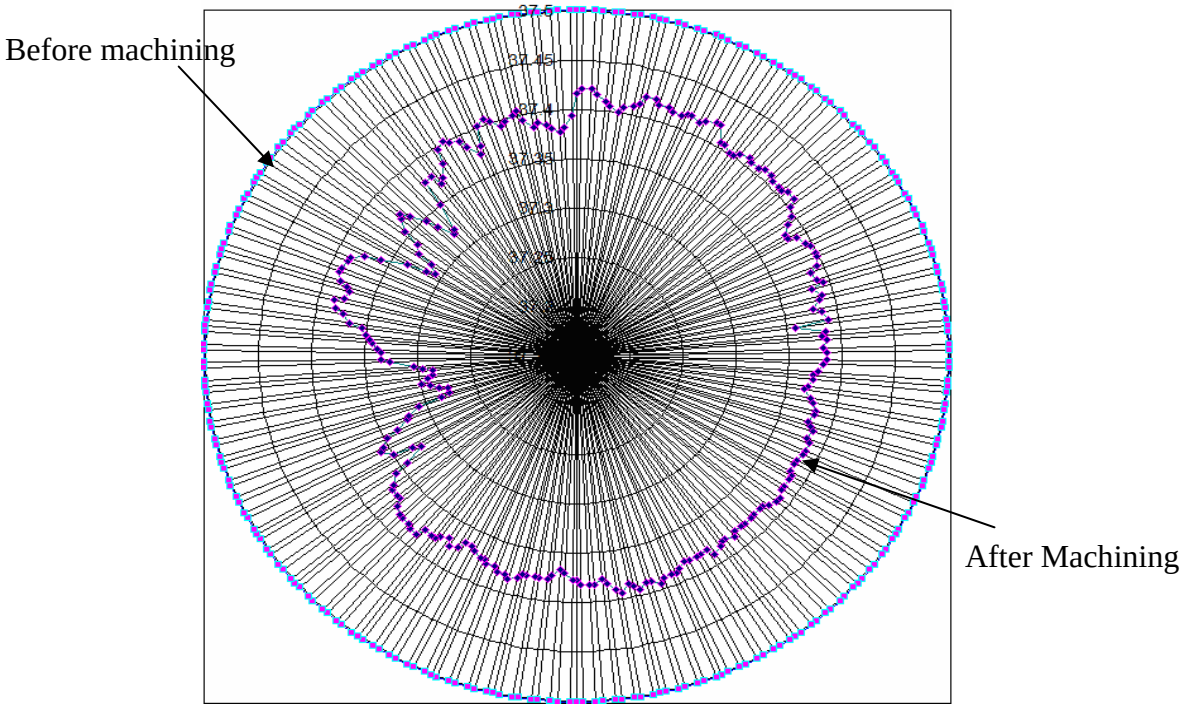

Figure 5.3: Wheel profile Measurement

Another reason for this higher wheel wear is due to another extra force exerted due to the rotation of the workpiece. The rotational movement of the workpiece exerts an extra force component on the weak oxide layer of the grinding wheel created by electrolysis. This force facilitates the break away of this layer from the grinding wheel and resulted into higher wheel wear. Due to this wheel wear grinding wheel diameter changes and tool path in the NC program was also updated to compensate this change in wheel diameter due to wear.

5.5 GROUND SURFACE PROFILE MEASUREMENT BY OMM SYSTEM

Ground surface profiles machined on the workpieces were measured by the on-machine measurement system. As described before firstly the starting point was set and other measurement parameters were selected. The coordinates measured were used for finding out the radius of the ground surface profile.

5.5.1 Profile measurement of Perspex workpiece

Before removing the workpiece from the machine the ground surface profile was measured and radius found was 254.35 mm. after setting the starting point of measurement the grid size was chosen 12mm×1mm at a feed speed of 200 mm/sec. The size of the measured area was 60mm×20mm. Co-ordinates measured in this were plotted using MATLAB as shown in figure 5.4.

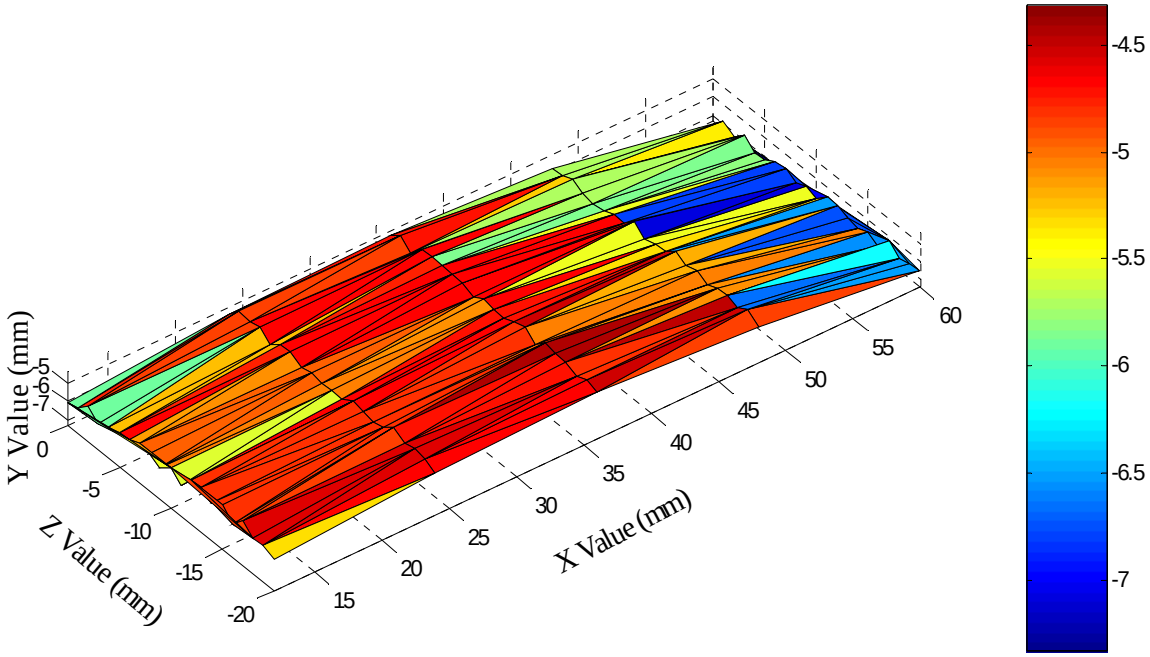

Figure 5.4: Surface Generated using the measured coordinates

Coordinates measured by the new system were saved in a text file which was later tabulated to study whether the system is working according to the set parameters or not. The coordinate values are shown in tabulated form in table 5.2. From this table it is quite clear that the system measured each point at a distance of 12 mm apart from each other while measuring in X direction and lowered down 1mm in Z direction after each line of measurement in X direction. And measurement was stopped after covering the area

60mm×20mm. So from the value showed in Table 5.2 it can be clearly stated that the OMM is working according to set parameter while measuring the coordinates on the ground surface. Figure 5.4 also shows that the OMM system is able to detect the variation of surface profile

Table 5.2: Coordinates measured by the OMM system

Serial No	X	Y	Z	Serial No	X	Y	Z
1	-0.0001	6.7255	0.0001	17	23.999	4.7625	-3
2	11.9971	6.0335	0.0001	18	35.9995	4.6668	-3
3	24.0006	5.4398	0.0001	19	48.0004	5.7058	-3
4	36.0009	5.1988	0.0001	20	59.9976	6.7047	-3
5	48.0023	5.7142	0.0001	21	12.0013	5.5977	-3.9996
6	11.9995	5.9173	-0.9995	22	24.0018	5.213	-4
7	23.999	4.772	-1.0001	23	36.0011	4.5735	-4.0001
8	35.999	4.73	-1	24	48.0011	5.8575	-4
9	48.0001	5.6885	-1	25	59.9976	7.2203	-4
10	59.9852	6.8637	-1	26	12.0035	5.393	-4.9995
11	12.0115	5.3982	-1.9995	27	24.0035	4.7562	-5
12	24.008	4.8753	-2	28	36.0052	4.5563	-5
13	36.0138	5.3042	-2	29	47.9997	5.7942	-5
14	48.0145	5.3972	-2	30	60.0032	7.186	-5
15	60.015	7.3362	-2	31	11.9984	5.4035	-5.9995
16	11.9995	5.8765	-2.9996	32	23.9996	4.6878	-6.0001

Serial No	X	Y	Z	Serial No	X	Y	Z
33	36.0013	4.6795	-6	55	59.9984	6.9955	-10
34	48.0008	5.542	-6	56	11.9988	5.5803	-10.9996
35	60.0009	6.8575	-6	57	24.0017	5.036	-11
36	11.9996	5.1475	-6.9995	58	35.9905	4.74	-11
37	24.0008	5.1005	-7	59	48	5.329	-11
38	36.0012	4.669	-7	60	60.0005	6.484	-11
39	47.9994	5.526	-7	61	11.998	4.8667	-11.9996
40	60.0005	6.799	-7	62	23.9996	4.6905	-12
41	11.9999	5.2415	-7.9996	63	36.0029	4.541	-12
42	23.9985	4.963	-8	64	48.001	4.8405	-12
43	36.0008	4.9425	-8	65	59.9917	6.4873	-12
44	47.9994	4.9772	-8	66	12.0064	4.8273	-12.9995
45	59.9951	7.071	-8	67	24.0089	4.7885	-13
46	12.0045	5.5255	-8.9996	68	36.009	4.355	-13
47	24.0034	5.0953	-9	69	48.009	5.1883	-13
48	36.0041	4.673	-9	70	60.0047	6.7293	-13
49	48.0046	5.5072	-9	71	12.0018	5.1682	-13.9995
50	60.0052	6.8327	-9	72	23.9986	4.956	-14
51	11.9971	5.08	-9.9995	73	36.0032	4.8693	-14
52	23.9996	5.055	-10	74	48.0066	5.0355	-14
53	35.9907	4.719	-10	75	60.003	6.9115	-14
54	48.001	5.388	-10	76	11.999	4.808	-14.9994

Serial No	X	Y	Z	Serial No	X	Y	Z
77	23.9919	4.8022	-15.0001	92	24.0007	4.5635	-18
78	36.0023	4.317	-15	93	35.9989	4.7973	-18.0001
79	48.0029	5.2745	-15	94	47.9956	5.1935	-18
80	60.0011	6.576	-15	95	59.9995	6.6545	-18
81	11.9983	5.487	-15.9996	96	11.9982	5.3092	-18.9993
82	23.9983	4.3158	-16	97	24.0007	4.6852	-19.0001
83	35.9961	4.425	-16.0001	98	35.9998	4.5465	-19
84	48.0008	5.0953	-16	99	48.0003	4.843	-19
85	59.989	6.8848	-16	100	60.0005	6.4932	-19
86	12.009	4.8505	-16.9995	101	12.0006	5.554	-19.9996
87	24.0109	4.725	-17.0001	102	23.997	5.0328	-20
88	36.0061	4.4727	-17	103	36.0015	4.7393	-20
89	48.0112	4.9893	-17.0001	104	47.9997	5.3285	-20
90	60.0116	6.199	-17	105	59.9986	6.458	-20
91	11.9977	5.3732	-17.9996				

5.5.2 Profile measurement of BK7 Glass workpiece

Profile of the aspheric surface machined on BK7 glass was measured in the same manner used in case of Perspex workpiece. After setting the starting point, an area of 30mm×8mm was selected in the middle region of the machined surface to read the

coordinates. Grid size of 5mm×1mm was chosen for measurement and using the coordinates measured a surface plotted as shown in figure 5.5.

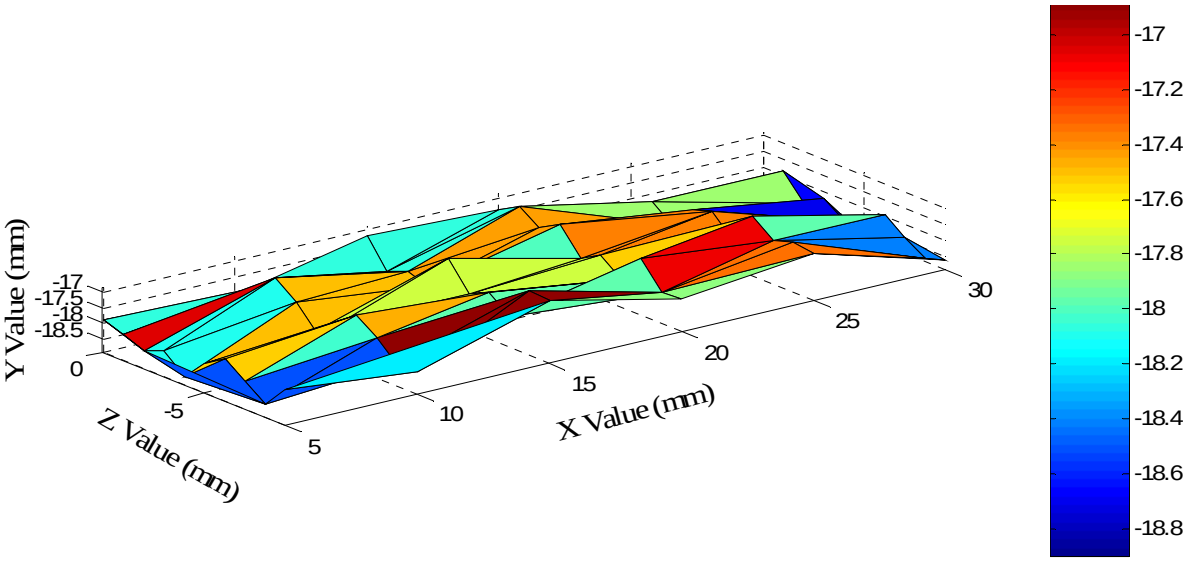

Figure 5.5: Surface Generated by the points measured in the OMM system

5.5.3 Analysis of different profile values measured

Perspex workpiece was machined mainly to check the overall performance of the newly developed system in grinding free form surfaces. The finished workpiece was measured in some other standard profile measurement system. Different profile values got from different system is shown in table 5.3.

Table 5.3: Comparison between different measuring methods

Measuring method	Radius of the lens(mm)
On machine measurement system	254.35
CMM Machine	257.30
Profile measurement system	244.74

From these three profile radius measured by three different system it is quite obvious that there is a variation in the measured values. Since the principle used in the CMM machine was very more similar with the principle used in the new system, value measured in the CMM as the reference in this study. Thus error in the measured value was 3.78%. There are many reasons for this variation in the measured values.

The stylus tip radius used for CMM, Profile Measurement Machine and the new system were 2 mm and 4 mm. One of the probable reasons for the variation of the radius measured in different machine is the different radius of the stylus tip. Based on experimental results Marek Dobosz et al have explained that there is always an offset exists between the actual contact point of the stylus tip with the triggering surface and of the coordinate measured. Inaccuracy incorporated for this offset is higher in case of measuring spherical surface than in case of flat surface. He also concluded that this offset changes with stylus tip radius and affects the overall accuracy of the measurement.

In case of the CMM machine points chosen were mainly at the middle region of the surface which is comparatively less machined. Less machined in another words means more flat i.e. higher profile radius. This may be one of the reasons for higher radius measured by the CMM machine.

In the Mitutoyo profile measurement machine the probe tip needed to be set up right at the middle of the surface so that it can give the biggest diameter which is the profile radius of the whole surface. In this case the setup was done manually and may be

the line of measurement was not right at the middle of the surface. As a result it gave a profile radius lower than the value measured by the other two systems.

5.6 PROFILE ACCURACY

Analysis of profile accuracy was one of the prime objectives of this study. Profile accuracy can be directly measured using the Mitutoyo form tracer CS-500 machine.

5.6.1 Profile accuracy of the Perspex workpiece

Profile accuracy of the Perspex workpiece was measured with the Mitutoyo machine with a sampling length and evaluation length of 2.5 mm and 12.5 mm respectively which were chosen as the maximum possible lengths in that specific measurement so that the profile accuracy calculated would be more accurate. Figure 5.6 showed the evaluation profile measured in Mitutoyo machine. The profile accuracy found was 2.985 µm.

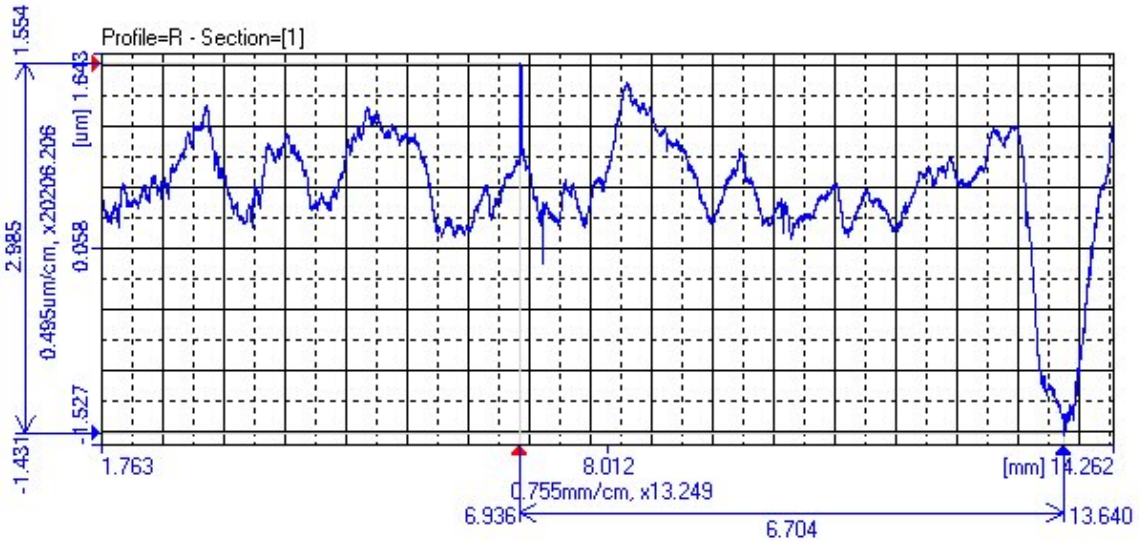

Figure 5.6: Profile accuracy of the Perspex workpiece measured in Mitutoyo machine

5.6.2 Profile accuracy of the BK7 workpiece

Profile accuracy of the BK7 workpiece was measured with the Mitutoyo machine with a sampling length and evaluation length of 2.5 mm and 12.5 mm respectively. Figure 5.7 showed the evaluation profile measured in Mitutoyo machine. The profile accuracy found was 1.234 µm.

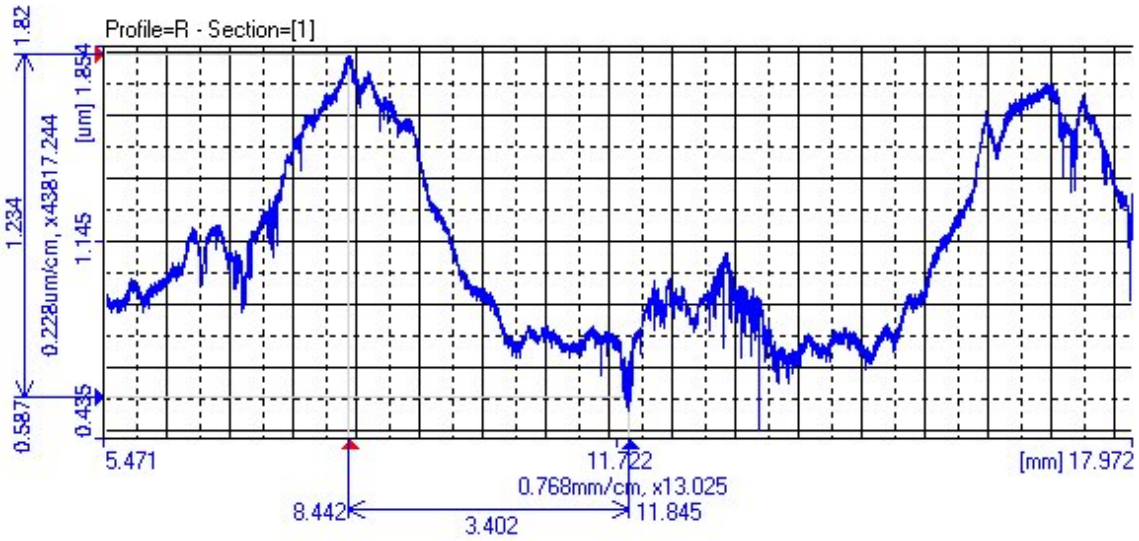

Figure 5.7: Profile accuracy of the BK7 Workpiece (With software compensation) measured in Mitutoyo form tracer

Another BK7 glass piece was machined without any software compensation to study the effect of software compensation in grinding aspheric surfaces on hard and brittle material. Profile accuracy of this workpiece was measured with the Mitutoyo machine with a sampling length and evaluation length of 0.25 mm and 1.25 mm respectively which were chosen to ensure higher accuracy described in the previous section. Figure 5.8 showed the evaluation profile measured in Mitutoyo machine. The profile accuracy found was 2.250 µm.

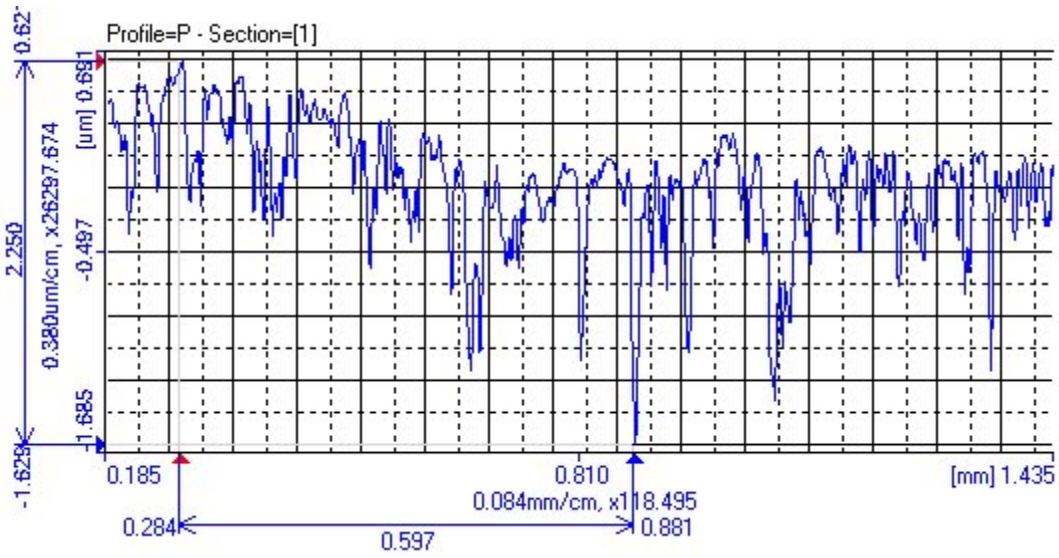

Figure 5.8: Profile accuracy of the BK7 workpiece (without software compensation) measured in Mitutoyo form tracer

From the above three figures it is quite clear that profile accuracy of the BK7 glass piece is higher than the other two values. One of the major reasons behind this higher accuracy is may be due to the frequent update of tool path according to the wheel diameter change due to wear. But there are too many variables in case of Perspex and BK7 glass piece to make any form comment that only software compensation was the reason for the more accurate profile. Likewise workpiece material as well as size of the workpiece and desired profile radius was different.

5.6.3 Effect of Software Compensation on Profile Accuracy

After removing from the machine profile radius of the both BK7 workpieces machined with and without software compensation was measured in the MAHR OMS 400 CMM machine and values obtained are shown in table 5.4. Taking the value measured in the CMM machine as the actual profile radius, error was calculated and

shown in this table. Error values showed in the table are the evidence for improvement of profile accuracy in the finished workpiece ground with software compensation.

Table 5.4: Table for different profile radius measured

Experimental condition	Desired Profile Radius	Achieved profile radius (mm)	Error (%)
With software Compensation	100	99.96	0.04
Without software Compensation	100	98.17	2.83

In this case all the parameters of the ELID grinding were similar. Unlike the case of Perspex both the workpiece material and dimension was same. Lastly the desired profile value was also same for both workpieces. Only significant difference was the compensation of tool path in the NC program due to wheel wear. This is popularly known as software compensation. Only due to this software compensation error in the surface profile was reduced from 2.83% to 0.04%.

5.7 FORM ACCURACY

In order to verify the form accuracy of the ground surface the finished part was set in the Mitutoyo CS-500 form tracer. Then coordinates along a line right at the middle of the surface was measured. It also gave the coordinate of the center of the circle which fits those points. Using these available values radius was calculated at each point using the standard formula of circle.

5.7.1 Form Accuracy BK7 Glass piece

The BK7 glass piece machined with software compensation was removed from the machine and coordinates were measured in the Mitutoyo machine as described before. Measurements were done for a sampling length of 30 mm which was maximum allowable sampling length for the 40 mm diameter workpiece capturing the whole profile and pitch size of 0.01 mm which was the smallest pitch size to ensure better measurement accuracy. The chosen speed of measurement was 0.2 mm/sec. Finally all those radius values at each point along the line of measurement were plotted versus desired value of the radius as shown in figure 5.9. From this figure overall form inaccuracy of the ground surface calculated was 15.35µm P-V.

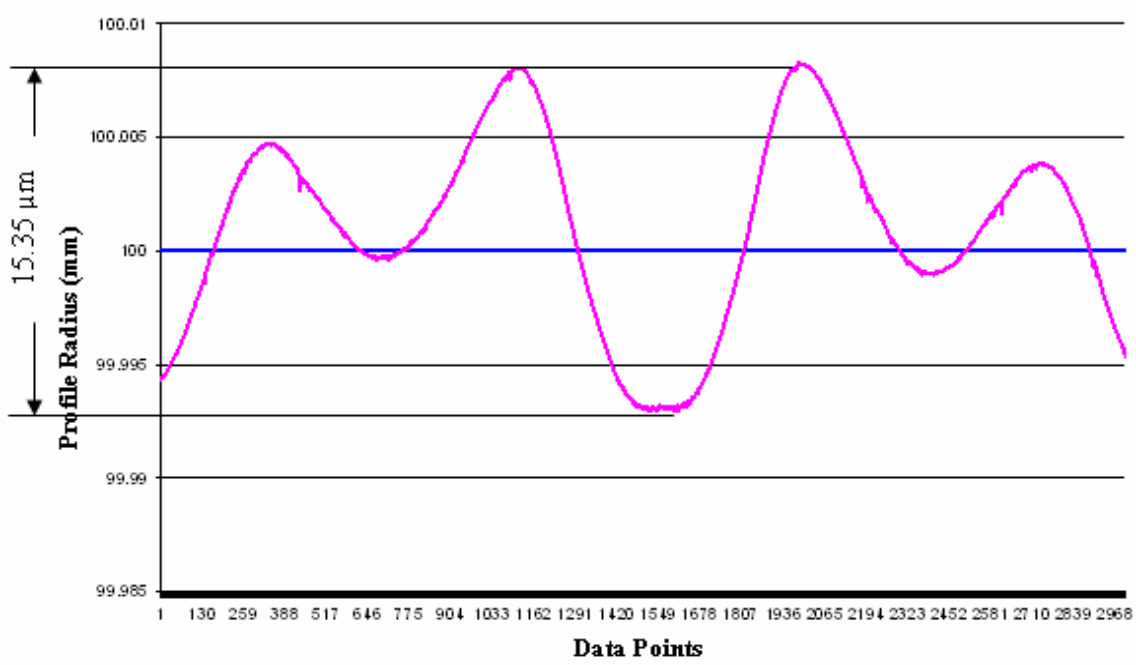

Figure 5.9: Form accuracy of the BK7 lens (with software compensation) using Mitutoyo CS-500

Another BK7 glass piece machined without software compensation was also measured in the Mitutoyo machine to get the coordinates along a line on the surface after removing from the machine. Coordinates were measured for a sampling length and pitch size of 20 mm and 0.05 mm respectively. The speed of measurement was 0.2 mm/sec. Finally all those radius values at each point along the line of measurement were plotted versus overall radius of the surface as shown in figure 5.10. From this figure overall form inaccuracy of the ground surface calculated was 30.4µm P-V.

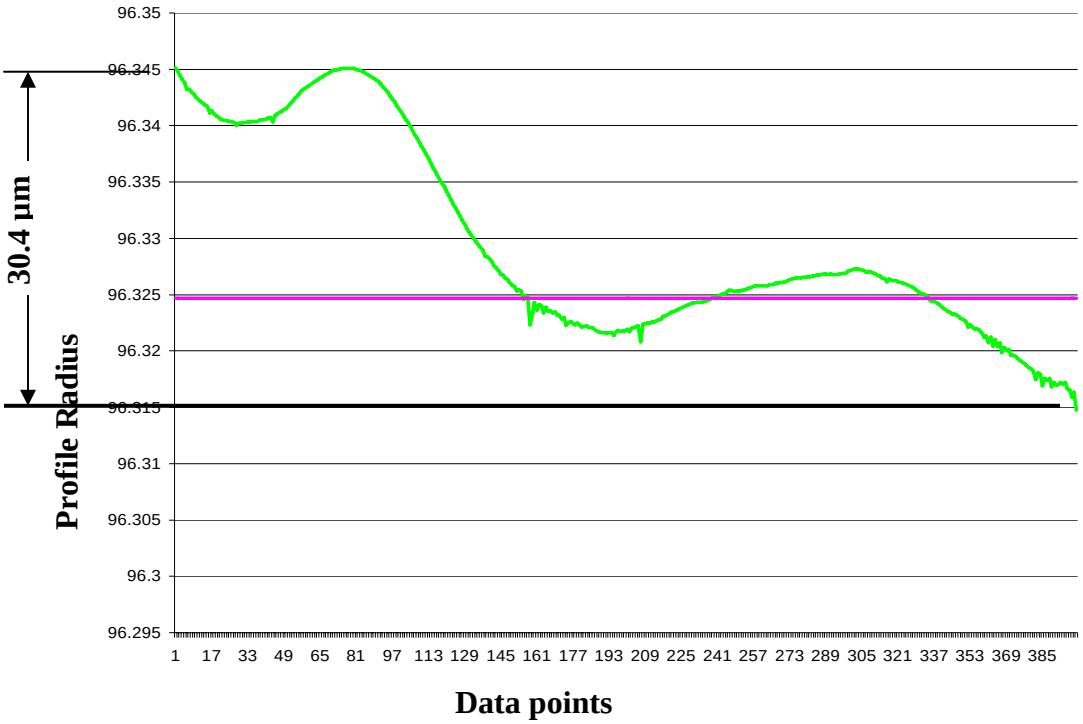

Figure 5.10: Form accuracy of the BK7 lens (without software compensation) using Mitutoyo CS-500

5.7.2 Form Accuracy of Perspex Workpiece

The Perspex workpiece was measured in the Mitutoyo machine to get the coordinates along a line on the surface after removing from the machine. Coordinates were measured for a sampling length and pitch size of 60 mm and 0.05 mm respectively.

The speed of measurement was 0.2 mm/sec. Finally all those radius values at each point along the line of measurement were plotted versus overall radius of the surface as shown in figure 5.11. From this figure overall form inaccuracy of the ground surface calculated was 142.7µm P-V. Since number of data points were too many for handling in Excel only part of the data points was used for plotting the graph.

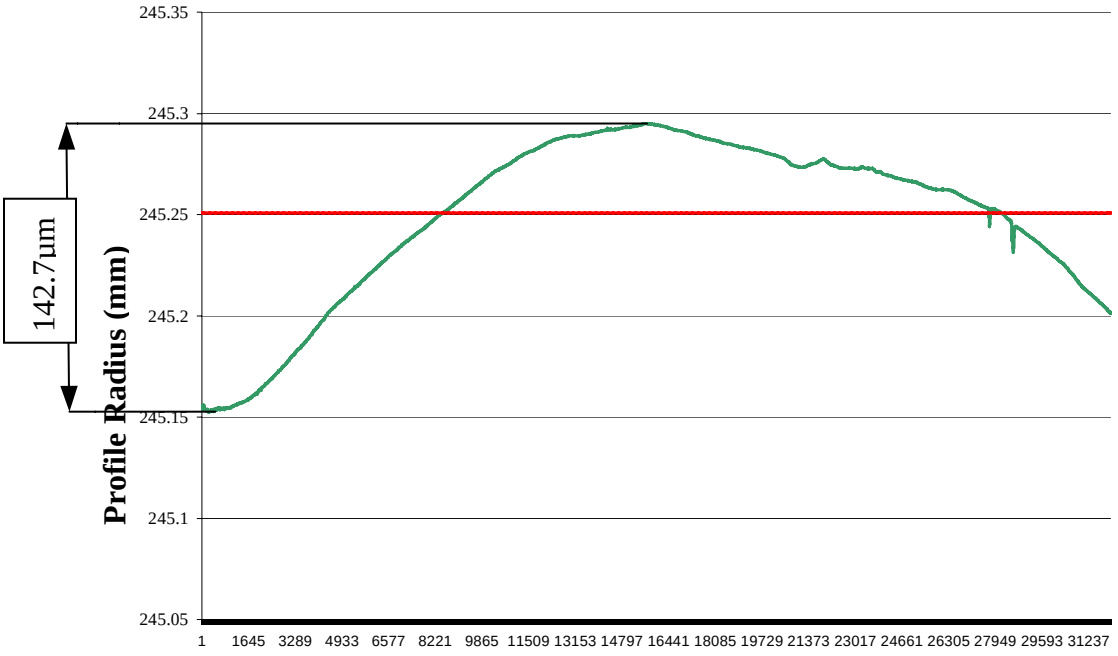

Figure 5.11: Form accuracy of the Perspex lens using Mitutoyo CS-500

5.7.3 Analysis of different form accuracy

From the nature of the above figures it is evident that form accuracy was also higher in case of workpiece machined with software compensation. In case of Perspex workpiece although the NC program was updated several times it was not enough as the wheel wear was higher due to the bigger size of the workpiece.

There is a similarity in all the three graphs plotted in the above three figures. From which one conclusion can be readily made that is error inherited from the machine itself. One of the crucial reasons behind this from inaccuracy is the positional inaccuracy of the machine tool.

Another factor which may affect the form accuracy is the shape of the grinding wheel cutting edge. For making a very precise spherical form, contact between workpiece and grinding wheel should be single point contact at a time like rolling. Application of a grinding wheel with round shaped working surface is one probable way to ensure this point contact.

The generated grinding force is larger on the outward surface than on the inward one. This is because the workpiece speed is higher on the outward surface [E. S. Lee et al.]. This is another factor for form inaccuracy.

5.8 MEASUREMENT OF SURFACE ROUGHNESS

Surface roughness is one of the major parameters studied in grinding. Specifically in grinding aspheric lenses for optoelectronics industry surface roughness is major concern of the manufacturers. In this study surface roughness of the finished products were measured in some standard instruments available in the lab.

5.8.1 Surface roughness of Perspex

Surface roughness of the Perspex workpiece was measured in the Mitutoyo profile measurement machine. All the measurement conditions are mentioned in table 5.5. Evaluation profile from this measurement is shown in figure 5.12. Different values of

roughness of the Perspex workpiece measured from this machine were Ra = 0.049 µm, Ry = 0.297 µm and Rt = 0.653 µm.

Table 5.5: Measurement condition

Stylus speed	0.2 mm/sec
Pitch	0.01 mm
Sampling length	10 mm
Stylus radius compensation	0.005 mm

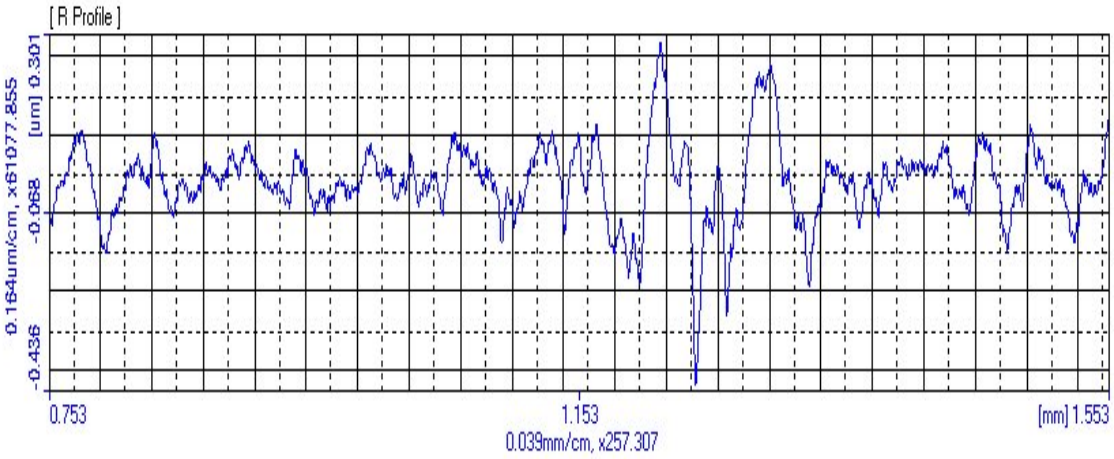

Figure 5.12: Surface Roughness of the Perspex workpiece

5.8.2 Surface Roughness of BK 7 Workpiece

Roughness of the final ground surface of the BK7 glass piece machined with software compensation was measured using Taylor-Hobson form Talysurf-120 machine as it is more reliable. During this measurement stylus speed was 0.05mm/sec. different roughness value measured are mentioned in table 5.6.

Table 5.6: Measured value of Roughness

Parameter	Value
Ra	0.0183 µm
Rt	0.4210 µm
Rz	0.1119 µm
Rc	0.1004 µm

Evaluation profile is shown in figure 5.13. From the figure itself it is quite obvious that the surface generated is quite uniform in nature. Surface roughness was also measured in AFM machine and values obtained are: Ra = 9.54 nm, P-V 44.48 nm and Measuring Length (L) = 80.71 µm.

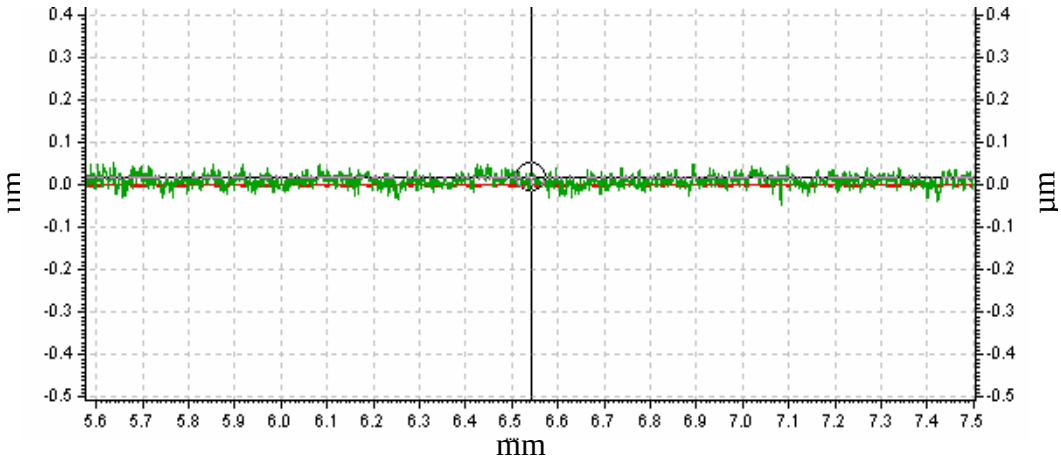

Figure 5.13: Surface Roughness of BK7 glass measured in Taylor Hobson machine

Surface roughness of the second glass piece machined was again measured in the Mitutoyo machine. All the measurement conditions were same as in case of Perspex except in this case sampling length was 30 mm. Evaluation profile obtained is shown in

figure 5.14. Different roughness parameters obtained from this measurement are tabulated in table 5.7.

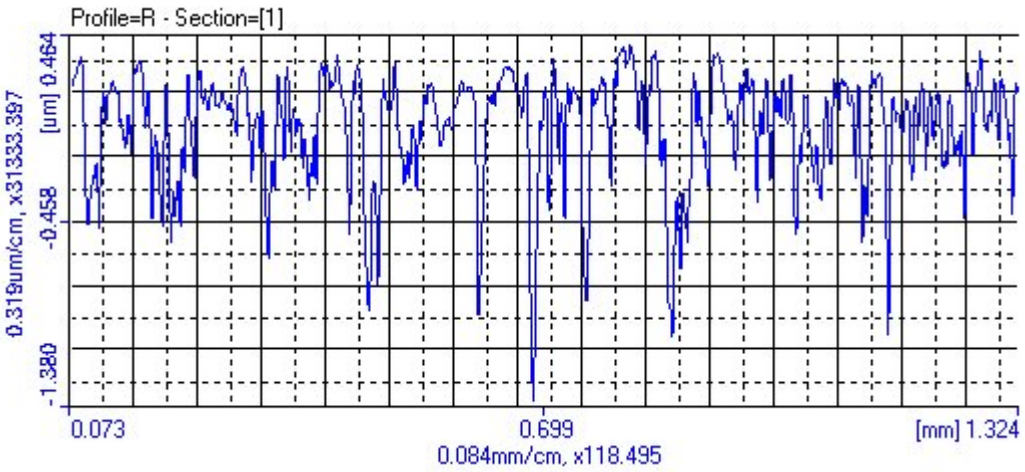

Figure 5.14: Surface roughness measured in Mitutoyo CS-500 form tracer

Table 5.7: Different Roughness values Measured

Parameter	Value (µm)
Ra	0.1981
Ry	0.8953
Rz	0.7613
Rp	0.3830
Rv	0.5123
Rq	0.2297

5.8.3 Analysis of Surface Roughness

General speaking, it is well known that the grit size of abrasive on the grinding wheel has profound effects on the attainable surface roughness. In order to obtain the better surface finish and the less damaged layer, needless to say, ultra-fine abrasives

wheel is necessary to be used [Shaohui Yina et al]. In this study the grinding wheel used for finishing was CIB-D grinding wheel with mesh size of 4000. So by using higher grades of grinding wheel surface roughness can be improved.

5.8.3.1 Influence of grinding wheel speed

In this study maximum grinding wheel speed used was 2000 RPM. Faster the rotational speed of the grinding wheel, the greater the improvement in the ground surface roughness [E.S. Lee et al]. This is attributed to changes in the material removal mechanism between the two grains. If the rotational speed of grinding wheel is increased, ground surface roughness is improved because grain effects affecting the circumference direction of workpiece are decreased.

5.8.3.2 Influence of work rotation speed

The work rotation speed has a dominant influence on the ground surface roughness finish of an aspheric surface. The ground surface roughness is improved with high rotation speed in the workpiece. Ground surface roughness is decreased if the ratio of the feedrate and rotational speed of the workpiece is greater than 3 [E.S. Lee].

5.8.3.3 Influence of feed rate

Increase of feederate causes degradation of ground surface roughness. In general, as the grit size decreases, the number of active cutting edges per unit area on the wheel surface increases, so the spacing between active cutting points reduces. The cutting chip

thickness is also significantly reduced, and thus, the ground surface roughness of an aspheric surface micro-lens greatly improves.

5.9 STUDY OF GROUND SURFACE INTEGRITY

In order to investigate the presence of sub-surface damages and grinding marks on the finished surface was observed under SEM and Keyence microscope. Photographs of the finished Perspex and glass workpieces are shown in figure 5.15 (a) and (b) respectively. From this figure it is evident that, surface created is very much transparent.

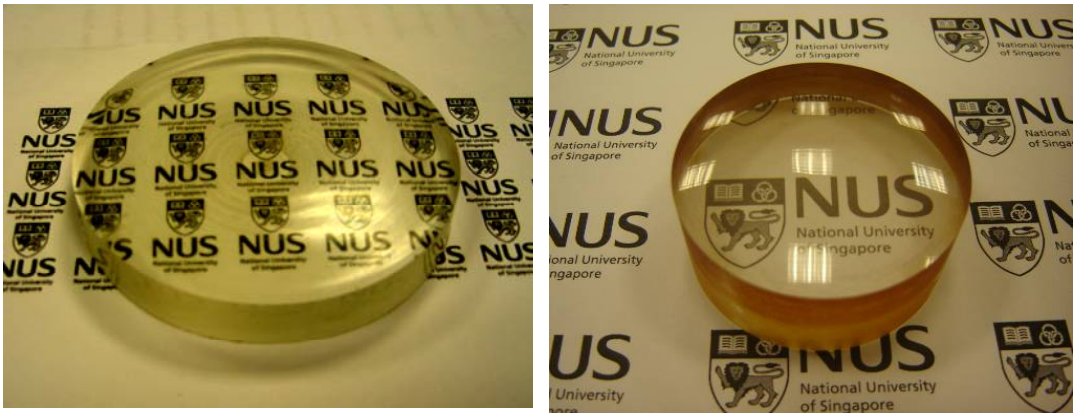

(a) (b)

Figure 5.15: Finished (a) Perspex and (b) Glass sample after grinding

Perspex workpiece was observed under Keyence microscope for studying ground surface quality. Two of the images obtained are shown in figure 5.16 (a) and (b).

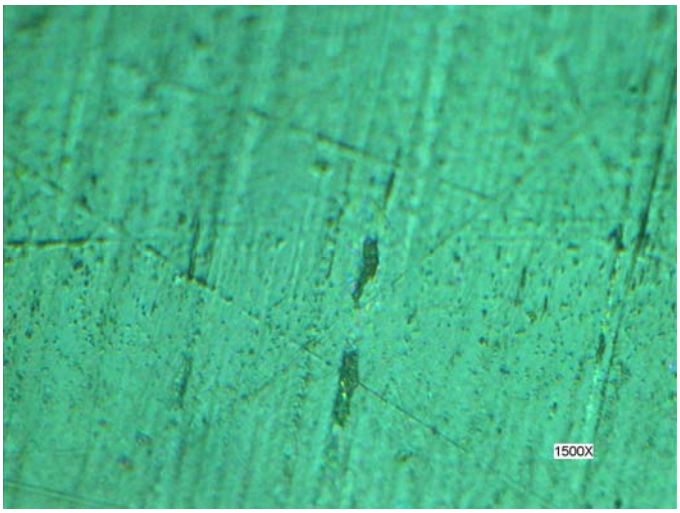

(a)

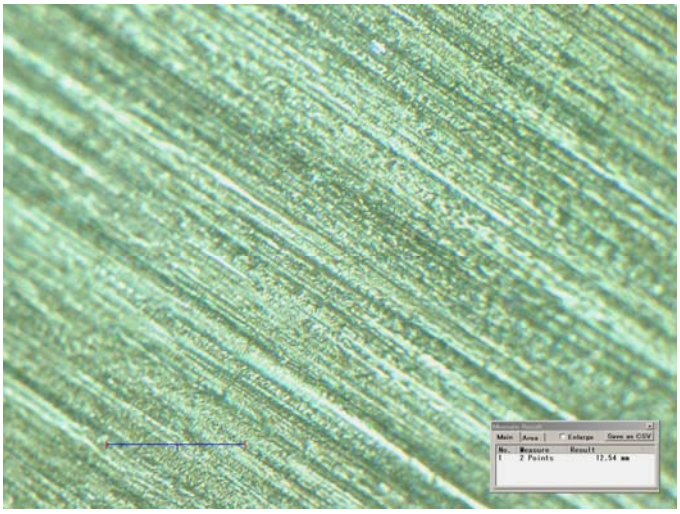

(b)

Figure 5.16: (a) 3D (b) 2D view of the Perspex surface under Keyence microscope

The glass workpiece was observed under Keyence microscope. A 2D and 3D image of the ground surface observed under Keyence microscope is shown in figure 5.17 and 5.18 respectively. Both of these cases the magnification was 3000X. From these two figures it can be stated a very high quality optical surface has been generated where grinding marks are quite regular and uniform.

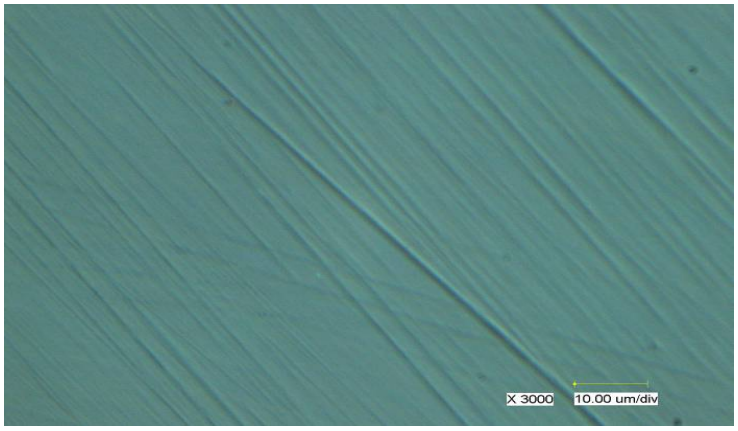

Figure 5.17: 2D image of the Ground glass Surface observed under Keyence microscope

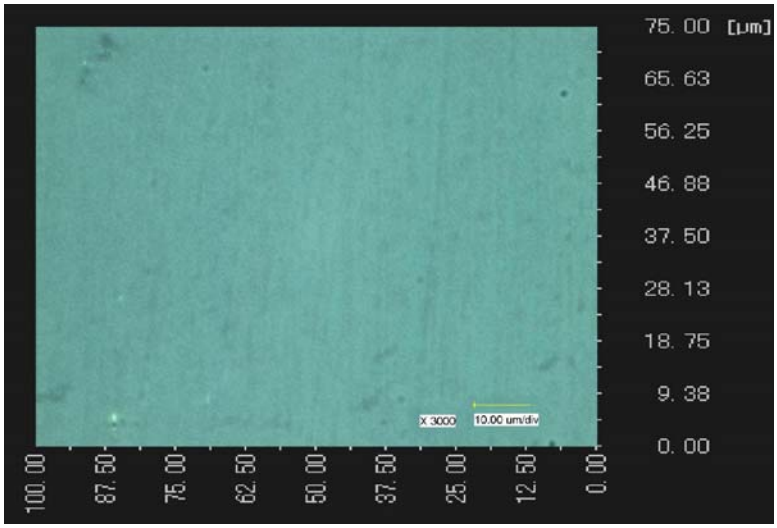

Figure 5.18: 3D image of the Ground glass Surface observed under Keyence microscope

One more picture was taken by the Keyence microscope to study the topography of the surface which is shown in figure 5.19. Curvature of the surface is clearly marked in this figure.

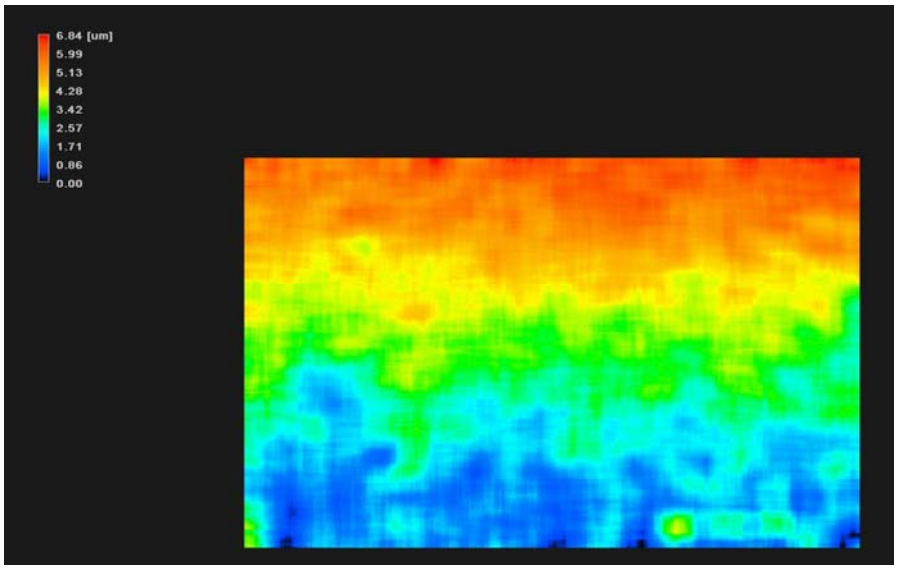

Figure 5.19: Surface topography of the glass piece observed under Keyence Microscope

One of the major goals of this study was to machine an aspheric surface free from any subsurface damage or cracks. To observe these surface and subsurface phenomena the glass piece was observed under SEM. Images obtained from the SEM are shown in figures 5.20 (a) and (b) respectively. The figures showed are after 2500X and 1500X times' magnification.

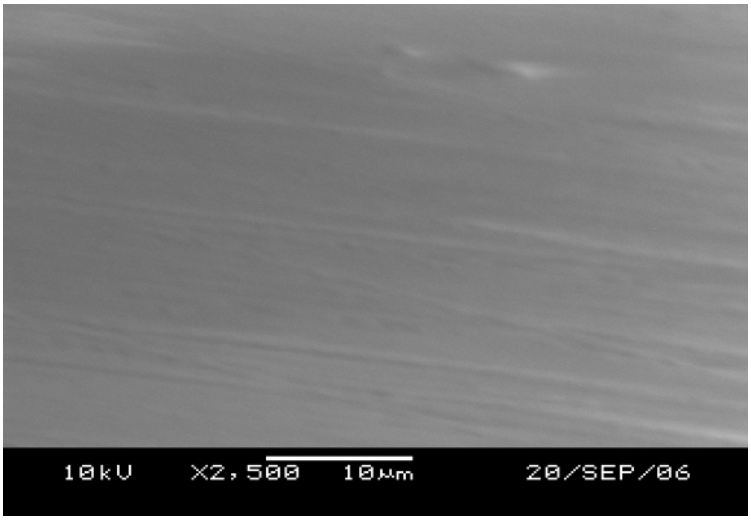

Figure 5.20 (a): SEM images of the ground surface after 2500 times' magnifications

The glass piece which was machined with software compensation was also observed under Keyence microscope. Figure 5.20 has shown a picture taken by this microscope after 1500 times magnification of the real image.

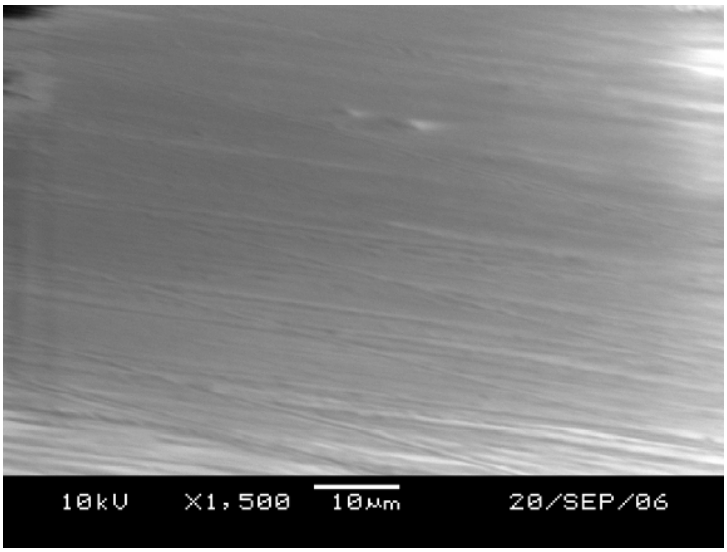

Figure 5.20(b): SEM images of the ground surface after 1500 times' magnifications

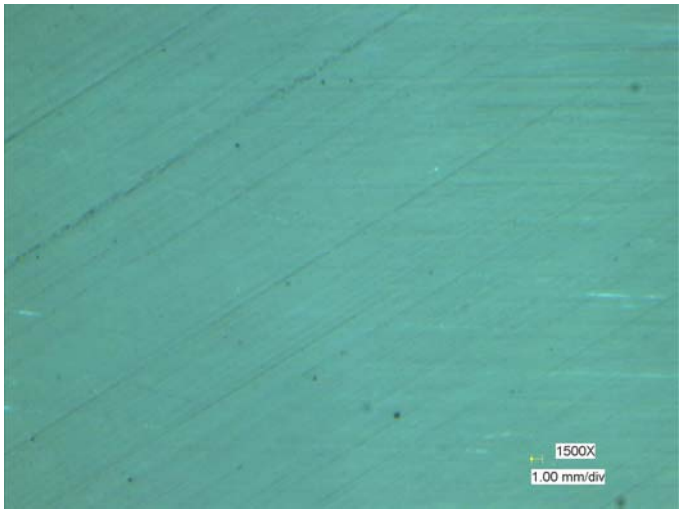

Figure 5.21: Ground glass (without software compensation) under Keyence microscope

5.9.1 Analysis of Surface Integrity

The passivating film created by electrolysis is one of the major reasons behind generation of optical quality surface on hard and brittle material [C.Z. Ren et al.]. Thickness of the film is several dozens of micron which is far larger than the size of the ultra fine abrasive. So it is difficult for the abrasive particle to create cutting action on the harder workpiece. As a result the materials are removed with a manner combining the micro-scale grinding of ultra fine abrasives and the lapping and polishing actions of the abrasives wrapped in the film. So even without lapping and polishing it is possible to generate surface with a surface roughness in submicron level which reduces the amount of time and money dedicated for these post processes

It is found that the application of the ELID technique improves the surface quality of the ground surface. The active sharp grits per unit area of the grinding wheel slowly start decreasing during the conventional grinding process. In the case of the ELID grinding technique, the active sharp grits per unit area of the wheel remain almost constant at better dressing conditions and this leads to improved surface integrity and surface roughness [Lim et al].

The metal bonded diamond grinding wheels have better grindability and stiffness. But, the wheel-working surface is harder because of its high bonding strength. The bonding strength of the wheel-working surface should be reduced for better grinding results. The efficient way of reducing the bonding strength is by using the electrolytic dressing process. Even though electrolytic dressing reduces the strength of the bonding

material, the layer has enough strength to hold the diamond grits while performing grinding.

CHAPTER SIX

CONCLUSIONS AND RECOMMENDATIONS

6.1 MAJOR CONTRIBUTIONS

In this study major contributions can be summarized into the following points:

- Design and development of a CNC ELID grinding machine
- Develop an on-machine measurement system for measuring ground surface profile
- Machining of aspheric surface on hard and brittle material with and without software compensation
- Report on improvement in dimensional accuracy of finished part ground with software compensation.

6.1.1 Design and development of a CNC ELID grinding machine

In this study a 4 axis CNC grinding machine was developed along with a power supply necessary for ELID. A workpiece rotational axis was also fabricated and attached into this system which is required for grinding free from surfaces. Performance of the developed systems was checked.

6.1.2 Develop an on-machine measurement system for measuring ground surface profile

An on machine profile measurement system based on CMM principle has been developed in this study to measure the profile of the ground surface. The developed on-machine measurement system is easy to implement, versatile and error measured is also within acceptable limit.

6.1.3 Machining of aspheric surface on hard and brittle material with and without software compensation

Optical quality aspheric surfaces were machined on BK7 glass and Perspex. Tool path was generated considering the desired profile and actual wheel diameter. During the grinding process achieved profile and wheel wear were taken into consideration for updating the tool path in the NC program.

6.1.4 Report on improvement in dimensional accuracy of finished part ground with software compensation

Error in the final profile radius of the finished part was improved from 2.83% to 0.04% only by implementing software compensations in grinding aspheric surface on BK7 glass piece.

6.2 RECOMMENDATIONS FOR FURTHER IMPROVEMENT

During this study it was observed that there is still quite a big opportunity in improving the performance of the system for generating free form surface. Due to time

constrain, all these recommendations could not be accommodated in this study but can be used as a guide for further moving forward with this research.

6.2.1 Possibility of improving the machine tool

Although performance of the CNC grinding machine was quite satisfactory but still there are premises for further improvement. Specifically the driving motor of Y axis can be changed to see whether it improves the repeatability or not. Recently many machine tool manufacturers are switching to linear motor. So installation of linear motor can also improve the performance of the machine tool itself.

6.2.2 Possibility of improving the ELID process

As comparatively new process there are still many scopes untried to improve the ELID process itself. There is a probability of controlling the electrolysis for ensuring the most efficient use of grinding wheel. Gap between electrode and grinding wheel can also be carefully maintained by developing some mechanism for controlling movement of electrode which in turn can ensure uniform electrolysis.

6.2.3 Possibility of improving the turntable

Replacing the existing sealed type ball bearing of the turn table with ceramic bearing or air bearing can improve the accuracy if the turntable. But this will definitely be a more expensive option.

6.2.4 Improvement of form accuracy

It was found in this study that form deviation in all the surfaces ground were almost identical which means that this was due to the error with the machine tool itself. There is very strong chance of removing this kind of deviation by controlling the grinding process. NC program can be modified in such a way that grinding wheel will go only to those specific points where there is some excess of material and remove that. Use of round edge grinding wheel instead of flat edge one can also contribute to improve the form accuracy of the ground surface.

REFERENCES

A. Taguchi, T. Miyochi, Y. Takaya, S. Takahashi, K. Saito 3D micro-profile measurement using optical inverse scattering phase method, Annals of the CIRP, 49/1/2000, p. 423

C.S. Han, S. Dong and Y.Y Tang; Geometric Models of the ultra precision grinding for large non-axisymmetric optical aspheric surfaces; Key engineering Materials Vol. 257-258 (2004) pp 57-62.

C.Z. Ren, J.M. Che, T.Y. Wang, W.D. Jin, ELID Grinding Based on state Control of passivating films Key engineering Materials Vol. 315-316 (July 2006) pp. 536-540.

Derk Visser, Tom G. Gijsbers, and Rob A. M. Jorna; Molds and measurements for replicated aspheric lenses for optical recording, Applied Optics, Vol. 24, No. 12 / 15 June 1985.

E.B. Hughes, A. Wilson, G.N. Peggs, Design of a high-accuracy CMM based on multi-lateration techniques , Annals of the CIRP, STC P, 49/1/2000, p. 391

E.S. Lee, S. Y. Baek, A study on optimum grinding factors for aspheric convex surface micro-lens using design of experiments, International Journal of Machine Tools & Manufacture 47 (2007) 509–520

G.N. Peggs, A.J. Lewis, S. Oldfield, Design for a compact high-accuracy CMM, Annals of the CIRP, STC P, 48/1/1999, p. 417

Hao-Bo Cheng, Zhi-Jing Feng, Kai Cheng and Ying-Wei Wang, Design of a six-axis high precision machine tool and its application in machining aspherical optical mirrors, International Journal of Machine Tools and Manufacture, Volume 45, Issue 9, July 2005, Pages 1085-1094.

H.J. Jing, Y.X. Yao, S.D Chen, Machining accuracy enhancement by modifying NC Program, Key engineering Materials Vol. 315-316 (July 2006) pp. 71-75.

H.S. Lim; K. Fathima; A. Senthil Kumar; M. Rahman, Electrolytic in process dressing (ELID) grinding; International Journal of Machine Tools & Manufacture 42 (2002) pp. 935–943.

H. Schwenke, M. Franke, J. Hannaford, H. Kunzmann, Error mapping of CMMs and machine tools by a single tracking interferometer, Annals of the CIRP 54/1/2005, p. 475

Ichirou Yamaguchi, Jun-ichi Kato, Hirokazu Matsuzaki; Measurement of surface shape and deformation by phase-shifting image digital holography, Opt. Eng. 42(5) pp. 1267–1271 (May 2003), Society of Photo-Optical Instrumentation Engineers.

J. Qian ,P. Vleugels, D. Hemschoote, A novel design for a high precision freeform ELID grinding machine, Proc. of 4th euspen International Conference- Glasgow, Scotland (UK), May-June 2004

Jung-Sik Heo, Yang Koo, Soung-Sam Choi, Grinding characteristics of conventional and ELID methods in difficult-to-cut and hardened brittle materials, Journal of Materials Processing Technology, Vol. 155–156 (2004) pp 1196–1200

Katsushi Furutani , Noriyuki Ohguro, Nguyen Trong Hieu, In-process measurement of topography change of grinding wheel by using hydrodynamic pressure, International Journal of Machine Tools & Manufacture 42 (2002) 1447–1453

Marek Dobosz; Adam Wo´zniak; "CMM touch trigger probes testing using a reference axis"; Precision Engineering vol. 29 (2005) pp.281–289

Ming Chang, Kao-Hui Lin, Non-contact probe for profilometric measurement of small-form parts, Opt. Eng. 40(10) 2057–2058 (October 2001), Society of Photo-Optical Instrumentation Engineers

M Zhou, X.D. Liu and S.N. Huang, Ultraprecision cutting of glass BK7, Key engineering Materials Vol. 315-316 (July 2006) pp. 536-540.

N. R. Sivakumar, W. K. Hui, K. Venkatakrishnan, B. K. A. Ngoi, Large surface profile measurement with instantaneous phase-shifting interferometry, Optical Engineering, Vol. 42 No. 2, February 2003

Ohmori H, Nakagawa T, Analysis of mirror surface generation of hard and brittle materials by ELID (electronic in-process dressing) grinding with superfine grain metallic bond wheels, Annals of the CIRP, Manufacturing Technology, 44/1/1995, pp. 287–290.

Pei-Lum Tso, Ho-chiao Chuang, A study on the form error compensation for aspheric lens machining, Key engineering Materials Vol. 238-239 (2003) pp. 369-374.

Peisen S. Huang, Qingying Hu, Fu-Pen Chiang; Error compensation for a three-dimensional shape measurement system, Opt. Eng. 42(2) 482–486 (February 2003)

Peisen S. Huang, Chengping Zhang, Fu-Pen Chiang, High-speed 3-D shape measurement based on digital fringe projection, Opt. Eng. 42(1) 163–168 (January 2003), Society of Photo-Optical Instrumentation Engineers.

Saroti, S. Zhang,G. X., Geometric error measurement and compensation of machines; annals of CIRP, 44/2 599-609.

S. Okuyama, T. Kitajima, A. Yui, Theoretical study on the effect of form error of grinding wheel surfaces under free form grinding, Key Engineering Materials 257–258 (2004) 147–152.

Shaohui Yin, Shin-ya Morita, Hitoshi Ohmori, Yoshihiro Uehara, Weimin Lin, Qing Liu, Toshinori Maihara, Fumihide Iwamuro and Daisaku Mochida, ELID precision grinding of large special Schmidt plate for fiber multi-object spectrograph for 8.2 m Subaru

telescope, International Journal of Machine Tools and Manufacture, Volume 45, Issue 14, November 2005, Pages 1598-1604

Shin-ya Moritaa, Hitoshi Ohmori, Yoshihiro Ueharaa, “ELID precision grinding of large special Schmidt plate for fiber multi-object spectrograph for 8.2 m Subaru telescope”; International Journal of Machine Tools & Manufacture 45 (2005) 1598–1604.

Stephan R. Clark, John E. Greivenkamp, Optical reference profilometry, Opt. Eng. 40(12) 2845–2851 (December 2001), Society of Photo-Optical Instrumentation Engineers

T. Enomoto, Y. Shimazaki, Y. Tani, T. Sata, Improvement of form accuracy in axisymmetrical grinding by considering the form generation mechanism, Annals of the CIRP,STC G, 45/1/1996, p. 351

T. Kawai, K. Ebihara, Y. Takeuch; Improvement of Machining Accuracy of 5-Axis Control Ultraprecision Machining by Means of Laminarization and Mirror Surface Fininshing; Annals of the CIRP, Vol 54, 2005, p. 329

Wei Gao, Satoshi Kiyono, High accuracy profile measurement of a machined surface by the combined method, *Measurement* Vol. 19, No. 1, pp. 55-64,1996

Y. Namba, M. Abe / A. Kobayashi Ultra-precision grinding of optical glasses to produce super-smoots surfaces, Annals of the CIRP, Vol 42, 1993, page 417

Y. Takaya, S. Takahashi, T. Miyoshi, K. Saito, Development of the nano-CMM probe based on laser trapping technology, Annals of the CIRP, STC P, 48/1/1999, p. 421

Young Kee Ryu, Choonsuk Oh, Jong-Seul Lim, Development of a noncontact optical sensor for measuring the shape of a surface and thickness of transparent objects, Opt. Eng. 40(4), pp. 500–502 (April 2001), Society of Photo-Optical Instrumentation Engineers

Yousef A. Gharbia, Jayantha Katupitiya, Experimental determination of optimum parameters for nano-grinding of optical fibre end faces, International Journal of Machine Tools & Manufacture 44 (2004) 725–731.

Y. Zhang, Y. B. Guo and K. Syoji Research on effect conditions of micro vibration in ultra-precision grinding of aspheric surface. Key engineering Materials Vol. 259-260 (2004), pp. 430-434.

Yoshioka J, Hashimoto F, Miyashita M, Kanai A, Abo T, Daito M, Ultraprecision grinding technology for brittle materials: Application to surface and centerless grinding processes, Milton C. Shaw Grinding Symposium, PED 16, pp. 209 – 227, 1985.

Z.Q. Liu, P.K. Venuvinod, Error compensation in CNC turning solely from dimensional measurements of previously machined parts, Annals of the CIRP, STC P, 48/1/1999, pp. 429

LIST OF PUBLICATIONS

A) Journal

1) T. Saleh, M. Sazedur Rahman, H.S. Lim, M. Rahman; "Development and performance evaluation of an ultra precision ELID grinding machine", accepted for Journal of Materials Processing Technology.

2) M. Sazedur Rahman, M. Rahman, Tanveer Saleh; "ELID precision grinding of an aspheric surface using software Compensation" to be submitted (Submitted and under review in the international journal of machine tools and manufacture)

B) Conference Proceedings

1) M. Sazedur Rahman, Tanveer Saleh, H. S. Lim, S. M. Son, and M. Rahman; "Development of an On-Machine Measurement System in Grinding Process for Machining Compensation"; Proceedings of CIRP 2nd International Conference on High Performance Cutting.

2) T. Saleh, M. Sazedur Rahman, H.S. Lim, M. Rahman; Development and performance evaluation of an ultra precision ELID grinding machine, Proceedings of 7th APCMP, 2006.

Appendix A

DETAILED DRAWINGS OF DIFFERENT DEVICES

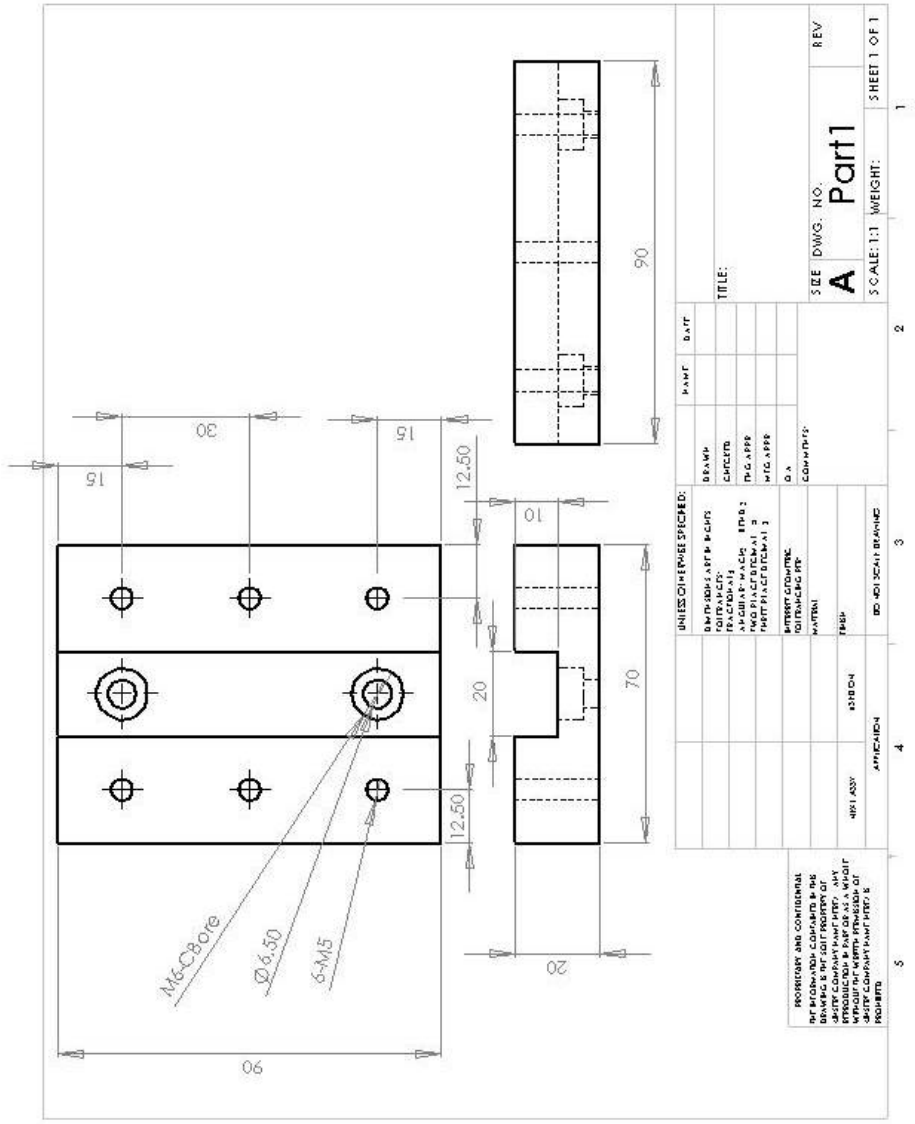

Fig A.1: Spindle Block attachment

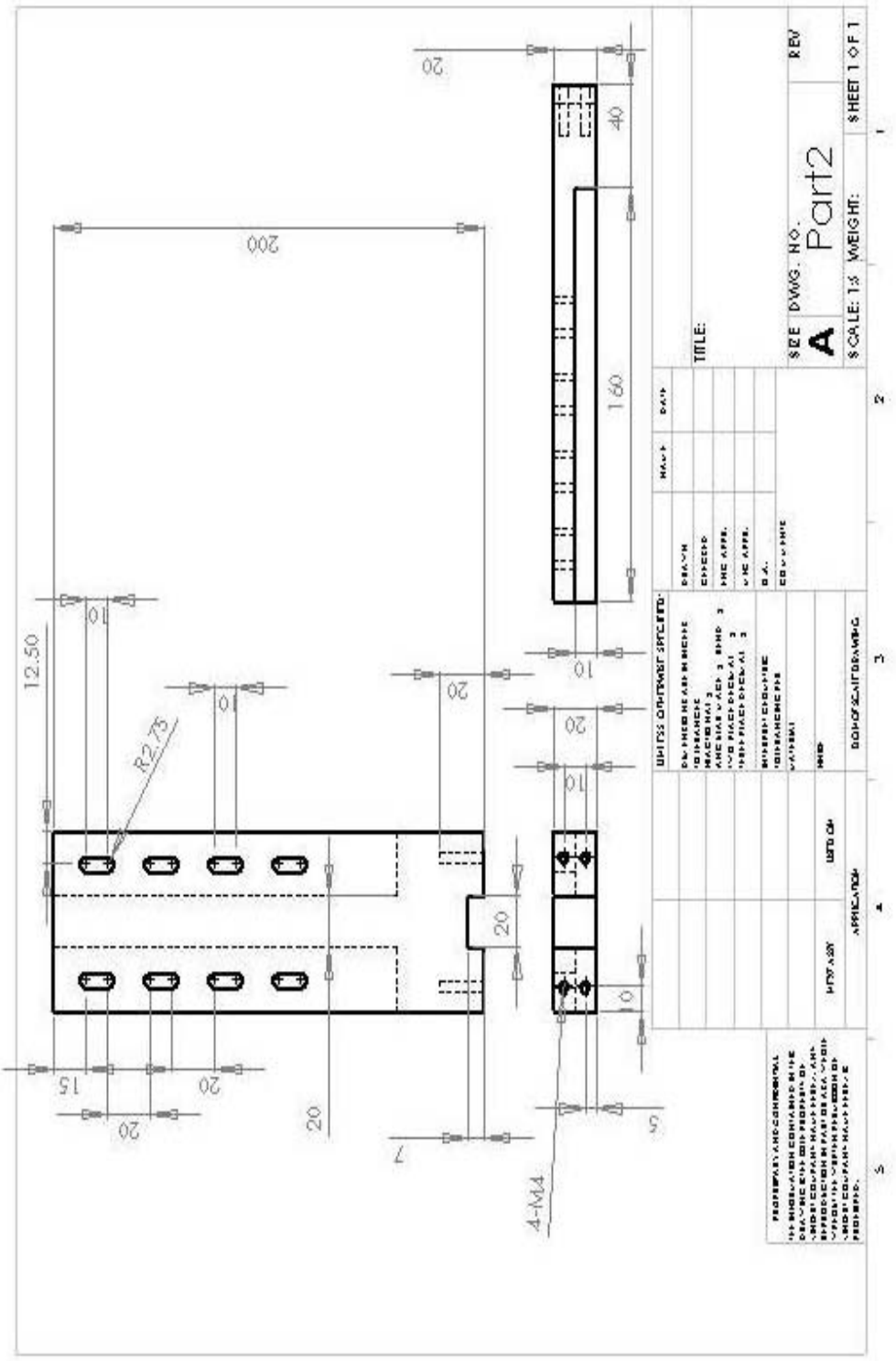

Fig A.2: Sliding Linkage

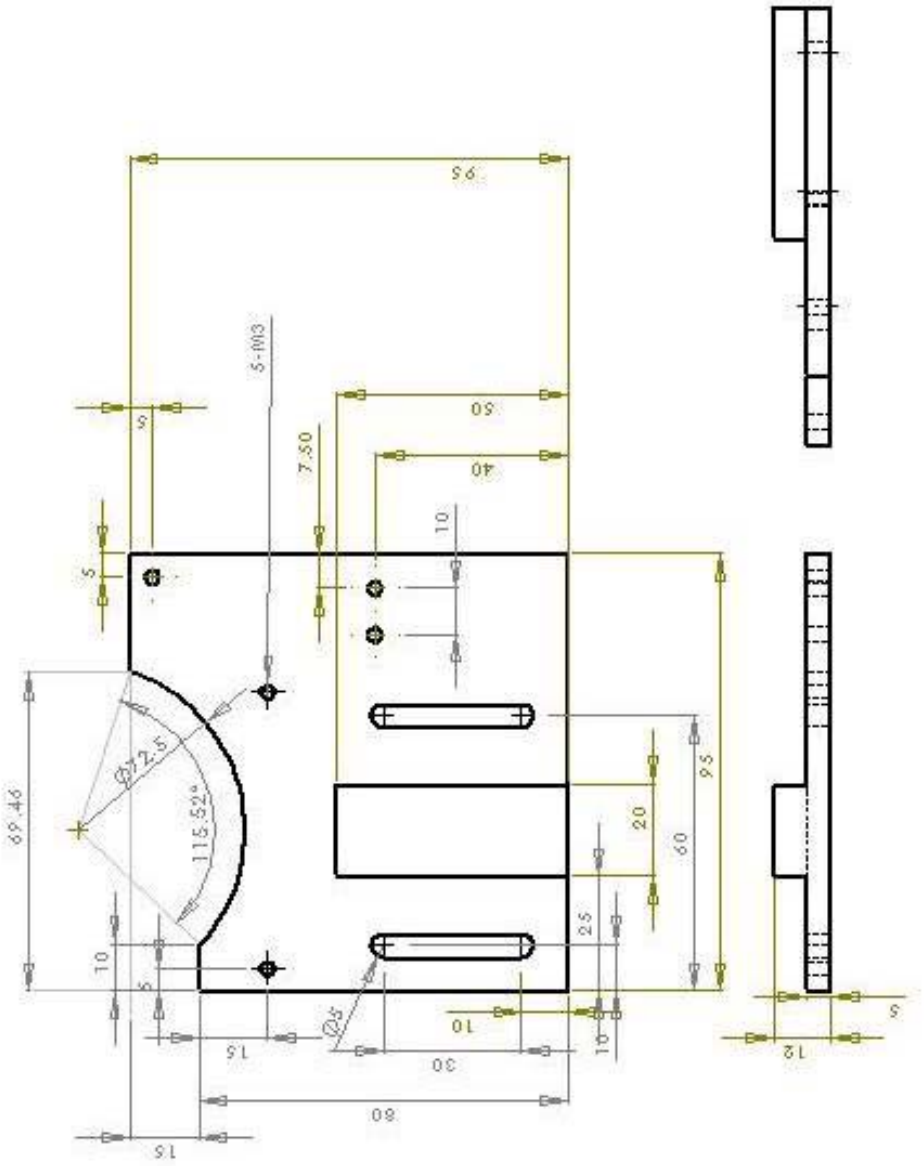

Fig A.3: Electrode holder

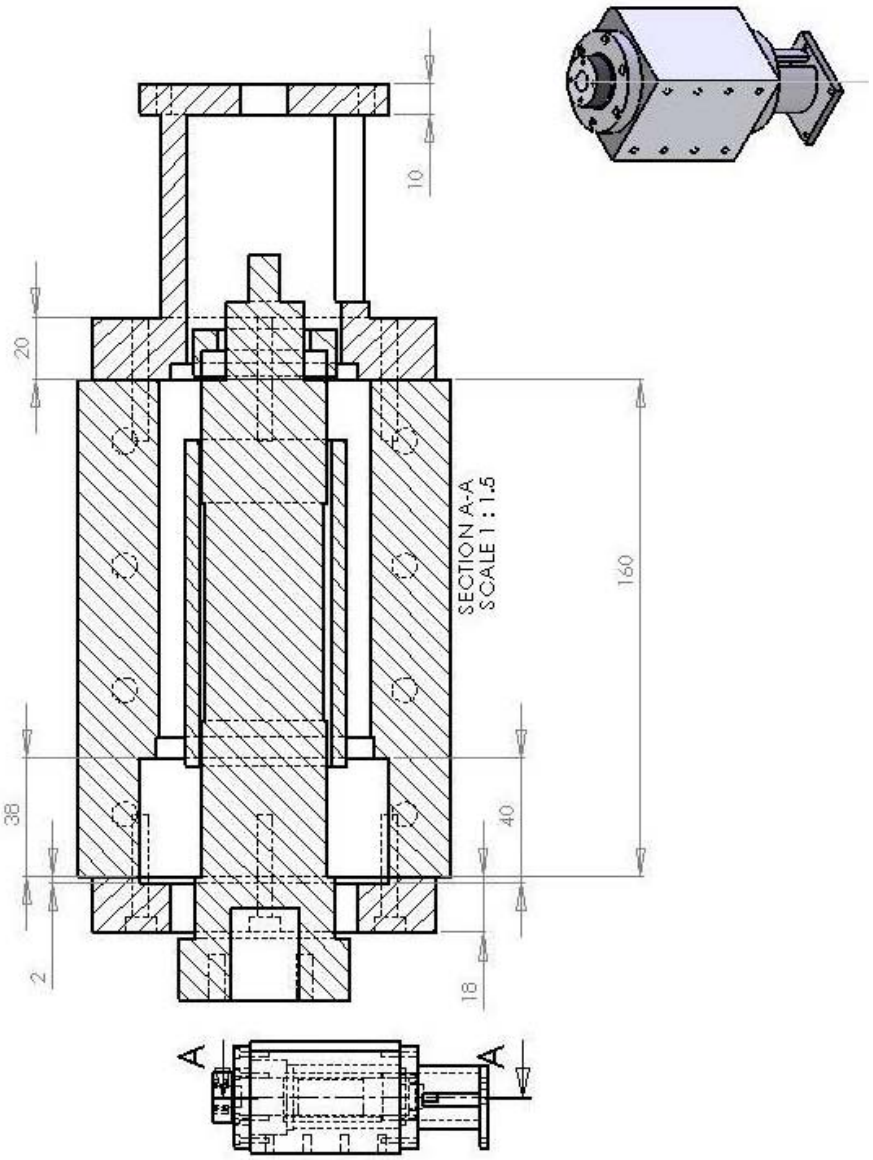

Fig A.4: Assembly of the turn-table

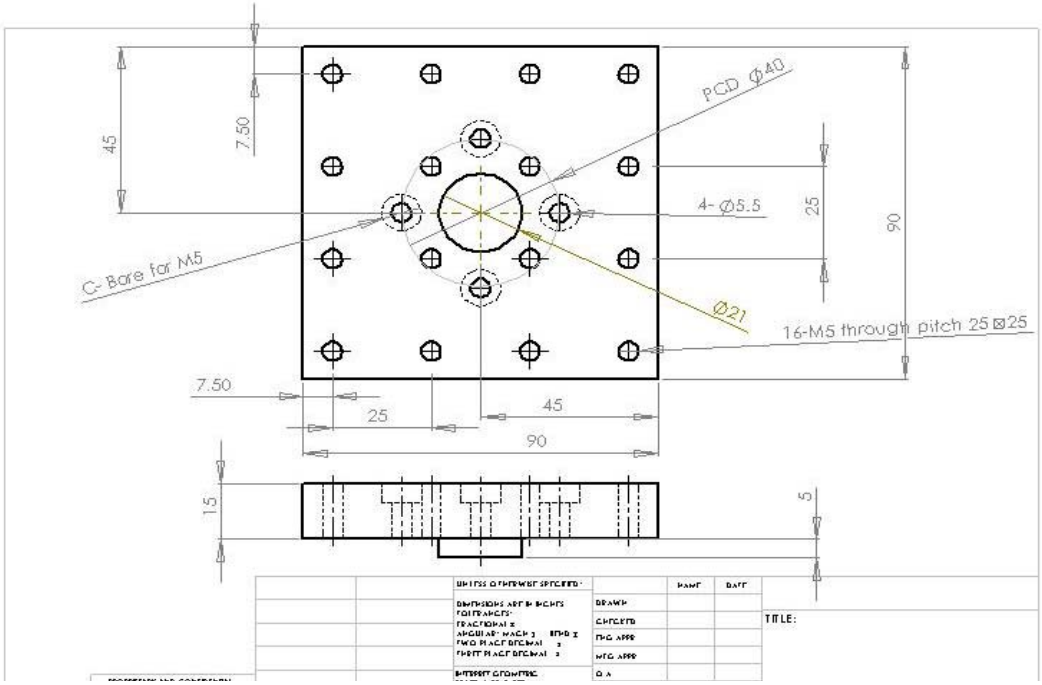

Fig A.5: Shaft Mounting Plate

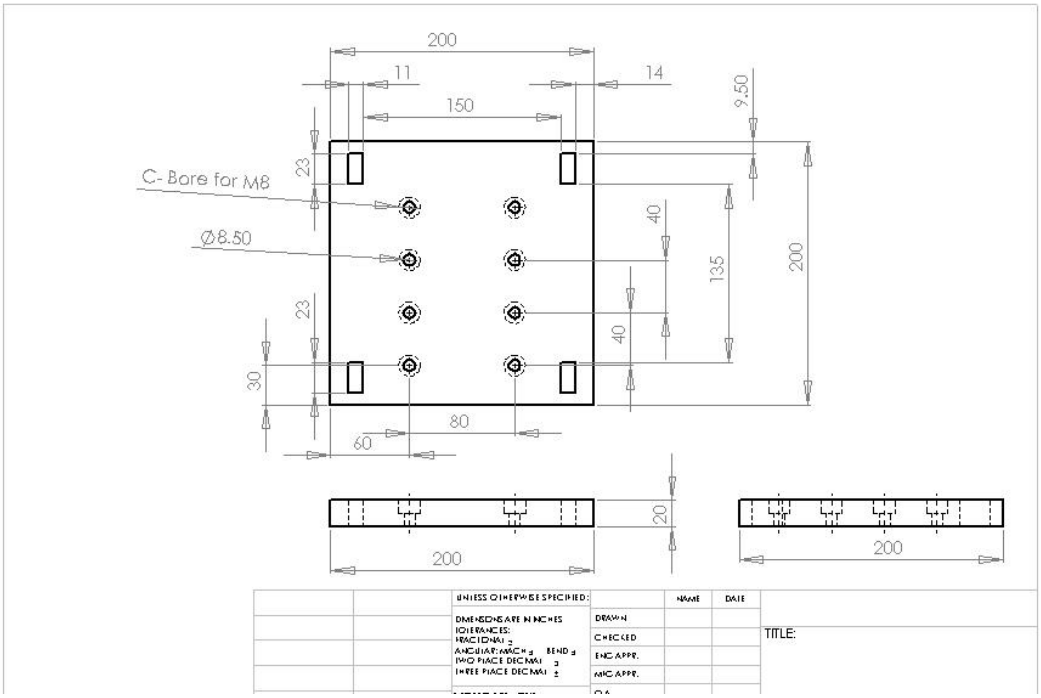

Fig A.6: Base Plate of the turn table

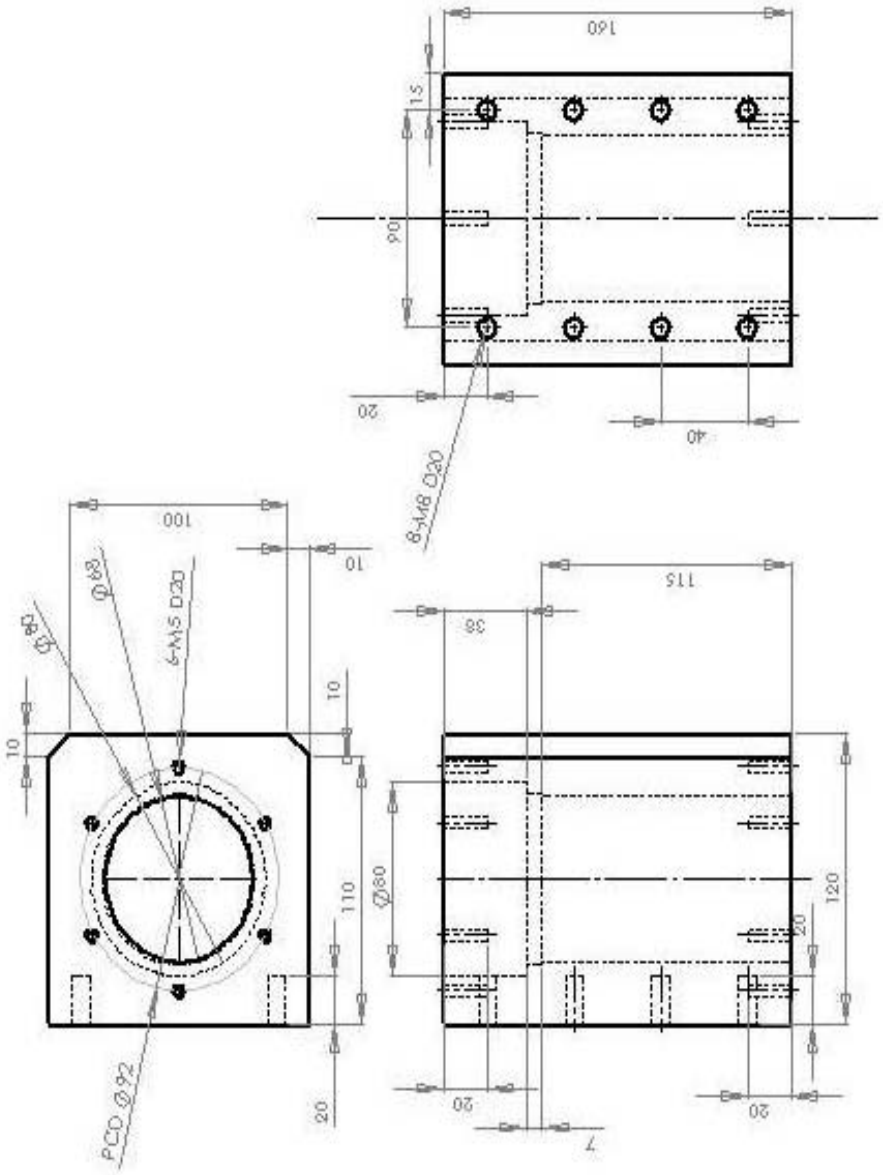

Fig A.7: Bearing Box of the turn table

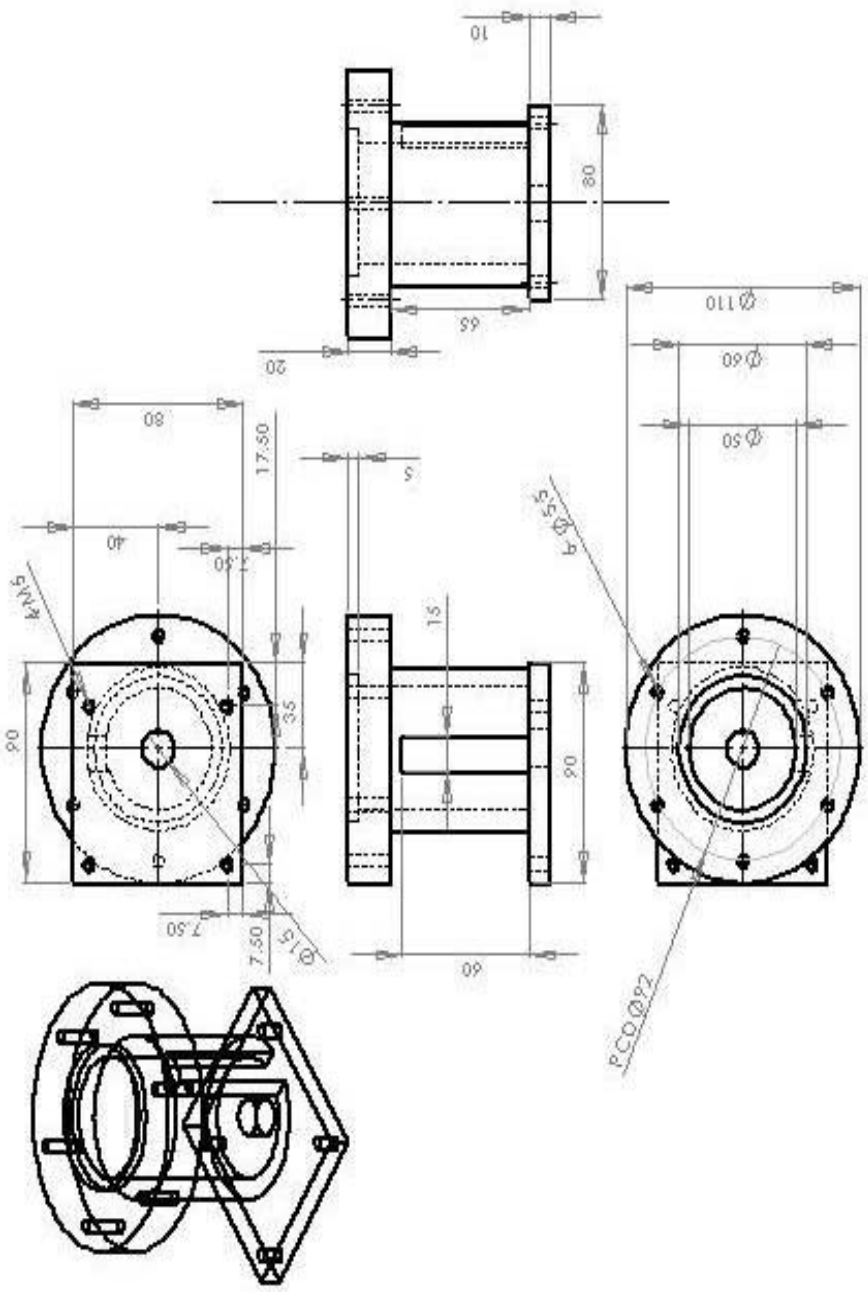

Fig A.8: Coupling cover

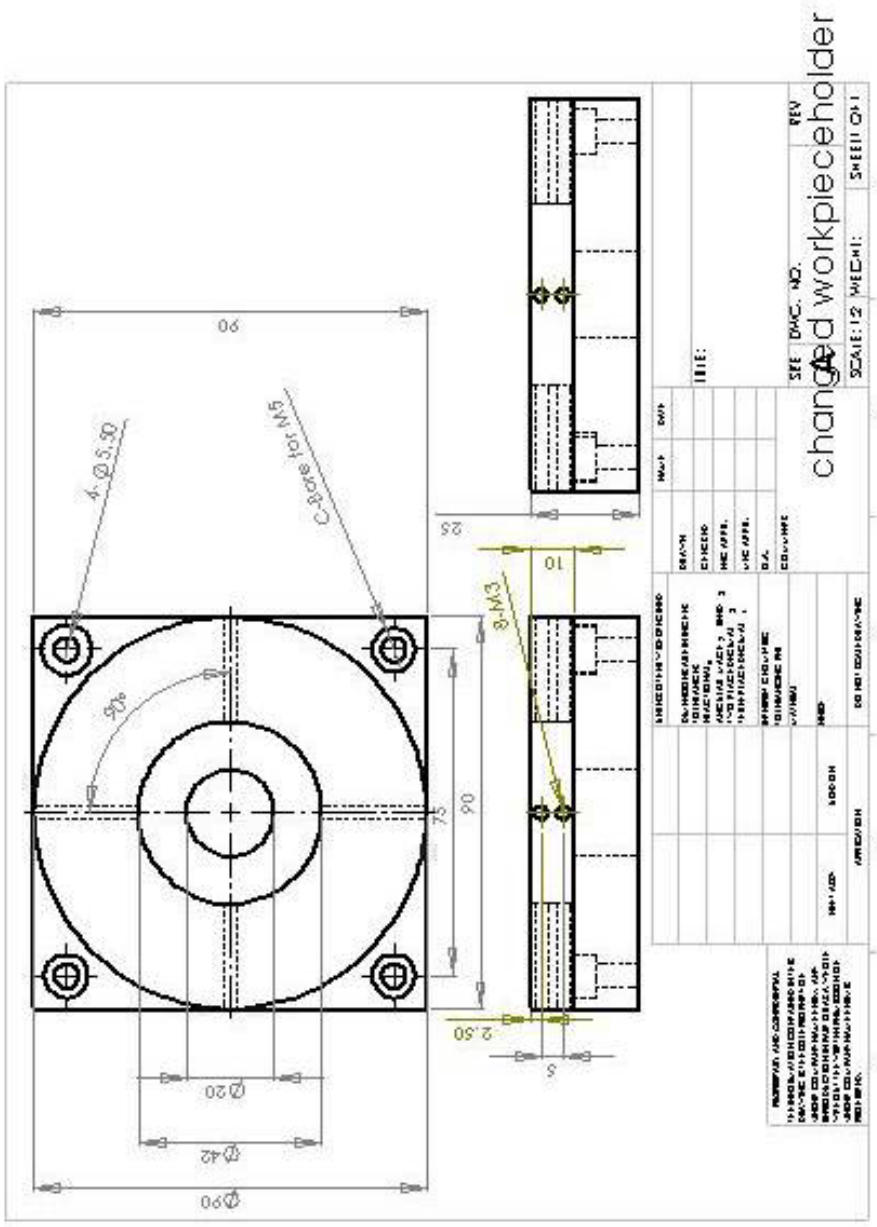

Fig A.9: Workpiece holding plate

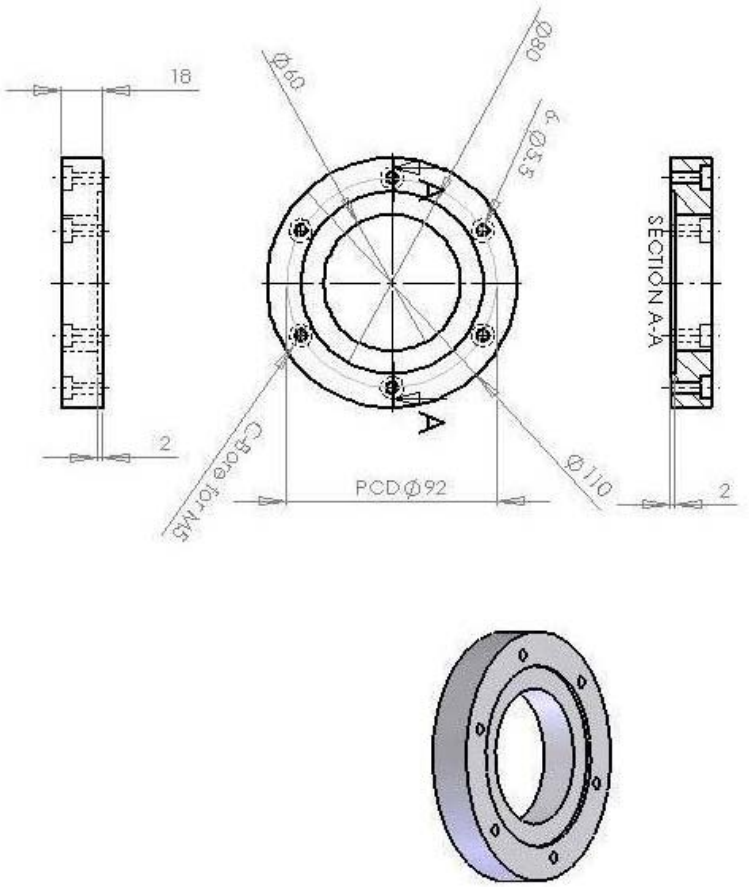

Fig A.10: Press Ring

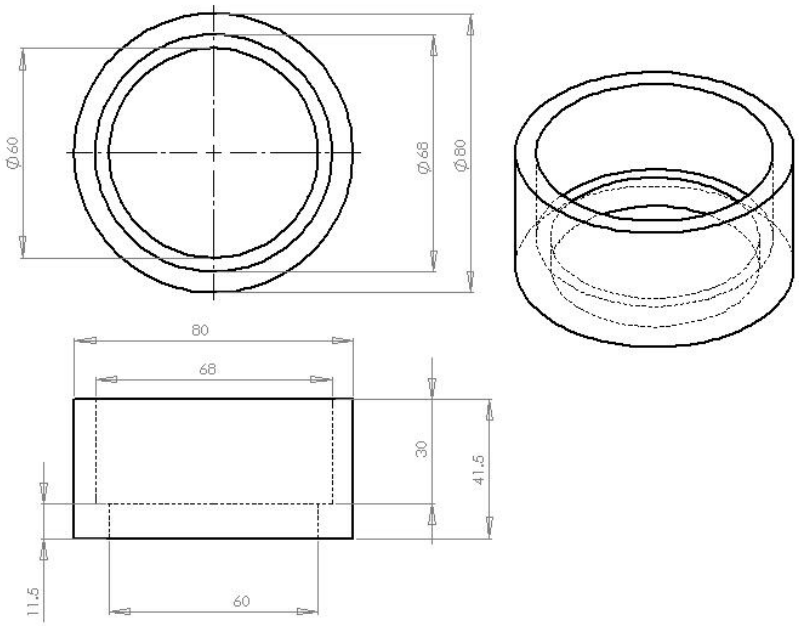

Fig A.11: Bearing fixing Ring

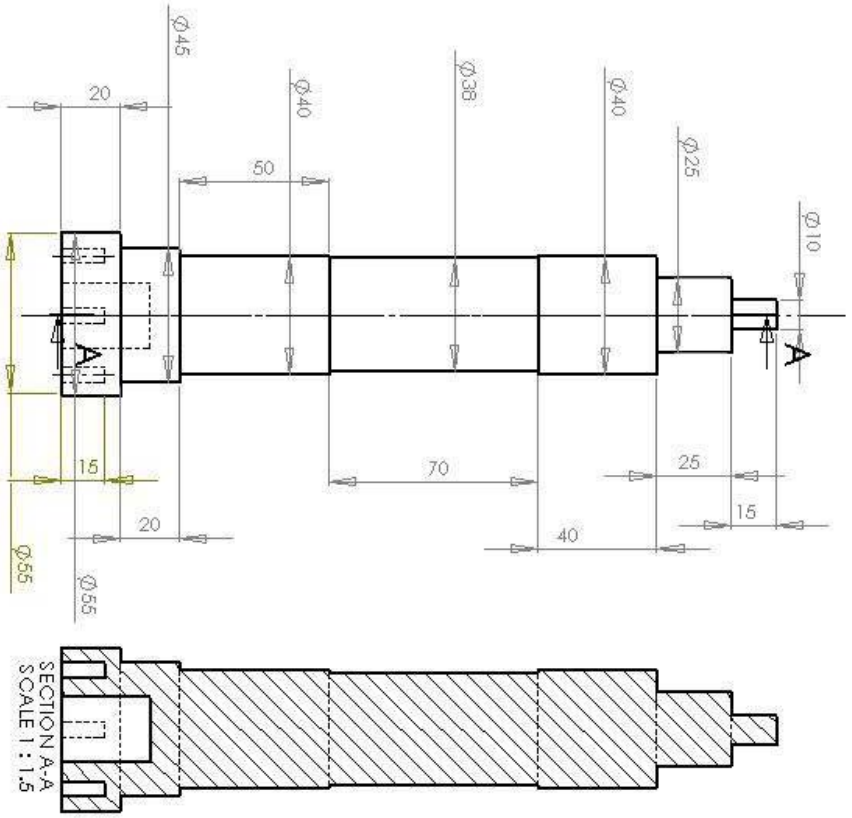

Fig A.12: Shaft of the turn table

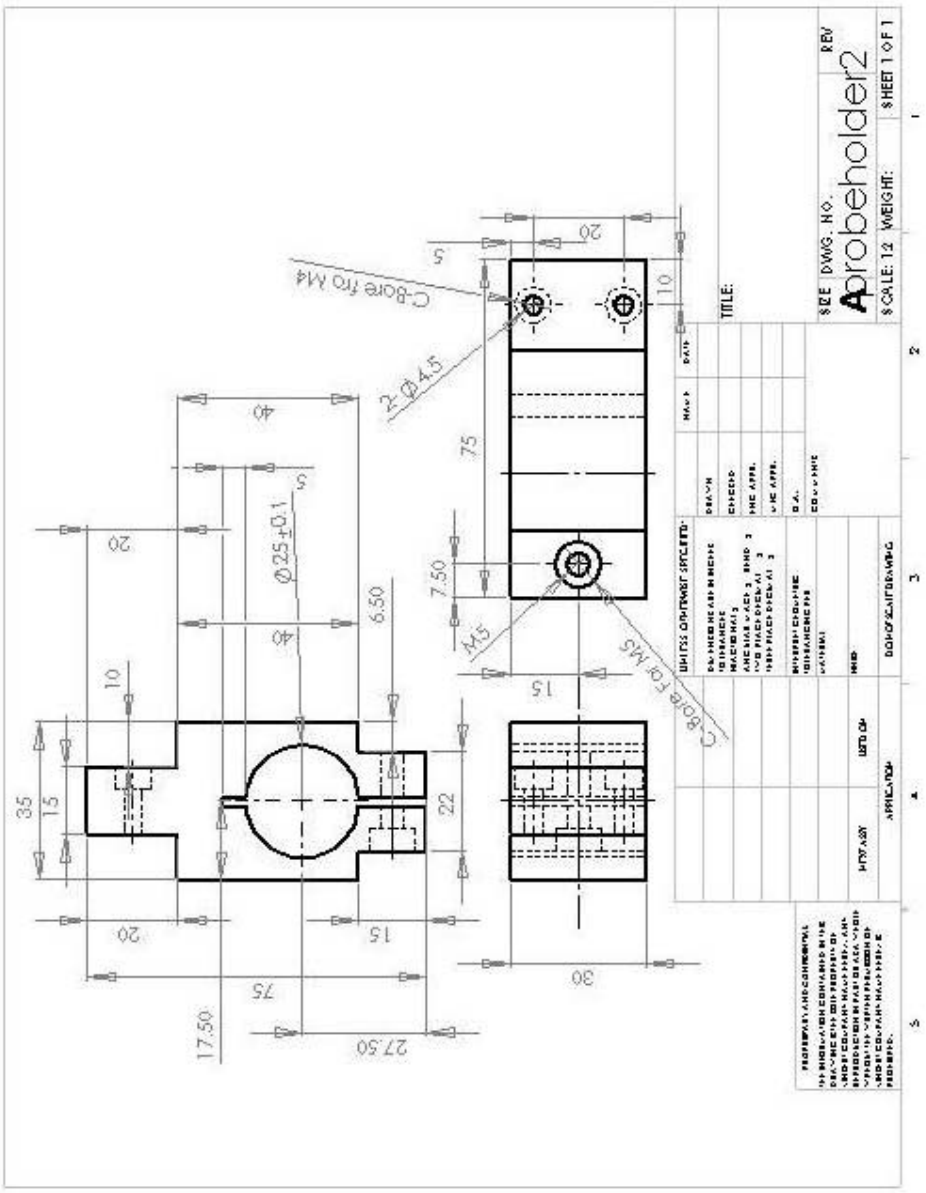

Fig A.13: Probe Holder

APPENDIX B

COMPONENT SPECIFICATION

Table B1: Specifications of the motors and drivers used in the machine

Part No.	Rated Power (W)	Resolution (C/T)	Power Supply (V)
TS4503N7000E200	100	2000	200
TA8110N141E103	100	2000	200
MSMA012A1A	100	2500	200
MSDA013A1A	100	2500	200

Table B2: Specifications of the motor used in the turntable

Model Number	S8125GX-V12
Size	80 sq. mm
Output Power	25 W
Voltage	220/240 V
Current	0.25/0.27 A
Frequency	1.5 µF
Speed	1200 RPM
Poles	4

Table B3: Specification for the LP2 Probe

Length (mm)	40.8
Diameter (mm)	25
Principal application	Lathes and grinders
Sense directions	± X, ± Y, +Z
Unidirectional repeatability	1.0 µm
Trigger force (+Z Axis)	5.85N
Stylus over travel XY plane +Z direction	 ±12.5° 6.5mm

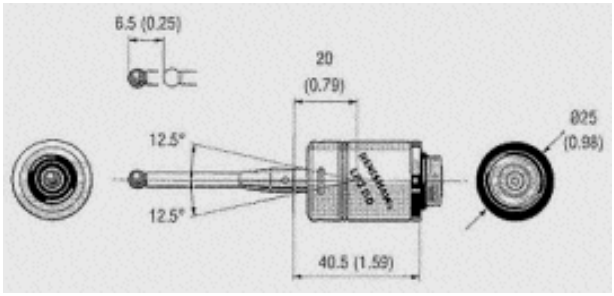

Figure B1: Schematic diagram of LP2 Probe

Table B4: Specification of the Stylus

Part Number	A-5003-4799
Ball Diameter	4 mm
Length	50 mm
Stem Dia	2.5 mm
Effective Length	38 mm
Mass	4.99 gram

Table B5: Specification of the FS1i Female socket

Principle application	Adjustable female socket with integral interface Used for holding the LP2 and LP2H probes.
System content	FS1i adjustable socket assembly, two adjusting screws, protective cover, allen key.
Length	45.5 mm
Diameter	25 mm
Weight	70 g
Storage temperature	-10°C to 70°C
Operating Temperature	10°C to 40°C
IP Rating	IPX8
Cable	4 core screen cable with polyurethane sheath. Each core 7/0.2 insulated. Ø4.35 mm x 1.0 m (3 ft 3 in)
Supply voltage	12 V to 30 V
Supply current	18 mA nominal, 25 mA max.

Output current max	50 mA
Output type	Voltage free SSR
Protection	Short circuit protected output. The interface must be powered from a suitably fused supply.

Table B6: Specification of the solenoid valve

Part Number	SY3120-5LZD-MS
Bore Size	M3×0.5
Rated Voltage	24V DC
Operating Pressure	-100 kPa to 0.7

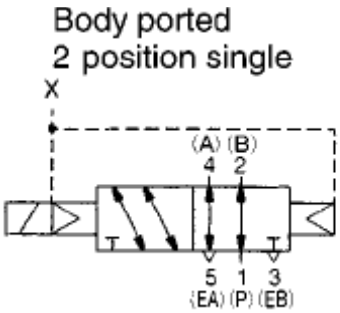

Figure B2: JIS symbol of the solenoid valve

Table B7: Specification of the Inductive Sensor

measuring range	0 to 1 mm
output voltage	0 to 5 V
resolution	0.04 % of F.S
linearity	±1% of F.S
response frequency	18 kHz